Title
Synaptic Organizing Complexes in the Modulation of Excitatory Transmission

Author
Lovero, Kathryn Lynn

Publication Date
2014

Peer reviewed|Thesis/dissertation

Synaptic organizing complexes in the modulation of excitatory transmission

by

Kathryn L. Lovero

DISSERTATION

Submitted in partial satisfaction of the requirements for the degree of

DOCTOR OF PHILOSOPHY

in

Neuroscience

in the

GRADUATE DIVISION

of the

UNIVERSITY OF CALIFORNIA, SAN FRANCISCO

Approved:

[redacted]

For my sister, Liz, who always leads the way

Acknowledgements

First and foremost, none of this work would have been possible without the outstanding mentorship of Roger Nicoll. I came to UCSF hoping to work with Roger – I had long admired both the research and researchers that came out of his lab – and feel so fortunate to have been able to spend my graduate career in the Nicoll lab. Roger's passion for science provides daily inspiration, and his scientific rigor and integrity will continue to be the gold standard to which I hold my own work.

I am also extremely indebted to Yuko and Masaki Fukata, who conducted the groundbreaking research that laid the foundation for the LGI1-ADAM project, and whose continued collaboration has been critical to its completion. Their biochemical work on the LGI1-ADAM complex has been essential in shaping the experiments I have carried out and our understanding of the data. In addition to their scientific prowess, Yuko and Masaki are also very kind and generous, and have been a joy to work with.

Similarly, the entire Nicoll lab has been vital to the growth of these projects, and also for making my time at UCSF truly enjoyable. All the postdocs I have overlapped with—Wei Lu, Yun Shi, John Gray, Maya Yamazaki, Nengyin Sheng, Jennifer Sun and Salvatore Incontro—have provided invaluable guidance throughout my graduate career. In particular, Sabine Schmid initiated the SynDIG1 project, and graciously continued collaborating with me after leaving the lab. I also owe a special thanks to Alex Jackson, who went above and beyond to share his extensive knowledge of electrophysiology with patience and kindness. Finally, Bruce Herring, both a fantastic scientist and good friend, was always willing to help me talk through an experimental issue or idea and was critical to the development of my work.

I am tremendously thankful to have shared my time in the lab with such a wonderful group of graduate students. Seth Shipman, Jon Levy, Carleton Goold and Adam Granger each started in the Nicoll Lab the year before me, and paved the way for my graduate experience. All of them are extraordinarily talented scientists, and whether it was technical advice, scientific guidance, or a laugh, they were always there to help. In particular, I owe a special thanks to Adam Granger, with whom I shared a little office for the majority of my time in the Nicoll Lab. I couldn't have picked a better roommate. Adam was the person I turned to first with every idea or problem I had, and our constant dialogue kept me motivated and focused, but most of all made every day in lab a good day. Quynh Anh Nguyen, Meryl Horn, and Sam Ancona Esselmann all joined the lab after me, and it has been a pleasure getting to know them and gaining their fresh input on my work. They are outstanding scientists, and I look forward to seeing all they accomplish in graduate school.

In addition to the wonderful postdocs and graduate students in the Nicoll Lab, none of this work could have been done without the technical help of Kirsten Bjorgan, Manuel Cerpas, and Dan Qin. Kirsten kept the lab full of supplies, slice cultures, and cheer. Manuel is a master of electroporation, and has seamlessly stepped in as lab manager and kept the lab afloat. Dan Qin joined the lab recently, and has quickly picked up mouse maintenance and genotyping, an often thankless but absolutely essential part of our research.

The UCSF neuroscience community as a whole has been a vibrant and inspiring place to work. This is largely due to the superb leadership of Louis Reichardt, and now Roger, and the terrific administrative support from Pat Veitch, Carrie Huckaba, and Lucita Nacionales. It is also because of the exceptional students this program draws,

who have been my classmates, collaborators, and friends. In particular, Meg Younger, who is a great friend and even better scientist, was especially helpful in keeping me upbeat and motivated during tough times in my project, as well as Caitlyn Gertz, my classmate and confidant who has supported me in every way and every part of this journey.

I am also very grateful to the members of my thesis committee, who have provided critical guidance throughout my graduate career. Robert Edwards, who graciously chaired my committee, has shared his seemingly unlimited knowledge of neuroscience and practical issues. Mark von Zastrow offered expert advice in cell biology and imaging, and provided a unique and important perspective in committee meetings. I had the pleasure of interacting with Grae Davis in a number of settings – as a rotation student, in the classroom, and in committee meetings Grae's thoughtful mentorship, enthusiasm, and creativity shaped me as a scientist and motivated me to think about my work in new and exciting ways. Finally, I am grateful to Hillel Adesnik, not only for serving as my out-of-institution committee member, but also for performing the initial experiments that were the basis for my work on LGI1 and for giving me invaluable advice for graduate school when I was still a student in San Diego.

Prior to coming to UCSF, I had a number of mentors and teachers without which I would never have pursued a PhD. Marilyn Rowan formally taught me math and language arts throughout elementary school, but it was her informal teaching of critical thinking skills and the joy of problem solving that laid the foundation for all of my future studies. In high school, Donna Schwan first showed me how much fun biology can be, an experience I consider a turning point in my educational path.

In college, I benefited enormously from the mentorship of Andrea Chiba, my first PI, who also taught the class that solidified my interest in pursuing graduate work in cell and molecular neuroscience. I owe a special thanks to Chris Cordova, the graduate student I worked with in the lab, for being patient with my inexperience and giving me invaluable advice about graduate programs. After college, I had the great fortune of working with Martin Paulus, an incredibly productive scientist who also took the time to be an especially dedicated mentor - giving me outstanding scientific opportunities as a research assistant and guiding me through the graduate application process.

While each of these people has helped me along the way, my family has been a constant source of support throughout this entire journey. Words can't possibly do justice to how appreciative I am of them. My sister is a true trailblazer - I am forever inspired by her intelligence and creativity, and grateful for her camaraderie. My parents have always encouraged my intellectual curiosity, and their unwavering support is what has given me the strength to pursue my own interests and take chances in life.

Finally, I consider myself tremendously fortunate to have met Sam Myers early in my time at UCSF and been able to share this experience with him. I am in awe of his dedication to research, his vast knowledge of science, and the joy he spreads to everyone around him. He has been my rock throughout graduate school, cheering me on in everything I do, lifting me up after every failure I've had, celebrating with me after every success I've enjoyed. I couldn't have done this without him.

Contributions

Initial characterization of the LGI1$^{-/-}$ mouse was conceived of by and carried out in collaboration with Yuko and Masaki Fukata. Biochemical studies of the LGI1-mediated transsynaptic complex were completed by Yuko and Masaki Fukata. Outside-out recordings for SynDIG1 and LGI1/ADAM22 experiments were performed by Yun Shi and Adam Granger, respectively. Sabine Schmid instigated the research on SynDIG1 as a potential auxiliary subunit, cloned the SynDIG1 constructs, and recorded a portion of the SynDIG1 overexpression and knockdown datasets. All other experiments were conceived of and carried out by Kathryn Lovero.

The work in Chapter 3 has previously been published in Proceedings of the National Academy of Science and is reproduced with permission:

> Fukata Y, Lovero KL, Iwanaga T, Watanabe A, Yokoi N, Tabuchi K, Shigemoto R, Nicoll RA, Fukata M. Disruption of LGI1-linked synaptic complex causes abnormal synaptic transmission and epilepsy. Proc Natl Acad Sci U S A. 2010 Feb 23;107(8):3799-804. Epub 2010 Feb 2.

The work presented in Chapter 4 has previously been published in PLOS ONE and is reproduced with permission:

> Lovero KL, Blankenship SM, Shi Y, Nicoll RA. SynDIG1 promotes excitatory synaptogenesis independent of AMPA receptor trafficking and biophysical regulation. PLOS ONE 2013 8(6): e66171. doi:10.1371/journal.pone.0066171.

ABSTRACT OF THE DISSERTATION

Synaptic organizing complexes in the modulation of excitatory transmission

By Kathryn Lynn Lovero

Doctor of Philosophy in Neuroscience

University of California, San Francisco, 2014

The remarkable ability of the brain to interpret vast amounts of stimuli and adapt to new situations is dependent upon not only the proper formation, but also the functional specialization of synaptic connections between neurons. On the molecular level, we are just beginning to understand the networks that regulate synapse development, termed synaptic organizing complexes. Recent work has identified a number of different proteins required for the formation of synapses, i.e. synaptogenesis. However, much less is understood about the protein networks that guide the maintenance and maturation of these nascent synapses. Here, I describe a novel synaptic organizing complex comprised of the secreted protein LGI1 and its transmembrane partners, ADAM22 and ADAM23. I present data demonstrating that LGI1 mediates a transsynaptic complex, including pre- and postsynaptic ADAMs and members of the MAGUK family of intracellular scaffolding proteins. I go on to characterize the functional impact of this transsynaptic complex, revealing that ADAM22 and ADAM23 are essential to maintaining excitatory synapses, and that LGI1 acts as a paracrine signal originating from axons and dendrites to modulate the strength of these synapses. Finally, I address the function of the AMPAR-interacting protein SynDIG1 in synaptic

organization, and show that, despite its previous implication in synaptic maturation and possible role as an AMPAR auxiliary subunit, it is specifically a synaptogenic molecule at excitatory synapses.

Table of Contents

List of Tables

CHAPTER 3

List of Figures

CHAPTER 3

CHAPTER 4

CHAPTER 5

CHAPTER 6

CHAPTER 1:

General Introduction

Information processing in the brain

The human brain is estimated to have billions of neurons and, between these neurons, form trillions of synaptic connections. These connections are what we have come to understand as the basic units of communication in the brain, and the signals they send mediate information processing, or as it is more commonly described, thinking. As abstract as "thinking" may be, centuries of research in neuroscience have revealed a very concrete basis for information transfer between neurons.

When activated, a neuron fires an action potential, an electrical signal that travels down the axon of the neuron. This action potential eventually reaches the presynaptic terminal, and causes a depolarization that results in the release of a synaptic vesicle into the synaptic cleft, the small space between pre- and postsynaptic neurons. Synaptic vesicles are full of neurotransmitter chemicals—e.g. glutamate, GABA, acetylcholine, dopamine—that serve as the language of neurons. When a vesicle is released, these neurotransmitters cross the synaptic cleft and activate their receptors in the postsynaptic cell, leading to an influx of ions that initiate signaling pathways specific to the receptor. Activation of certain postsynaptic receptors results in excitation of the postsynaptic neuron, generating an action potential in the cell and propagation of the signal to another neuron; activation of others results in inhibition of the postsynaptic neuron and decreases the likelihood the cell will fire an action potential and propagate the signal.

How does our ability to distinguish stimuli, to remember specific events, to carry out a complex motor task arise from just a handful of different neurotransmitters? The remarkable capacity of the brain to process enormous amounts of information is dependent upon the proper development and specialization of the trillions of synaptic

connections between neurons. Specifically, information is encoded not only in the neurotransmitter identity, but also in the diverse locations and molecular composition of synaptic connections. These properties can be modulated by adding or subtracting synaptic connections, changing the probability that a vesicle will be released following depolarization of the presynaptic terminal, altering the molecular identity of the postsynaptic receptors, modifying the biophysical properties of the existing receptors, or varying the number of postsynaptic receptors. With the added layer of complexity derived from synapse specialization, the simple processing power of neurons through action potentials and neurotransmitter release becomes exponentially greater.

The majority of fast, excitatory transmission in the brain occurs at glutamatergic synapses. There, synaptic vesicles are packed with glutamate, which can activate three different postsynaptic receptors upon release into the cleft – AMPA (AMPARs), NMDA (NMDARs), and Kainate receptors (KARs). There is mounting genetic evidence in humans that the proper development and specialization of excitatory synapses is critical to healthy neurological function, with mutations in proteins involved in this process being implicated in autism, schizophrenia, epilepsy, and bipolar disorder (Kalachikov et al., 2002; Redies et al., 2012; Sousa et al., 2010; Wang et al., 2009; Yan et al., 2005). Thus, a greater understanding of excitatory synapse development and maturation is crucial not only to our understanding of information processing, but also to our ability to successfully diagnose and treat these, often debilitating, disorders.

The function of synaptic organizing proteins

The process of excitatory synapse development is a carefully and elegantly orchestrated series of events, which we have only recently begun to understand. Beginning with axo-dendritic contact and the recruitment of multiple adhesion molecules, the first step in synaptic development is functional pre- and postsynaptic differentiation, or, synaptogenesis. Following the establishment of this nascent synapse, many more proteins act to mature, maintain, and modulate the function of these specializations over an organism's lifetime.

In the last decade, the molecular identities of many of the proteins involved in synaptic development have been uncovered. Collectively, proteins involved in this process are called synaptic organizing proteins, and can be broadly separated into three categories: transmembrane adhesion molecules, secreted factors, and cytoplasmic scaffolding proteins. At the glutamatergic synapse, these proteins come together in different combinations to confer many critical properties of the synapse, including laminar specificity, probability of glutamatergic vesicle release, and postsynaptic AMPAR content—features that impart the ability of a neuron to generate specific patterns of connectivity and modulate the strength of its synapses.

Much of the research on synaptic organizing proteins has focused on the first step in synaptic development, synaptogenesis. A number of protein families have been shown to modulate this process, including neuroligins, neurexins, LRRTMs, Cbln1, ephs, ephrins, netrin-G ligands, and netrins (Siddiqui and Craig, 2011). However, the proteins involved in synapse maturation and maintenance are less well understood. Many studies have investigated the molecular mechanisms of synaptic plasticity (Bredt

and Nicoll, 2003; Kessels and Malinow, 2009; Yang and Calakos, 2013), but it is uncertain if similar mechanisms regulate synapse development.

LGI1 is an epilepsy-associated protein that modulates synaptic strength

LGI1 was recently identified as a potential synaptic organizer through a screen for proteins that interact with PSD-95, a member of the MAGUK family of cytoplasmic scaffolding proteins known to have critical roles in synapse development and plasticity (El-Husseini et al., 2000; Kim and Sheng, 2004; Migaud et al., 1998). Functional studies of LGI1 revealed that its application to hippocampal slices increases synaptic AMPARs, but does not alter long-term potentiation. This indicates that LGI1 strengthens synapses independent of classic mechanisms of plasticity (Fukata et al., 2006), acting through an unknown pathway to modulate synaptic content. LGI1 was also found to co-purify with the potassium channel subunit Kv1.1 and prevent its inactivation by the Kvβ1 subunit when expressed in oocytes (Schulte et al., 2006). However, it is unclear how a secreted protein would alter the activity of the intracellular Kvβ1 subunit, and if the observed effect on inactivation has any impact on synaptic transmission.

The protein domain structure of LGI1 indicates it may mediate a number of protein interactions. Following the N-terminal signal peptide, LGI1 has 4 LRR repeats, found in many synaptic organizing proteins (Siddiqui and Craig, 2011), followed by 7 EPTP domains, predicted to fold into a β-propeller structure (Kegel et al., 2013). Biochemical data indicate that the EPTP domains of LGI1 directly bind a disintegrin and metalloproteases 22 and 23 (ADAM22 and ADAM23), transmembrane proteins located diffusely along the dendrite and axon (Fukata et al., 2006). It is possible that LGI1 acts

through these transmembrane proteins to regulate transmission, though the function of ADAMs at the synapse has yet to be studied.

ADAM22 and ADAM23 are potential synaptic organizing proteins

ADAM22 and ADAM23 are catalytically inactive members of the ADAM family of metalloproteases (Novak, 2004; Sagane et al., 2005). They are single pass transmembrane proteins with disintegrin, cysteine-rich, and EGF-like domains in their extracellular region. ADAM22 has an SH3 binding site and PDZ-binding motif in its intracellular C-terminus, which has been shown to interact with the third PDZ domain of PSD-95 (Fukata et al., 2006) and is potentially indicative of a role in regulation of postsynaptic transmission. Moreover, along with LGI1, ADAM22 is also found in complex with Kv1.1, suggesting it may regulate presynaptic release as well. Though data on ADAM23 interactions with synaptic proteins are lacking, in mice, deletion of ADAM22 or ADAM23 results in a similar lethal epilepsy phenotype (Mitchell et al., 2001; Sagane et al., 2005), indicating that both of these proteins may have parallel, critical synaptic functions.

LGI1-ADAM complex in health and disease

Like many of the previously identified synaptic organizing proteins, mutations in *LGI1* and *ADAM* genes have been implicated in a number of neurological disorders. LGI1 was initially identified as a potential tumor suppressor due to its decreased expression in malignant gliomas, though further research indicated that LGI1 expression in all glial

cells is very low (Malatesta et al., 2009; Morante-Redolat et al., 2002; Piepoli et al., 2006; Senechal et al., 2005), resulting in a shift away from this research focus. More recently, however, LGI1 has become of clinical interest again, this time in relation to a hereditary form of epilepsy. Mutations in *LGI1* were found to be associated with human autosomal dominant temporal lobe epilepsy (ADTLE), a disorder characterized by frequent partial seizures with auditory auras (Ottman et al., 1995; Winawer et al., 2000). Linkage analysis in ADTLE families identified over 30 different mutations in *LGI1* in individuals afflicted by the disease, most of which disrupt secretion of the protein (Kalachikov et al., 2002; Kawamata et al., 2010; Morante-Redolat et al., 2002; Striano et al., 2008). Moreover, mutations in *ADAM23* have been implicated in canine epilepsy (Seppala et al., 2012), though its connection to human epilepsy remains unexplored. More recently, the role of LGI1 in epileptic disorders has been expanded by the discovery of antibodies against LGI1 in patients with autoimmune limbic encephalitis (Irani et al., 2010; Lai et al., 2010), which produces cognitive deficits, like amnesia, in addition to seizures. Finally, there is evidence in one family that mutations in *LGI1* are associated with hyperactivity (Berghuis et al., 2013), a finding that indicates *LGI1* mutations may have more diverse effects than currently appreciated.

Among genes associated with human epilepsy syndromes, *LGI1* is unusual in that it does not code for an ion channel subunit, but rather for a secreted protein (Noebels, 2003; Steinlein, 2004). Similarly, research on limbic encephalitis has largely focused on ion channel dysfunction (Dalmau et al., 2008; Lai et al., 2009; Lai et al., 2010). Thus, a deeper understanding of the function of the LGI1-ADAM complex may lead to novel treatment pathways for individuals afflicted with ADTLE, limbic encephalitis, and hyperactive disorders.

SynDIG1 is an AMPAR-interacting protein that may organize synapses

A subset of synaptic organizing proteins bind glutamate receptors directly, including LRRTM2 and Cbln1—molecules that induce synapse formation (de Wit et al., 2009; Linhoff et al., 2009; Matsuda et al., 2010; Uemura et al., 2010)—and neuronal pentraxins—which cluster AMPARs at the synapse (Koch and Ullian, 2010; Sia et al., 2007). Recently, synapse differentiation induced gene 1 (SynDIG1), a type II transmembrane protein, was identified as a gene highly upregulated during synapse development (Diaz et al., 2002). Further research on SynDIG1 showed that it directly interacts with the AMPAR subunits GluA1 and GluA2 in heterologous cells and copurifies with these receptors in the brain. Modulation of SynDIG1 expression in dissociated hippocampal cultures altered both mEPSC amplitude and frequency, and caused corresponding changes in synaptic AMPAR puncta density and size. However, overexpression of SynDIG1 did not affect NR1 or VGLUT distribution, leading the authors to conclude that SynDIG1 regulates synapse unsilencing and strengthening (Kalashnikova et al., 2010).

In this study, SynDIG1 was also found to impact the surface expression of AMPARs (Kalashnikova et al., 2010), which suggests a role in AMPAR trafficking or stabilization. It is unclear then if the previously described effect of SynDIG1 on synaptic transmission is the result of a synaptic targeting deficit or an overall decrease in available AMPARs at the surface. A key feature of the previously identified AMPAR auxiliary subunits—TARPs, CNIHs, and CKAMP44—is their regulation of surface trafficking of AMPARs (Jackson and Nicoll, 2011). Like SynDIG1, these auxiliary subunits are all transmembrane proteins that bind directly to AMPARs. However, no characterization of the biophysical impact of SynDIG1 association with AMPARs has

been carried out. Thus the question remains, is SynDIG1 an auxiliary subunit, a synaptic organizing protein, or perhaps both?

The aim of my graduate work was to elucidate the roles of recently discovered proteins thought to impact synapse development. Specifically, I characterized the regulation of excitatory transmission by secreted LGI1, transmembrane ADAMs 22 and 23, and the AMPAR-interacting protein SynDIG1. In chapter 3, I describe initial work analyzing the LGI1 interactome, and provide evidence for its coordination of a transsynaptic complex including ADAM22, ADAM23, and intracellular MAGUKs. I also show that deletion of *LGI1* results in decreased strength of excitatory synapses and seizures, the first evidence of a direct link between loss of functional LGI1 and epilepsy. In chapter 4, I extend these findings and demonstrate a requirement for ADAM22 and ADAM23 in maintenance of excitatory synapses, and show that LGI1 acts as a paracrine signal released from the pre- and postsynaptic cell to modulate AMPAR-content via intracellular ADAM-MAGUK interactions. Finally, in chapter 5, I describe the role of SynDIG1, a recently identified AMPAR-interacting protein, in synaptogenesis and synaptic maintenance, and rule out its potential role as a novel AMPAR auxiliary subunit.

CHAPTER 2:

Methods

Mouse genetics

All animals were housed according to the IACUC guidelines at the University of California, San Francisco.

For construction of the LGI1$^{-/-}$ targeting vector, a 11.2kb region containing exon 1 - 2 was subcloned from C57BL/6 BAC clone (RPCI-23-127G7) into pSP72 backbone vector (Promega) using a homologous recombination-based technique. The Neo cassette replaces 1.9kb of the region including exon 1 – 2, resulting in the long homology arm (7.5 kb long) on the 5′ side of exon 1 and the short homology arm (1.8 kb long) on the 3′ side of exon 2. The targeting vector was linearized and electroporated into iTL BA1 hybrid (C57BL/6 x 129/SvEv) embryonic stem cells. ES cell clones with the targeted *LGI1* locus were injected into C57BL/6 blastocysts. The chimeras were crossed into C57BL/6 for germ line transmission by iTL Inc. (New York). The genotypes were determined by Southern blotting or PCR using PCR primers: 5′-CCTCTTGCATGCCTGACCATTTGA-3′ and 5′-AGAAGGCTTATCCGAATACATGCC-3′ for the WT allele; 5′-AGCGCATCGCCTTCTATCGCCTTC-3′ and 5′-AGAAGGCTTATCCGAATACATGCC-3′ for the targeted alleles.

To specifically express LGI1 in the hippocampal dentate gyrus, we took advantage of prospero homeobox 1 (Prox1) promoter (kindly suggested by Drs. Sebastian Jessberger at University of Zurich and Ryuta Koyama at The University of Tokyo). The cDNAs of rat LGI1 tagged with FLAG and His x 6 (LGI1-FH) (Fukata Y et al PNAS 2010) and kanamycin resistant gene were inserted at the locus of the start codon of a Prox1 gene in the Prox1 containing BAC clone (RP23-360I16) by Red/ET recombination system (gene bridges). This linearized modified BAC DNA was

microinjected into C57BL/6 oocytes to produce transgenic mice (PhoenixBio). Genotyping was performed using PCR primers: 5′-GCTTGACCAGATTCATTGGCGACT-3′ & 5′-CTAATGGTGATGGTGATGATGACC-3′ for LGI1-FH. To visualize the Prox1-promoter driven LGI1, the LGI1-FH (Tg^{prox1}) transgenic mouse was crossbred with an $LGI1^{+/-}$mouse. Obtained $LGI1^{+/-}$; Tg^{prox1} was crossed with $LGI1^{+/-}$ to obtain $LGI1^{-/-}$;Tg^{prox1}. Immunohistochemical analysis of LGI1 (at P17) was performed as described previously (Fukata Y et al PNAS 2010).

ADAM22$^{fl/fl}$ mice were generated and genotyped as previously described(Ozkaynak et al., 2010). *ADAM22*$^{-/-}$ mice were generated by crossing the *ADAM22*$^{fl/fl}$ line with mice expressing Cre recombinase driven by the beta-actin promoter (βactin-Cre). Mice were determined by PCR to be ADAM22$^{-/-}$ using the forward primer 5′-TGCACTCAAGGCATGGTCTC-3′ and the reverse primer 5'-CTGCACTCCTCATCACCTTA-3'.

Cloning and plasmid construction

LGI1 and ADAM22 constructs were cloned by Masaki and Yuko Fukata as previously described (Fukata et al., 2006). For biolistic expression, LGI1, ADAM22, and ADAM22 mutants were subcloned into the into the NheI and XmaI sites of pCAGGS-IRES-mCherry vector using PCR and In-Fusion® HD Cloning System (Invitrogen). LGI1 used in lentivirus was subcloned into FUGW-GFP-IRES so that infected cells could be readily identified. pCAGGS-PSD95-IRES-GFP was a generous gift from Jon Levy. ADAM23 shRNA was generated using a previously described shRNA targeting sequence, AAGTGCCTACAGATTCAAGCC (Sun et al., 2007), which was inserted

behind the H1 promoter of a GFP expressing FHUGW vector using the AscI and BstbI sites.

The following cDNAs were cloned from brain total RNA by RT-PCR using primers based on the GenBank databases: mouse LGI2B (AY841361), rat LGI3 (NM_001107277), mouse LGI4 (NM_144556), rat ADAM11 (NM_009613), rat $Kva_{1.1}$ (NM_173095), rat $Kva_{1.2}$ (NM_012970), rat Kvb_2 (NM_017304) and mouse NPAS4 (NM_153553). All PCR products were analyzed by DNA sequencing. LGI subfamily members were subcloned into pCAGGS-FLAG. ADAM11, $Kva_{1.1}$ and $Kva_{1.1}$ were subcloned into a cytomegalovirus promoter-driven vector. Kvb_2 was subcloned into pEF-Bos-myc. To obtain LGI1-FH and LGI3-FH, LGI1 and LGI3 were subcloned into the EcoRI and BamHI sites of pcDNA3.1-FLAG-His, respectively, which was generated by inserting a synthetic DNA fragment obtained by annealing sense synthetic nucleotide 5′-GATCCGAATTCGACTACAAGGATGACGACGACAAGGGAGGTCATCATCACCATCACCATTAGC-3′, and antisense nucleotide 5′-TCGAGCTAATGGTGATGGTGATGATGACCTCCCTTGTCGTCGTCATCCTTGTAGTCGAATTCG-3′ into BamHI and XhoI sites of pcDNA3.1 (+). Other LGI1 and ADAMs constructs were described previously(Fukata et al., 2006).

The SynDIG1 sequence from mouse (Accession number BC147352) was purchased from Open Biosystems, amplified and from the pCR4-TOPO vector (*sense primer* 5′ ctcaagcttcgaattcgccaccATGGATGGCATCATTGAGC A 3′, *antisense primer* 5′ ccgcggtaccgtcgacTCACAGGTGGTTGTTTTTGG 3′), and inserted into the pIRES2-EGFP and pIRES2-DsRed vectors (Clontech) for expression in HEK cells and cultured slices. To knockdown SynDIG1 expression, we used an shRNA sequence (GCTGTGGCCAAAGGAGAC) that was previously verified by Kalashnikova et al.

(Kalashnikova et al., 2010). Initially the shRNA oligo was cloned into pSuper (Oligoengine) and then transferred into the FUGW vector (Addgene). To control for off target effects of the shRNA, the shRNA construct was co-expressed with an RNAi proof form of SynDIG1, containing three point mutations in the target region (GCCGTGGCCAAGGGGGAC). RNAi proof SynDIG1 was cloned into pIRES2-DsRed to be able to detect expression of both shRNA (EGFP) and RNAi proof target (DsRed) by using different fluorophores.

Antibodies

The following antibodies were used: rabbit polyclonal antibodies to LGI1 (Abcam), ADAM23 (Abcam), HA (Santa Cruz Biotechnology), SAP102(El-Husseini Ael et al., 2002), $Kv_{1.1}$a (SIGMA), and c-fos (Santa Cruz Biotechnology); and mouse monoclonal antibodies to PSD-95 (MA1-046, Affinity Bioreagents), FLAG (M2, SIGMA), HA (HA.11, Covans), $Kv_{1.1}$a (K20/78, NeuroMab), $Kv_{1.2}$a (K14/16, NeuroMab), Na^+K^+ATPase a3 (XVIF9-G10, Novus Biologicals), N-cadherin (BD Biosciences). Rabbit polyclonal antibodies to ADAM22 and NPAS4 were raised against GST-ADAM22 (aa 858-898) and His-NPAS4 (aa 626-802), respectively. Antisera were affinity purified on CNBr-activated sepharose 4B (GE Healthcare, Buckinghamshire, UK) column containing immunizing antigens.

Immunoaffinity purification of LGI1-FH

LGI1-FH expressed in HEK293 cells (one 10-cm plate) was tandemly purified using anti-

FLAG M2 agarose and Ni^{+}-NTA agarose. HEK293 cells were extracted with buffer A (20 mM Tris-HCl [pH 7.4], 150 mM NaCl, 1% TritonX-100, and 50 μg/mL PMSF) containing 20 mM imidazole. After centrifugation at 20, 000 x g for 1 h, the supernatant was incubated with 75 μl of FLAG-M2 agarose (SIGMA) for 2 h, washed with buffer A six times and eluted with 375 μl of buffer A containing 0.25 mg/mL FLAG peptide and 20 mM imidazole. The eluate was mixed with 75 μl of Ni^{+}-NTA agarose (QIAGEN, Venlo, Netherlands) for 2 h and washed with buffer A containing 20 mM imidazole four times. The final eluate was obtained with 250 μl of 250 mM imidazole in buffer A.

For purification of LGI1-FH from the transgenic mouse, brains from one wildtype or transgenic mouse were homogenized with buffer B (10 mM Tris-HCl [pH 8.0], 5 mM EDTA, 320 mM sucrose, and 100 μg/mL PMSF). P2 membrane fractions were solubilized with buffer A for 1 h. After centrifugation at 100,000 x g for 1 h, the supernatant was incubated with 75 μl of FLAG-M2 agarose for 2 h, washed with buffer A six times, and eluted with 375 μl of buffer A containing 0.25 mg/mL FLAG peptide and 20 mM imidazole. The eluate was mixed with 50 μl of Ni^{+}-NTA agarose for 1 h and washed with buffer A containing 20 mM imidazole four times. The final eluate was obtained with 250 μl of 250 mM imidazole in buffer A. Purified proteins were separated by SDS-PAGE and subjected to silver staining or Western blotting. For reprecipitation of ADAM22, ADAM23, or Kva1.1, the eluate from FLAG-M2 agarose was incubated with anti-ADAM22, anti-ADAM23, or anti-Kva1.1 antibody, and then with protein A sepharose (GE Healthcare). For quantitative Western blotting, blotted membranes were scanned with Light-Capture II (ATTO, Tokyo, Japan), and the optimal specific band was analyzed with the CS Analyzer 3.0 software (ATTO). Purified LGI1-FH from transfected HEK293 cells was quantitated by Coomassie brilliant staining using bovine serum

albumin for calibration.

For immunoprecipitation of endogenous ADAM22 or ADAM23, one mouse brain was homogenized in buffer C (320 mM sucrose, 20 mM Tris, pH 8.0, and 2 mM EDTA) containing 200 mg/ml PMSF. Homogenates were spun at 20,000 *g* for 1 h and pellets were resuspended in buffer D (20 mM Tris, pH 8.0, 1 mM EDTA, and 1.3% Triton X-100). The lysates were spun at 100,000 *g* for 1 h. Precleared lysates (5 mg protein) were immunoprecipitated with 5 μg of antibodies. Immunoprecipitates were separated by SDS-PAGE and gels subjected to Western blotting.

Mass spectrometry

For the in-gel digestion, the specific protein bands were excised from a silver- stained gel, reduced with dithiothreitol, and alkylated with iodoacetamide. Band slices were digested with trypsin (12 μg/mL) overnight and desalted with ZipTip C18 (Millipore). For the in-solution digestion, the method is basically followed as described(Yoshimura et al., 2004). Briefly, the eluates from tandem purification were concentrated by trichloroacetic acid precipitation. The samples were reduced with dithiothreitol and alkylated with iodoacetamide. The S-carbamoylmethylated proteins were precipitated by the methanol-chloroform precipitation. Precipitated protein was solubilized in 1.2 M urea and 80 mM Tris-HCl (pH 8.5) and digested with trypsin overnight. The obtained peptides were then separated via nano-flow liquid chromatography (nanoLC) (Paradigm MS4, AMR, Tokyo, Japan) using a reverse-phase C18 column. The LC eluent was coupled to a micro ion spray source attached to a LCQ Advantage or Fleet mass spectrometer (Thermo Fisher Scientific, Waltham, MA). For protein identification and

semi-quantification, we used the cross-correlation score (XC) of the SEQUEST algorithm from BioWorks software (Thermo Fisher Scientific). The specificity was determined by subtracting the results obtained from wild-type mice.

Subcellular fractionation

A mouse brain was homogenized in buffer C. The homogenate was centrifuged for 1 h at 20,000 x g to produce a pellet (P2) and the pellet was homogenized in buffer D (20 mM Tris, pH 8.0, 1 mM EDTA, and 1.3% Triton X-100). The resuspended P2 fraction was centrifuged at 100,000 x g for 1 h to produce a supernatant (P2 sol) and a pellet. The pellet (P2 insol) was resuspended into equal volume with "P2 sol". Each fraction was subjected to quantitative Western blotting as described above. For the Supplemental Fig. 2c, we followed the procedure as described previously(Carlin et al., 1980).

Immunofluorescence analysis

For cell-surface binding assay, COS7 cells were seeded onto three 12-mm cover slips in each well of a six-well cell culture plate (3×10^5 cells/well) and co-transfected with LGIs-FLAG and ADAM22-GFP. 24 h after transfection, cells were fixed with 4% paraformaldehyde at room temperature for 10 min and blocked with PBS containing 2 mg/ml bovine serum albumin (BSA) for 10 min on ice. The fixed cells were stained with anti-FLAG antibody without permeabilization, followed by Cy3-conjugated secondary antibody.

Cultured hippocampal neurons (5×10^4 cells) were seeded onto 12-mm cover slips.

The neurons (DIV21) were transfected with Thy1:LGI1-FH by Lipofectamine 2000. Transfected neurons were fixed with 2% paraformaldehyde/100 mM HEPES (pH 7.4) at room temperature for 20 min and blocked with PBS containing 10 mg/mL BSA for 10 min on ice. Surface-bound LGI1 was stained with anti-FLAG antibody, followed by Cy3-conjugated secondary antibody. Fluorescent images were taken with a confocal laser scanning microscopy system (LSM5 Exciter, Carl Zeiss) equipped with a Plan Apochromat 63×/1.40 NA oil immersion objective lens. Microscope control and all image analysis were performed with Carl Zeiss ZEN software.

Immunohistochemistry

Littermate mice (P17-19) were anesthetized and perfused with 4% PFA in 0.1 M phosphate buffer (PB, pH 7.4). The brain was removed and immersed in the same fixative for 4 h at 4°C and then cryoprotected in 20% sucrose in PBS overnight at 4°C. 60-μm free-floating sections were cut on a cryostat (Leica CM1950). Sections were pretreated with 2 mg/ml pepsin (DAKO)(Fukaya and Watanabe, 2000). Sections were blocked for 1 h in PBS containing 3% normal goat serum and 0.3%TritonX-100 at room temperature, and then incubated in the same buffer containing indicated antibodies (1 μg/ml) overnight at 4°C. Endogenous peroxidase activity was inactivated by incubating brain sections in 1% H_2O_2 for 30 min. Immunohistochemical staining was performed with an avidin/biotin/peroxidase system (ABC Elite; Vector Laboratories) and DAB (Vector Laboratories).

Preembedding peroxidase immunoelectron microscopy

Animals were anaesthetized and perfused with an ice-cold fixative containing 4% paraformaldehyde, 0.05% glutaraldehyde, 15% saturated picric acid, and 0.1 M PB for 12 min. The brains were immediately removed and the tissue blocks containing hippocampus were cut on a vibratome (Leica VT1000S, Wetzlar, Germany) into 50-μm-thick sections and collected in 0.1 M PB. Free-floating sections were pretreated with 2 mg/ml pepsin (DAKO)(Fukaya and Watanabe, 2000) and then blocked in 10% normal goat serum (NGS) diluted in 50 mM Tris HCl (pH 7.4) and 0.9% NaCl (TBS, pH 7.4) for 1 hr. at room temperature followed by sequential incubation with rabbit anti-LGI11 antibody (1–2 μg/ml in TBS containing 1% NGS) for 48 hr. at 4°C, and biotinylated goat anti-rabbit antibody (1:100; Vector Labs, Burlingame, CA) for 4 hr. at RT. After several washes in PBS, the sections were postfixed in 1% glutaraldehyde diluted in the same buffer for 10 min. After washing with PBS and TBS, the sections were incubated with ABC complex (1:100, ABC Elite Kit, Vector Labs) for 2 hr. and then DAB-H2O2 solution. After treatment with 1% osmium tetraoxide in 0.1 M PB, the sections were stained with uranyl acetate, dehydrated in graded series of ethanol, and flat-embedded on glass slides in Durcupan resin (Fluka, Buchs, Switzerland). Regions of interest were cut at 70 nm thickness on an ultramicrotome (Leica) and collected on grids. Ultrastructural analyses were performed with JEM1010 transmission electron microscope (JEOL, Japan). To test the specificity of immunolabeling for LGI1 with EM, sections from LGI1 null mouse were also processed. Under this condition, no selective labeling was observed.

Staining with AP fusions

LGI1-AP was prepared as described previously(Fukata et al., 2006). COS7 cells transfected with ADAMs were washed with Hank's balanced salt solution containing 0.5 mg/ml BSA and 20 mM Hepes, pH7.4 (HBH) and incubated for 90 min at 25°C with LGI1-AP. The cells were then washed with HBH, fixed with 4% paraformaldehyde for 15 min, and incubated for 100 min at 65°C to inactivate endogenous phosphatase activity. The cells were stained by 5-bromo-4-chloro-3-indolyl phosphate (BCIP) and nitroblue tetrazolium (NBT) solution (DAKO cytomation) for several hours to visualize AP activity. The reaction was stopped by the addition of PBS.

mRNA expression analysis

Microarray analysis was performed on brain tissues from P13-14 wildtype (n = 2) or LGI1 knockout mice (n = 3). Brain tissues were lysed in TRIZOL reagent (Invitrogen), and total RNA was subsequently isolated from the aqueous phase using an RNeasy kit (QIAGEN). The KURABO Industries performed cDNA amplification, labeling, and hybridization to Mouse Genome 430 2.0 array chips (Affymetrix). Data were analyzed with DNA Microarray Viewer (Affymetrix).

Lentivirus production

To create the LGI1 lentivirus, 3 T-75 flasks of rapidly-dividing HEK293T cells (ATCC) were transfected with FUGW-GFP-IRES-LGI1 and the helper plasmids pVSV-G and psPAX2 using FuGENE HD (Promega). After 40 hours of incubation, the supernatant was collected, filtered and concentrated using PEG-it Virus Precipitation Solution

(System Biosciences). The resulting pellet was resuspended in 400 μL Opti-mem, flash-frozen in liquid nitrogen, and stored at -80° C.

In utero electroporation

At E15.5, ADAM22$^{fl/fl}$ mice were anesthetized with 2.5% isoflurane and oxygen and injected with buprenorphine for analgesic. The uterus was temporarily removed from the abdomen and the left ventricle of embryos were injected with 2 μl of mixed plasmid DNA each via a beveled micropipette. pCAGGS-Cre:mCherry was typically diluted to approximately 0.5 μg/μl in 2–3 μg/μl of the replacement pCAGGs-ADAM22 plasmids. Embryos were then individually electroporated with 5x50 ms, 35 volt pulses, with the positive electrode placed against the lower right hemisphere and the negative electrode placed against the upper left hemisphere. Following electroporation, the uterus was placed back into the abdomen and the wound was sutured.

Acute slice preparation

Transverse hippocampal slices (300 μm) were obtained from P14-P15 mice with a Leica vibratome in a high sucrose cutting solution containing (in mM): NaCl 50, KCl 2.5, $CaCl_2$ 0.5, $MgCl_2$ 7.0, NaH_2PO_4 1.0, $NaHCO_3$ 25, glucose 10 and sucrose 150. Slices were transferred to artificial cerebrospinal fluid (ACSF) containing (in mM) NaCl 119, KCl 2.5, $NaHCO_3$ 26.2, Na_2PO4 1, glucose 11, $CaCl_2$ 2.5, $MgCl_2$ 1.3 in an incubating chamber, recovered at 35° C for 30 minutes, then moved to room temperature for the duration of the experiment.

Slice culture preparation and transfection

Hippocampal slice cultures were prepared from 6- to 8-day-old Sprague Dawley rats or mice as previously described (Stoppini et al., 1991). At 4 days *in vitro,* for overexpression experiments, or 1 day *in vitro*, for RNAi-mediated knockdown, slice cultures were transfected using a Helios Gene Gun (BioRad). For biolistic transfection, 50 ug total of each construct was coated on 1 uM-diameter gold particles, which were then coated onto PVC tubing and stored at 4 degrees. For experiments where bullets were coated with two different constructs, co-expression was visually confirmed by using different fluorophores for each construct.

Slice culture viral injections

LGI1-expressing lentivirus was introduced into slice cultures using a microinjection technique. Virus was loaded into a glass pipette, and 2.3 nL was injections were made into slices using a Micro4 microsyringe pump (WPI). Injections sites were visualized under 10x magnification and confirmed by visible depression of the slice culture after injection burst. For both CA3 and dentate gyrus, three injections were made into the region to ensure robust coverage.

Slice electrophysiology

Recordings were made using 3–4 MΩ glass electrodes filled with an internal solution consisting of 135 mM $CsMeSO_3$, 8 mM NaCl, 10 mM Hepes, 4 mM Mg-ATP, 0.3 mM Na-GTP, 0.3 mM EGTA, 5 mM QX314-Cl, and 0.1 mM spermine, pH 7.2 with CsOH.

External perfusion medium consisted of 140 mM NaCl, 2.4 mM KCl, 1 mM NaH_2PO_4, 26.2 mM $NaHCO_3$, and 10 mM glucose, and 100 μM picrotoxin, saturated with 95% O_2 and 5% CO_2. In rat slice culture recordings, 10 μM gabazine was included as well. For acute slice recordings, 2.5 mM $CaCl_2$ and 1.3 mM $MgSO_4$ was added to the external solution; for slice culture recordings, 4 mM $CaCl_2$ and 4 mM $MgSO_4$ were added. Transfected pyramidal cells were identified using fluorescence microscopy. In all paired experiments, transfected and neighboring control neurons were recorded simultaneously.

For synaptic recordings, a bipolar stimulating electrode was placed in stratum radiatum. After gaining whole cell access, cells were held at -70mV and stimulated for 5 minutes to allow for response stabilization. After this period, 20 trials were obtained at 0.2 Hz while holding the cells at −70 mV, followed by 20 trials at +40 mV. AMPA EPSCs were measured as the peak amplitude of the averaged traces recorded at -70 mV, and the NMDA EPSC was measured at +40 mV as the average amplitude of the current 100 ms after stimulation, at which the AMPA receptor mediated EPSC has completely decayed. Series resistances typically ranged from 10 to 20 MΩ; a cell pair was discarded if the series resistances differed substantially between the two cells. For coefficient of variation analysis, 100 trials were acquired at -70 mv. Paired-pulse ratios were obtained by recording the responses to a pair of stimuli given 40ms apart. The two resulting EPSCs were measured and the peak amplitude of the second EPSC divided by the peak amplitude of the first EPSC gives the paired-pulse ratio. Miniature excitatory postsynaptic currents (mEPSCs) were obtained in the presence of 1 μM Tetrodotoxin (Tocris Bioscience). Surface AMPAR EPSCs were elicited by local application of 500 nM S-AMPA (Abcam Biochemicals) and 50 μM cyclothiazide simultaneously to neighboring neurons for .5 ms.

Outside-out patches were taken from CA1 pyramidal neurons by patching the cell bodies with 4-5 MΩ patch pipettes. After obtaining whole-access and clamping the cell to -70 mV, the patch pipette was slowly pulled away from the cell body until a gigaohm seal reformed. The tip of the pipette was perfused with HEPES-ACSF containing (in mM): 150 NaCl, 2.5 KCl, 10 HEPES, 10 glucose, 1 $MgCl_2$, 2 CaCl1, 0.1 D-AP5, 0.1 picrotoxin, 0.1 cyclothiazide, and 0.5 μM TTX. To evoke glutamate currents, the solution was switched to HEPES-ACSF containing 1 mM L-glutamic acid. A ValveLink 8 (AutoMate Scientific Inc.) was used for fast perfusion of the control and glutamate containing HEPES-ACSF. Outside-out patches from experimental cells were interleaved with non-transfected control neurons to ensure the most consistent and direct comparisons.

HEK cell transfection

HEK cells were used for expression of GluA1(Q)flip, GluA2(Q)flip, SynDIG1 and TARP γ-2. The cells were cultured in a 37 °C incubator supplied with 5% CO_2. Transfection was performed in 6-well plates using lipofectomine2000 reagents according to the manufacturer's protocol (Invitrogen). For co-expressions, the ratio of GluA2 to SynDIG1 or TARP γ-2 cDNA was 1:1. After 2–3 h, PBS was used to stop the transfection. Cells were immediately dissociated with 0.05% trypsin and plated on coverslips pretreated with poly-D-lysine (BD Bioscience). To avoid cell death due to activation of exogenous glutamate receptors, the medium was supplemented with the competitive AMPAR antagonist NBQX (50 μM, Tocris Bioscience).

HEK cell electrophysiology

Recordings were made 1-2 days after transfection, using 4-5 MΩ glass electrodes filled with an internal solution consisting of 135 mM CsF, 2 mM $MgCl_2$, 1 mM $CaCl_2$, 10 mM Hepes, 11 mM EGTA, and 0.1 mM spermine, pH 7.4. External perfusion medium consisted of 140 mM NaCl, 5 mM KCl, 5 mM EGTA, 1.4 mM $MgSO_4$, 1 mM NaH_2PO_4, 10 mM glucose, and 10 mM Hepes, pH 7.2. Agonists were applied in the presence of 100 μM cyclothiazide (Abcam Biochemicals) to inhibit AMPAR desensitization. 15 sec pulses of 1mM glutamate (Abcam Biochemicals) or 1 mM kainate (Sigma) were applied to record whole cell current amplitudes.

Current voltage relationships were recorded from outside-out patches of transfected cells under the same conditions used to obtain whole cell current responses. Prior to recording a ramp, the patch was held at -100 mV for 50 ms. The voltage was then ramped up to +100 mV at a rate of 2 mV/ms. Ramp sweeps were recorded before and during agonist application and at least 5-10 ramp sweeps from each condition averaged. To subtract background leak conductance, the average ramp sweep before agonist application was then subtracted from the average ramp sweep recorded during agonist application. The resulting current voltage relationships from 2-5 patches were averaged and plotted.

Fast responses to glutamate were recorded from outside-out patches using the following internal solution: 135 mM KF, 33 mM KOH, 2 mM $MgCl_2$, 1mM $CaCl_2$, 11 mM EGTA, 10mM Hepes, and 0.1 mM spermine, pH 7.2. Glutamate (1 mM) pulses of 1 ms were applied to patches every 5 s using a piezoelectric controller (Siskiyou). To measure the kinetics of AMPA receptor deactivation we fitted the peak-normalized currents as a

single weighted decay and calculated the rate of deactivation from the area under peak-normalized currents as described in a previous study (Kato et al., 2007). Statistical significance was calculated using the Wilcoxon-Mann-Whitney test for unpaired data (Kaleidagraph).

Confocal imaging

Images were acquired using a Zeiss LSM 5 Pascal scanning confocal microscope. For SynDIG1 experiments, hippocampal slices were imaged at DIV 7-8, corresponding to 3-4 days of SynDIG1 overexpression or 6-7 days of SynDIG1 knockdown. In the ADAM22 conditional knockout, imaging was carried out at DIV17-21 to allow for complete turnover of existing ADAM22 after Cre-mediated deletion. For quantification of spine density, 100µm of the primary apical dendrite of transfected CA1 cells were imaged starting 100µm away from the soma. To ensure bright enough fluorescence to visualize spines, a vector driving mCherry or GFP expression under the strong hybrid CAG promoter (pCAGGS) was co-transfected with SynDIG1, SynDIG1 shRNA, and Cre. Double fluorescence was imaged to verify expression of both constructs. Spine density was quantified manually using ImageJ software.

Statistical analysis

Sample size (n) for all evoked data refers to number of pairs. All statistical analyses were preformed in Prism 5 (GraphPad). Paired-recording statistics were calculated using the Wilcoxon signed-rank test, while unpaired recording statistics were calculated

using the Wilcoxon-Mann-Whitney test. Statistics on spine density analysis also employed the Wilcoxon-Mann-Whitney test. Coefficient of variation was calculated as the square of the variance over the mean.

CHAPTER 3:

Disruption of LGI1-linked synaptic complex causes abnormal synaptic transmission and epilepsy

Introduction

Affecting 1-2% of the population, epilepsy is one of the most common neurological disorders. Epilepsy is characterized by recurrent unprovoked seizures and is caused by disturbances in the delicate balance between excitation and inhibition in neural circuits (Noebels, 2003; Steinlein, 2004). Recent human genetic studies establish the channelopathy concept for idiopathic (inherited) epilepsies: Many of the genes whose mutations cause human epilepsy encode ion channel subunits (Noebels, 2003; Reid et al., 2009; Steinlein, 2004). Examples include voltage-gated ion channels (K^+, Na^+, Ca^{2+} and Cl^- channels) and ligand-gated ion channels (nicotinic acetylcholine and $GABA_A$ receptors), which regulate neuronal excitability.

Leucine-rich glioma inactivated 1 (LGI1) is the unique human epilepsy-related gene that does not encode an ion channel subunit (Gu et al., 2002; Kalachikov et al., 2002; Morante-Redolat et al., 2002; Ottman et al., 2004), but is a neuronal secreted protein (Nishino et al., 2010) Mutations in LGI1 are linked to autosomal dominant partial epilepsy with auditory features (ADPEAF, also known as autosomal dominant lateral temporal epilepsy [ADLTE]), which is an inherited epileptic syndrome characterized by partial seizures with acoustic or visual hallucinations. So far, over 30 LGI1 mutations have been described in familial ADPEAF patients and sporadic cases (Nobile et al., 2009). Interestingly, at least 6 tested ADPEAF mutations all abolish LGI1 secretion (Fukata et al., 2006; Senechal et al., 2005)

Recent proteomic analysis identified LGI1 as a subunit of presynaptic Kv_1 (shaker type)-voltage gated potassium channels (Schulte et al., 2006). Using the *Xenopus* oocyte expression system, it was shown that LGI1 selectively prevents inactivation of the

Kv_1 channel mediated by a cytoplasmic regulatory protein, Kvb. Because LGI1 is a secreted protein, it remains unclear how LGI1 modulates a cytosolic potassium channel mechanism. LGI1 was also isolated from the brain as a component of a protein complex mediated by PSD-95, a representative postsynaptic scaffolding protein. LGI1 functions as a ligand for the epilepsy-related ADAM22 transmembrane protein, which is anchored by PSD-95, and LGI1 enhances AMPA-type glutamate receptor (AMPAR)-mediated synaptic transmission in hippocampal slices (Fukata et al., 2006). In contrast to the roles of LGI1 in synaptic transmission, an alternative hypothesis that LGI1 regulates neuronal development was proposed by analyzing transgenic mice carrying the human ADPEAF mutation 835delC, which truncates the C-terminal EPTP domain of LGI1 (Zhou et al., 2009). Thus, the physiological function of LGI1 in the brain remains controversial. Another uncertainty is how LGI1 mutations contribute to epileptogenesis, either by haploinsufficiency or in a dominant-negative manner.

Here, we found that loss of LGI1 in mice ($LGI1^{-/-}$) causes specific lethal epilepsy and that heterozygous mice for LGI1 mutation ($LGI1^{+/-}$) show seizure susceptibility. We identified two epilepsy-related proteins, ADAM22 and ADAM23, as the major LGI1 receptors in the brain. Extracellulary secreted LGI1 links these two receptors and organizes a *trans*synaptic protein complex including both pre- and postsynaptic proteins. Reduction in this protein linkage is strongly associated with the epileptic phenotype. Loss of LGI1 selectively reduces AMPAR -mediated synaptic transmission. Thus, we propose that LGI1 is a unique antiepileptogenic secreted protein, which connects pre- and postsynaptic protein complexes for finely tuned synaptic transmission.

Results

Loss of LGI1 gene in mice specifically causes the epileptic phenotype

To define the physiological roles of LGI1 in the brain, we targeted disruption of the mouse LGI1 (Figure 1) and confirmed the absence of LGI1 protein by Western blotting (Figure 2A). LGI1 mutant mice were born at the expected Mendelian ratios without apparent anatomical defects. Homozygous null LGI1$^{-/-}$ mice showed growth failure beginning around postnatal day 14 (P14) (Figure 3). All LGI1$^{-/-}$ mice showed spontaneous recurrent generalized seizures after P14, with a sudden onset of wild running and jumping, followed by limb clonus and tonic limb extension (Figure 2B and C). Episodes occurred approximately once each hour. Almost all LGI1$^{-/-}$ mice died suddenly during the postnatal third week (P14-21) (Figure 2A and B). No mice survived more than 25 days after birth. We often observed generalized seizures immediately preceding death and all mice that died unobserved showed full tonic postures, suggesting that the cause of death is fatal apnea during seizures.

In contrast to homozygous LGI1 knockout mice (LGI1$^{-/-}$), heterozygous LGI1$^{+/-}$ mice displayed no overt abnormalities. As ADPEAF is an autosomal dominant disease (i.e., patients are heterozygous for the LGI1 mutant allele), we investigated if the lack of one LGI1 allele lowers the threshold for seizure induction by pentylenetetrazole (PTZ), a $GABA_A$ receptor antagonist. A significantly greater fraction of LGI1$^{+/-}$ mice responded to 35 mg/kg injections of PTZ than observed for LGI1$^{+/+}$ mice (Figure 2D). Generalized clonic or tonic seizures were observed in 8 LGI1$^{+/-}$ mice (42.1%) compared to only 1 wild type mouse (8.3%) (Figure 2E). This result indicates that heterozygous mice for LGI1 mutation have increased susceptibility to seizure-inducing stimuli.

Epilepsy observed in LGI1$^{-/-}$ mice is the "monogenic" disorder, as the lethal epileptic phenotype was rescued by crossbreeding with transgenic mice expressing LGI1 under the neuron-specific Thy1 promoter (Figure 4A and B; LGI1$^{-/-;Tg1/+}$). The mice did not show obvious seizures, survived normally, and were fertile. In contrast, expression of LGI3, which is another member of LGI family and does not bind to ADAM22 (Figure 4C), could not rescue the LGI1 knockout mice (Figure 4B; LGI1$^{-/-;Tg3/+}$). Given that ADAM22$^{-/-}$ mice show a similar epileptic phenotype (Sagane et al., 2005), it suggests that lack of ligand/receptor interaction between LGI1/ADAM22 can cause epilepsy. Supporting this, the LGI1 point mutation (E383A) observed in patients with ADPEAF prevented its neuronal secretion and binding to ADAM22 in hippocampal neurons, whereas secreted wild-type LGI1 bound to ADAM22 at dendritic spines (Figure 4C). Together, these results clearly suggest that LGI1 mutations in ADPEAF represent loss-of-function mutations.

Identification of global LGI1-containing protein network in the brain

To clarify the mode of action of LGI1 in the brain, we isolated the protein–protein interaction with LGI1. Because our designed epitope-tagged LGI1 with FLAG and His x 6 (LGI1-FH; Figure 4A) rescued loss of the endogenous LGI1 gene, we used this transgenic mouse to purify LGI1 physiologically expressed in the brain. Tandem affinity purification (TAP) of LGI1-FH from transgenic mouse brain extracts yielded selective protein bands of 100 kDa (p100), 90 kDa (p90), 80 kDa (p80), 65 kDa (p65), 55 kDa (p55), and 30 kDa (p30) proteins (Figure 5A). The bands from transgenic mouse brain are highly specific as we saw few bands from a wild-type mouse brain. Mass spectrometry

and Western blotting indicated that p100 contained ADAM22 and PSD-95, p90 was ADAM22, p80 was ADAM22 and ADAM23, p65 was LGI1, p55 contained tubulin, and p30 was 14-3-3 (Figure 5B and Table 1). Quantitative Western blotting revealed that more than 90% of expressed LGI1-FH in the brain was recovered (Figure 5C). As ADAM22 and ADAM23 were both quantitatively and similarly enriched with LGI1-FH, ADAM23 as well as ADAM22 are major LGI1 receptors in the brain. Consistently, LGI1 directly bound to both ADAM22 and ADAM23 in vitro (Figure 6) (Fukata et al., 2006; Owuor et al., 2009; Sagane et al., 2008). Furthermore, to identify overall constituents of the LGI1 complex including indirect interactions, we conducted large-scale purification combined with shotgun proteomic analysis. The global LGI1 protein complex included ADAM22 subfamily members (ADAM22, ADAM23, and ADAM11) as its receptors and postsynaptic scaffolding proteins (PSD-95, PSD-93, and SAP97) (Figure 5D). In addition, presynaptic potassium channels (Kv_1) and presynaptic scaffolding proteins (CASK and Lin7) were identified at a relatively low amount but with reproducibility. 14-3-3 was reported as a binding partner with ADAM22 (Godde et al., 2006). Interestingly, each targeted disruption of ADAM22 (Sagane et al., 2005), ADAM23 (Mitchell et al., 2001; Owuor et al., 2009), and Kv_1 channel ($Kv_{1.1}$ (Smart et al., 1998) and $Kv_{1.2}$ (Brew et al., 2007), which form heterotetramer in the brain) causes a similar epileptic phenotype (generalized tonic-clonic seizures beginning around the postnatal second or third week) and premature death in mice, suggesting that LGI1, ADAM22, ADAM23 and Kv_1 are genetically associated and functionally related.

LGI1 connects pre- and postsynaptic machinery through ADAM22 and ADAM23 receptors

We analyzed interactions between constituents of the LGI1-associated protein complex. Using a cell surface-binding assay, we found that secreted LGI1 directly bound to the ectodomain of ADAM22 and ADAM23 on the cell surface but not to $Kv_{1.1}$ (Figure 6). To examine whether our purified LGI1 complex exists as a single protein complex or multiple ones with distinct compositions, we reprecipitated the purified LGI1 protein complexes from the transgenic mouse brain with antibodies against either ADAM22 or $Kv_{1.1}$. ADAM22 reprecipitation enriched ADAM23 and $Kv_{1.1}$ together with LGI1, but not Na^+K^+ATPase (Figure 7A). $Kv_{1.1}$ reprecipitates contained ADAM22 and ADAM23 together with LGI1 (Figure 7A**)**. This finding indicates that LGI1, ADAM22, ADAM23, and $Kv_{1.1}$ exist in a single protein complex. Furthermore, ADAM22 and ADAM23 were coimmunoprecipitated with each other from wild-type mouse brain extracts (Figure 7B). Importantly, this interaction was completely lost in the $LGI1^{-/-}$ mouse brain. In contrast, the interaction of ADAMs with $Kv_{1.2}$ was still detected in the $LGI1^{-/-}$ mouse. These results indicate that LGI1 directly links between ADAM22 and ADAM23 to form a ternary complex and that the Kv_1 channel was indirectly associated with LGI1 via ADAM22 or ADAM23. PSD-95, which directly interacts with one major ADAM22 isoform with a PDZ-binding motif (Fukata et al., 2006), was also coimmunoprecipitated with ADAM22 and ADAM23 in wild-type mouse brain. Given that the LGI1 protein complex contains both presynaptic and postsynaptic proteins (Figure 5D), it is conceivable that LGI1 mediates a transsynaptic interaction between ADAM22 and ADAM23.

LGI1 Is Specifically Required for Synaptic Localization of ADAM22 and ADAM23

We next asked whether LGI1 controls subcellular distributions of ADAM22, ADAM23, and Kv_1. LGI1, ADAM22, and ADAM23 similarly distributed both presynaptically and postsynaptically (Figure 8). Loss of LGI1 reduced the amount of both ADAM22 and ADAM23 in Triton X-100–insoluble crude synaptic fractions by ≈80% and inversely increased in Triton X-100–soluble fractions (Figure 9A). This is consistent with the data that the interaction of ADAM22 with postsynaptic PSD-95 is reduced in the $LGI1^{-/-}$ mouse (Figure 7B). The amount of $Kv_{1.1}$ both in the total homogenate and in the Triton X-100–insoluble fraction was reduced by 50%, whereas that of N-cadherin did not change. Mislocalization of ADAM22 and ADAM23 solely depended on the expression levels of LGI1, as (i) the effect was LGI1 gene dose-dependent (Figure 9A) and (ii) the mislocalization was restored by Thy1-driven LGI1-FH ($^{Tg1/+}$) but not LGI3-FH ($^{Tg3/+}$) (Figure 9B). Consistently, ADAM22-ADAM23 interaction was specifically detected in the rescued mouse $LGI1^{-/-;Tg1/+}$ but not in the $LGI1^{-/-;Tg3/+}$ mouse (Figure 8B).

Immunohistochemical analysis showed that LGI1 predominantly occurs in the hippocampus and entorhinal cortex. The staining is specific, as it is lost in the $LGI1^{-/-}$ mouse and appears in the $LGI1^{-/-}$ mouse brain expressing LGI1-FH (Figure 9C). Specific strong staining was observed in the neuropil of the hippocampus (Figure 9C and D) immunofluorescent microscopic examination, LGI1 was detected as tiny puncta at the molecular layers of the hippocampal regions (Figure 9E). LGI1 was often apposed or colocalized with PSD-95. Furthermore, immunoelectron microscopic analysis showed that gold particles for LGI1 were often detected at or around the synaptic cleft in the hippocampal dentate gyrus region (Figure 9F, arrowheads). ADAM22, ADAM23, and $Kv_{1.2}$ were also expressed in the overlapping regions (Figure 9D). Consistent with

biochemical data, neuropil staining of ADAM22 and ADAM23 was apparently reduced in the LGI1$^{-/-}$ mouse, especially in the dentate gyrus (Figure 9D, arrowheads). $Kv_{1.2}$, but not $Kv_{4.2}$, also showed slightly reduced staining in the hippocampus (Figure 9D).

Essential Role of LGI1 in AMPAR-Mediated Synaptic Transmission

Because we previously showed that LGI1 application to hippocampal slices specifically increases AMPAR-mediated synaptic transmission (Fukata et al., 2006), we next examined whether loss of LGI1 affects AMPAR-mediated synaptic transmission in the hippocampus. Two methods were used to measure synaptic AMPAR function. First, we compared the AMPA/NMDA ratio in control and wild-type (LGI1$^{-/-\ +/+}$) and LGI1$^{-/-}$ mice. A clear reduction in this ratio was observed (Figure 10A). This decrease could result from either a selective increase in NMDA synaptic currents or a selective decrease in AMPA synaptic currents. To distinguish between these alternatives, we recorded miniature excitatory postsynaptic currents (mEPSCs) in the presence of tetrodotoxin. Indeed, a significant decrease in the average amplitude of mEPSCs, but not frequency, was found (Figure 10C and D). Finally, we examined paired pulse ratio to determine whether the probability of transmitter release is changed in the LGI1$^{-/-}$ mice. No change in the paired pulse ratio was detected (Figure 10B). These results indicate that the loss of LGI1 reduces AMPAR-mediated synaptic currents in the hippocampus.

Discussion

Our data establish LGI1 as an antiepileptogenic ligand that regulates AMPAR-mediated synaptic transmission. We found that loss of neuronal LGI1 specifically reduces AMPAR-mediated synaptic transmission. This result is complementary to the previous report that LGI1 application to hippocampal slices specifically augments AMPAR-mediated synaptic transmission through ADAM22 (Fukata et al., 2006). How might dysregulation of AMPAR-mediated synaptic transmission induce epilepsy? LGI1 and ADAM22/ADAM23 are expressed in inhibitory interneurons as well as in excitatory neurons in the hippocampus (Fukata et al., 2006). Decreased AMPAR function in inhibitory interneurons may induce an increase in overall excitability of the hippocampus, for example. By analogy, mutations in stargazin, an AMPAR auxiliary subunit, cause loss of AMPARs in inhibitory neurons of the thalamic reticular nucleus and contribute to absence epilepsy (Menuz and Nicoll, 2008). It may be worthwhile to investigate whether specific expression of the LGI1 transgene in certain particular neuronal populations, such as inhibitory interneurons or principal excitatory neurons in the hippocampus, could rescue the LGI1 null mice.

How do LGI1 mutations in humans contribute to epileptogenesis, either by haploinsufficiency or in a dominant-negative manner? A recent study using the transgenic mouse expressing ADPEAF mutant LGI1 835delC proposes a dominant-negative mechanism (Zhou et al., 2009), because endogenous LGI1 in the transgenic mice is expressed at a level similar to that in wild-type mice. The 835delC mutation, which truncates the C-terminal EPTP repeat and expresses only the N-terminal LRR region, arrests maturation of excitatory glutamatergic synapses. However, because this transgenic mouse does not show any spontaneous epileptic phenotype, it remains

unknown whether the mutant mouse is a reliable model of ADPEAF. Also, uncertain is how LGI1 835delC functions in a dominant negative manner. Alternatively, another group suggests a loss of function mechanism based on the genetic facts that various types of mutations are associated with a rather homogenous phenotype (Nobile et al., 2009). Phenotypes of LGI1 gene-targeted mice, increased seizure susceptibility in heterozygous LGI1$^{+/-}$ mice and lethal epileptic seizures in homozygous LGI1$^{-/-}$ mice provide supportive evidence for the haploinsufficiency mechanism of ADPEAF mutations in human; ADPEAF mutations perturb LGI1 secretion and reduce the LGI1-mediated transsynaptic connection between ADAM22 and ADAM23, leading to abnormal synaptic transmission and epilepsy. Because heterozygous mice for ADAM23 gene disruption show the similar susceptibility to PTZ (Owuor et al., 2009) and homozygous mice for ADAM22 or ADAM23 mutation show spontaneous lethal seizures (Mitchell et al., 2001; Owuor et al., 2009; Sagane et al., 2005), it is strongly suggested that the amount of LGI1/ADAM22/ADAM23 complex determines seizure susceptibility. One may ask about the relationship between the phenotype of heterozygous LGI1$^{+/-}$ mice and the clinical features of ADPEAF patients. It is likely that the subtle abnormalities in LGI1$^{+/-}$ mice are not noticed because of the mild nature or infrequency of the seizures. This is consistent with the clinical features of ADPEAF: generalized tonic–clonic seizures occur infrequently (about one per year).

LGI1 may have two different functions: (*i*) regulating AMPAR-mediated synaptic transmission and (*ii*) recruiting presynaptic machinery containing potassium channels. Here, we propose a novel type of transsynaptic protein interaction: Extracellularly secreted LGI1 connects presynaptic ADAM23 to postsynaptic ADAM22 at the synaptic cleft. A unique EPTP repeat domain of LGI1 is responsible for ADAM22 binding

(Fukata et al., 2006). The EPTP domain is supposed to form a seven-bladed β propeller structure, which contains potential multiple protein–protein interfaces. It is conceivable that EPTP domain allows the simultaneous binding of ADAM22 and ADAM23 to LGI1. Unlike classical cell adhesion molecules, such as N-cadherin and Neurexin/Neuroligin, LGI1-mediated transsynaptic interaction is unique in that the amount of secreted LGI1 determines the strength of the interaction. Such ligand-dependent cell–cell adhesive machinery has not been reported to date and could provide an important mechanism for regulating synaptic transmission. If secretion of LGI1 is regulated in a synaptic activity-dependent manner, LGI1 may emerge as a major determinant of brain excitation. Therefore, the LGI1/ADAMs (ligand/receptors) complex represents an exciting therapeutic target for human epilepsy. In addition, the LGI1-targeted mouse will be a resource to elucidate pathogenesis of and therapeutics for human epilepsy.

Figure 1. **Targeting construct and characterization of LGI1 knockout mice.**

(A) Restriction maps of wild-type murine LGI1 allele (Upper), pSP72 targeting plasmid (Middle), and targeted allele (Lower). Black filled bars indicate LGI1 exons; red filled bars denote Southern probes; and blue filled bars specify PCR genotyping fragments. B, BamHI; S, SpeI; Neo, neomycin. (B) Southern blots from wild-type (+/+), heterozygote (+/−), and null (−/−) mice. Using a 5′ probe and SpeI digestion, the wild-type and the targeted loci generated 13.3- and 11.4-kb bands, respectively. The neomycin cassette probe recognized a 8.7-kb band in the targeted locus after BamHI digestion. Using a 3′ probe and BamHI digestion, the wild-type and the targeted loci generated 10.1- and 8.7-kb bands, respectively. (C) PCR genotyping. Wild-type (W) and targeted loci (T) gave 493- and 337-bp PCR products, respectively.

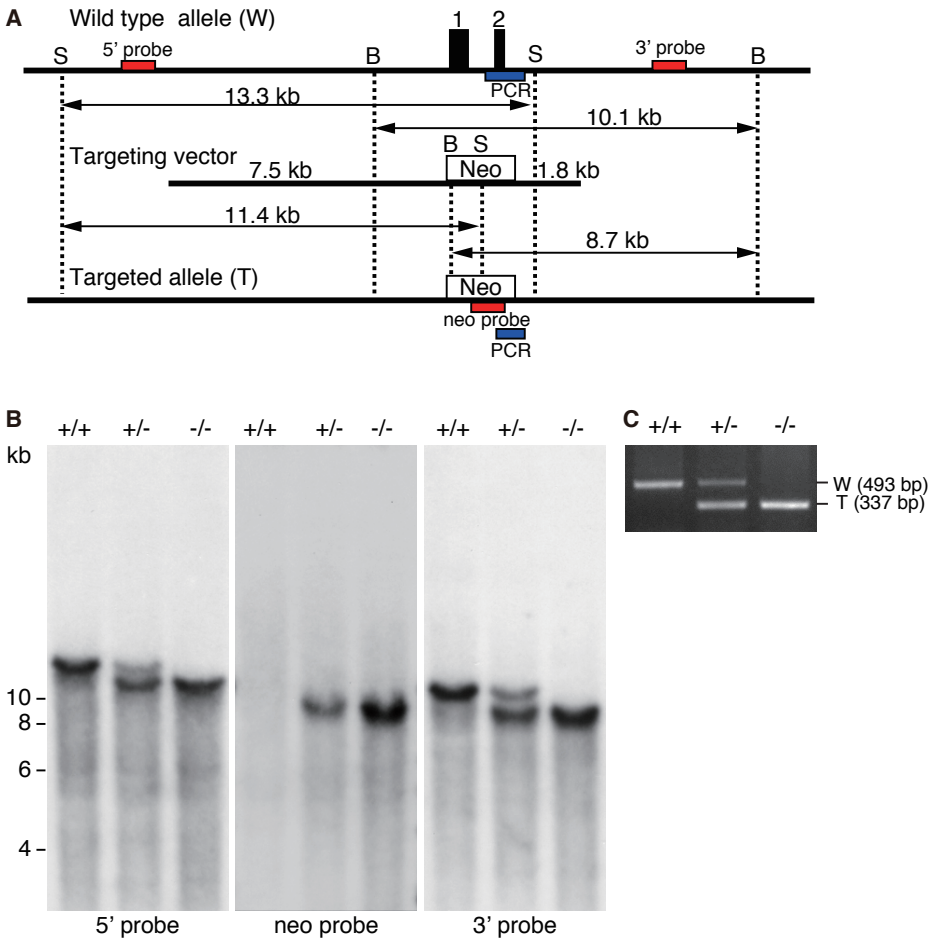
A
Wild type allele (W)
1
2
S
5' probe
B
S
3' probe
B
PCR
13.3 kb
10.1 kb
B S
Targeting vector
7.5 kb
Neo
1.8 kb
11.4 kb
8.7 kb
Targeted allele (T)
Neo
neo probe
PCR
B
+/+ +/- -/- +/+ +/- -/- +/+ +/- -/-
kb
10
8
6
4
5' probe
neo probe
3' probe
C
+/+ +/- -/-
W (493 bp)
T (337 bp)

Figure 2. Loss of LGI1 causes lethal epilepsy in mice.

(A) Survival plot of LGI1 mutant mice. The absence of LGI1 protein in the brain was confirmed with anti-LGI1 antibody (Inset). (B) Observed epileptic or lethal phenotype in $LGI1^{-/-}$ mice (n = 27) during the postnatal third week. (C) Epileptic behaviors of $LGI1^{-/-}$ mice at P17. The mutant animal had spontaneous generalized seizures (resulting in a blurred image; Upper), followed by full tonic extension (Lower; arrowheads indicate limb extension). (D) Response of 1-month old wild-type ($LGI1^{+/+}$) and $LGI1^{+/-}$ mice to PTZ (35 mg/kg). Data are mean ± SEM. Student's t test: ***$p < 0.001$ ($LGI1^{+/+}$, n = 12; $LGI1^{+/-}$, n = 19). (E) Quantification of reaction to PTZ injection. Each criterion (0–5) is as follows. 0, no reaction; 1, twitching; 2, myoclonic body jerks; 3, clonic forelimb convulsions; 4, generalized clonic convulsions; 5, generalized tonic convulsions.

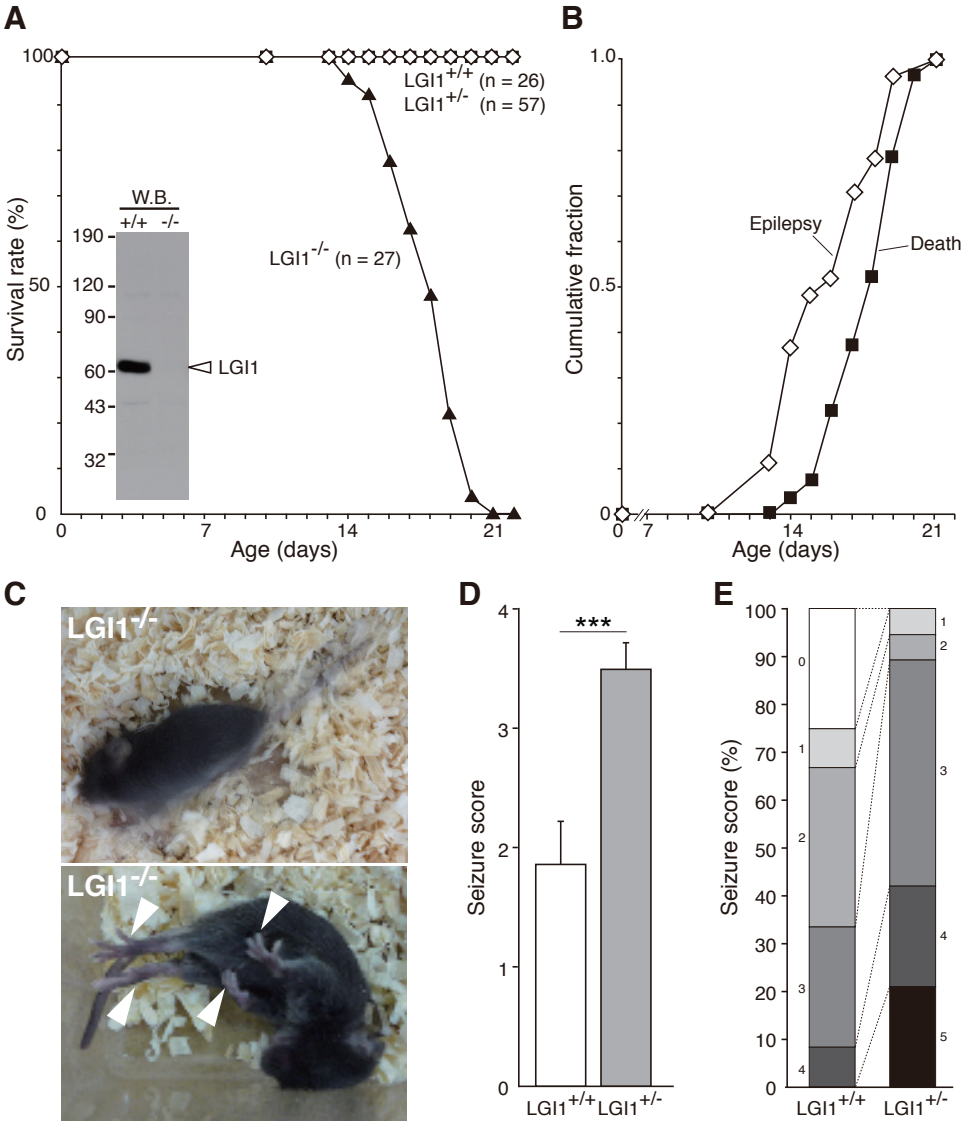
A
100
50
0
Survival rate (%)
0
7
14
21
Age (days)
LGI1+/+ (n = 26)
LGI1+/- (n = 57)
LGI1-/- (n = 27)
W.B.
+/+ -/-
190
120
90
60
43
32
LGI1
B
1.0
0.5
0
Cumulative fraction
Epilepsy
Death
C
LGI1-/-
LGI1-/-
D
***
Seizure score
LGI1+/+
LGI1+/-
E
Seizure score (%)
LGI1+/+
LGI1+/-

Figure 3. Growth failure of LGI1$^{-/-}$ mice in first three weeks of life.

Beginning at P10, LGI1$^{-/-}$ mice are significantly smaller than their littermates ($p < 0.05$). During the second and third week, while littermates increase in size on average 2g, the LGI1$^{-/-}$ mice do not increase in size at all.

Postnatal day	LGI1 genotype body weight (g)		
	$^{+/+}$	$^{+/-}$	$^{-/-}$
P10	5.76 ± 0.89	5.51 ± 1.17 ($P = 0.429$)	5.01 ± 1.04 ($P = 0.031$)
P12	6.07 ± 0.94	6.11 ± 1.41 ($P = 0.437$)	5.51 ± 0.99 ($P = 0.014$)
P14	6.69 ± 0.53	6.83 ± 0.89 ($P = 0.545$)	5.82 ± 0.96 ($P = 0.015$)
P17	7.77 ± 1.29	7.70 ± 1.01 ($P = 0.866$)	5.29 ± 0.99 ($P < 0.001$)

$^{+/+}$ Wild type;
$^{+/-}$ heterozygote; $^{-/-}$ homozygote,

Figure 4. Neuronal expression of LGI1, but not LGI3, completely rescues the epileptic phenotype of LGI1$^{-/-}$ mice.

(A) Thy1 promoter-driven LGI1 or LGI3 tagged with Flag and His Å~ 6 (-FH) designed for generating transgenic mice. (B) Neuronal expression of LGI1-FH transgene (Tg1/+), but not LGI3 (Tg3/+), completely rescued the lethal epileptic phenotype of LGI1 knockout mice (LGI1$^{-/-;+/+}$). (C) Thy1 promoter-driven LGI1-FH was functionally secreted and bound to surface expressed ADAM22 (green) in cultured hippocampal neurons. LGI1 E383A-FH, an ADPEAF mutant, was not secreted and failed to bind to ADAM22. LGI3-FH did not show the binding to ADAM22-GFP–expressing neurons. Red, surface-bound LGIs-FH; blue, total expression of LGIs-FH (tLGI1). (Scale bars, 10 μm [Upper]; 5 μm [Lower; dendritic regions were magnified]).

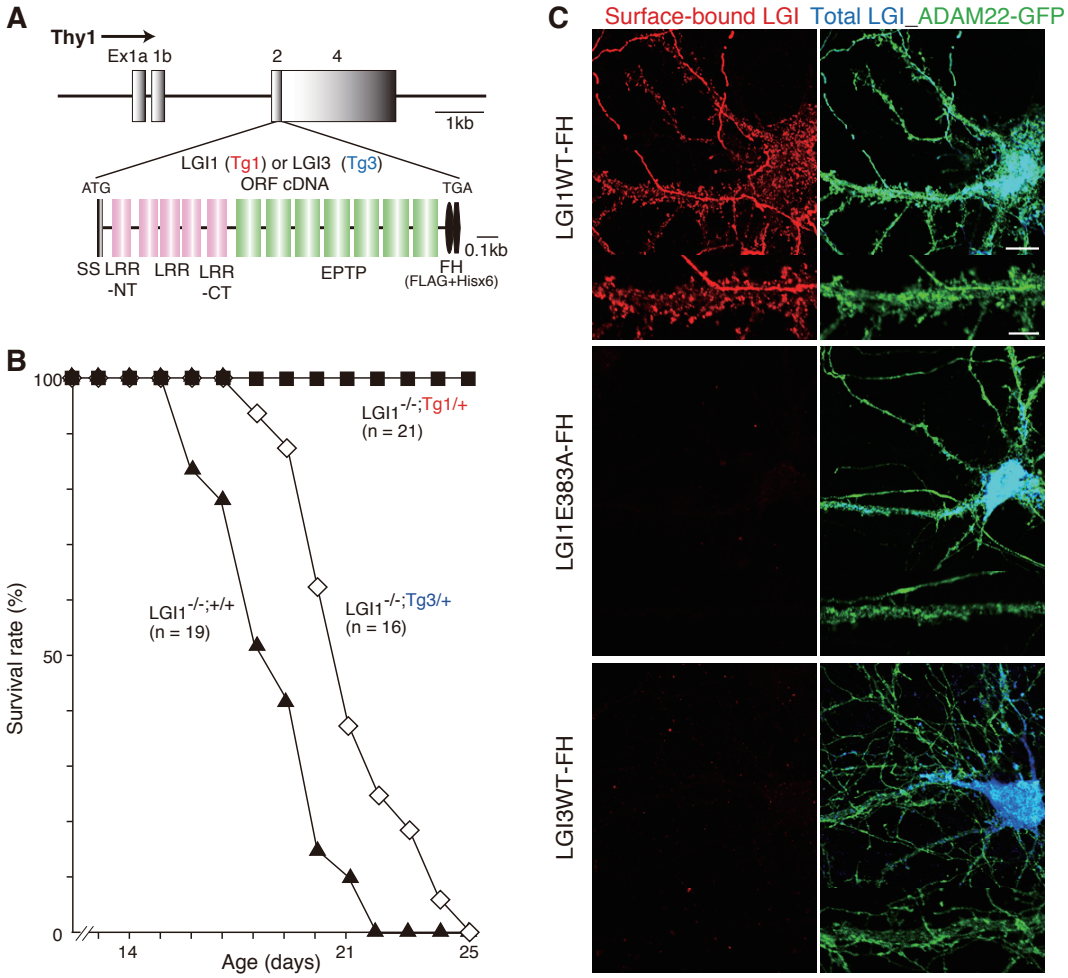
A
Thy1
Ex1a 1b
2
4
1kb
LGI1 (Tg1) or LGI3 (Tg3)
ORF cDNA
ATG
TGA
0.1kb
SS
LRR -NT
LRR
LRR -CT
EPTP
FH (FLAG+Hisx6)
B
100
50
0
Survival rate (%)
LGI1-/-;Tg1/+ (n = 21)
LGI1-/-;Tg3/+ (n = 16)
LGI1-/-;+/+ (n = 19)
14
21
25
Age (days)
C
Surface-bound LGI
Total LGI_ADAM22-GFP
LGI1WT-FH
LGI1E383A-FH
LGI3WT-FH

Figure 5. Identification of global LGI1-containing protein complex in the brain.

(A) In vivo LGI1-associated protein complex purified from the LGI1-FH–expressing mouse (Tg1), including p100, 90, 80, 65, 55, and 30 (arrowheads, from Top). (B) Major constituents of LGI1 complex contained ADAM23 as well as ADAM22 and PSD-95. Closed arrowheads, LGI1-FH; asterisk, nonspecific band; open arrowhead, endogenous LGI1; Ft, flow through; Elu, elution; Res, resin after elution. (C) More than 90% of expressed LGI1-FH was isolated by TAP. (D) LGI1-associated protein network analyzed by shotgun mass spectrometry. The identified specific proteins were lined up according to the SEQUEST score that is used for protein identification and semiquantification. Error bars, ±SD (n = 3).

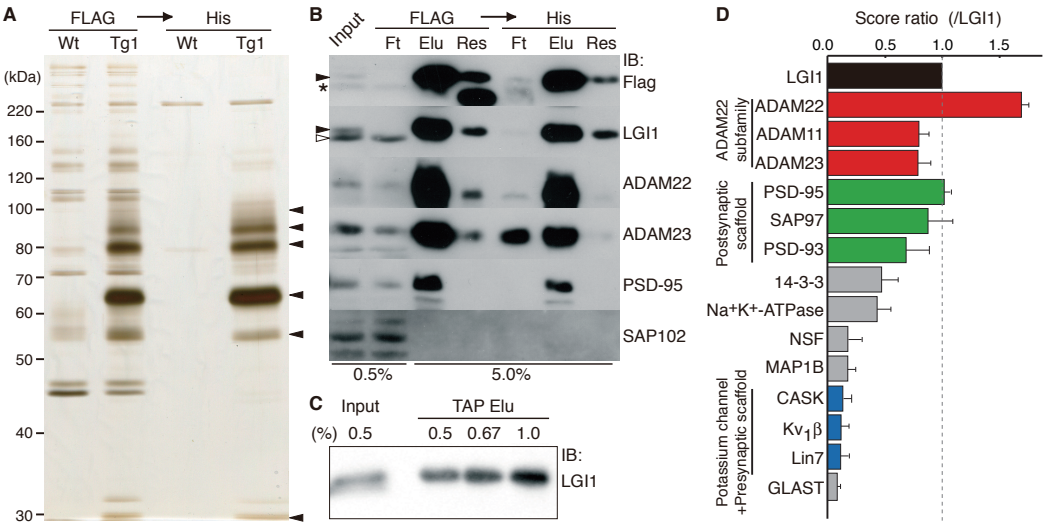
A
FLAG
His
Wt
Tg1
Wt
Tg1
(kDa)
220
160
120
100
80
70
60
50
40
30
B
Input
FLAG
His
Ft
Elu
Res
Ft
Elu
Res
IB:
Flag
LGI1
ADAM22
ADAM23
PSD-95
SAP102
0.5%
5.0%
C
Input
TAP Elu
(%) 0.5
0.5
0.67
1.0
IB:
LGI1
D
Score ratio (/LGI1)
0.0
0.5
1.0
1.5
LGI1
ADAM22
ADAM11
ADAM23
ADAM22 subfamily
PSD-95
SAP97
PSD-93
Postsynaptic scaffold
14-3-3
Na+K+-ATPase
NSF
MAP1B
CASK
Kv1β
Lin7
GLAST
Potassium channel +Presynaptic scaffold

Figure 6. ADAM22 subfamily members, but not Kv_1 channel, are LGI1 receptors.

(*A*) Binding of LGI1-AP, a secreted alkaline phosphatase (AP) fusion protein of LGI1, to ADAM-expressing COS7 cells. LGI1-AP bound to the cell surface was detected by the AP reaction. Note that LGI1-AP is bound to the ADAM22 subfamily (ADAM22, ADAM23, and ADAM11) but not to a distant ADAM member, ADAM9. Scale bar, 20 μm. (*B*) Indicated cDNAs were cotransfected into COS7 cells. At 24 h after transfection, surface-bound FLAG-tagged proteins (red) were labeled before cell permeabilization, and then HA-tagged proteins were stained (green). Secreted LGI1 specifically bound to ADAM22 and ADAM23, but not to $Kv_{1.1}$a in the presence of Kvb_2. LGI1 E383A, an ADPEAF mutant, did not bind to ADAM22. Scale bar, 10 μm.

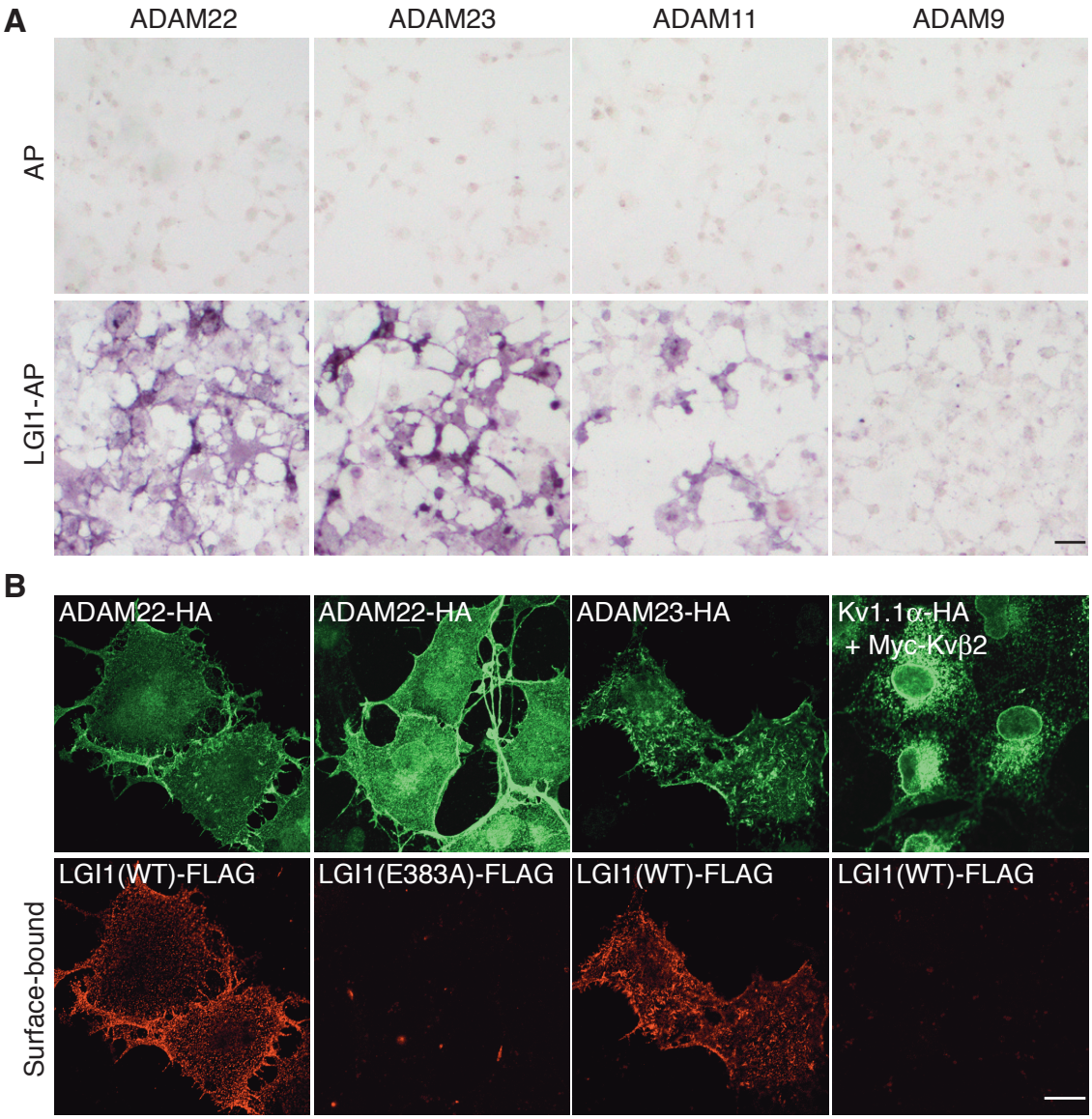
A
ADAM22
ADAM23
ADAM11
ADAM9
AP
LGI1-AP
B
ADAM22-HA
ADAM22-HA
ADAM23-HA
Kv1.1α-HA
+ Myc-Kvβ2
LGI1(WT)-FLAG
LGI1(E383A)-FLAG
LGI1(WT)-FLAG
LGI1(WT)-FLAG
Surface-bound

Figure 7. LGI1 mediates the interaction between two receptors, ADAM22 and ADAM23.

(A) LGI1, ADAM22, ADAM23, and Kv1 channel occur in a single protein complex. Purified LGI1 complex from the LGI1-FH expressing mouse was sequentially reprecipitated with antibodies to either ADAM22 or Kv1.1 (second IP). Open and closed arrowheads indicate ADAM22 and LGI1, respectively. (B) LGI1 connects between ADAM22 and ADAM23. ADAM22 (Left) or ADAM23 (Right) was immunoprecipitated from LGI1+/+ or LGI1$^{-/-}$ mouse brain extracts. Note that both Immunoprecipitates includes postsynaptic PSD-95 and presynaptic Kv1.2.

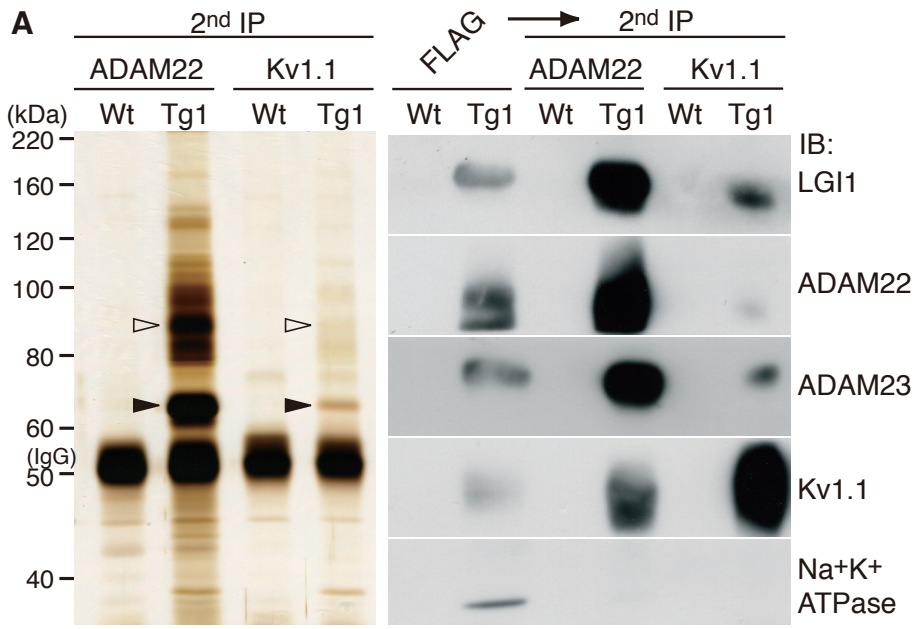
A
2nd IP
ADAM22
Kv1.1
(kDa)
Wt
Tg1
Wt
Tg1
220
160
120
100
80
60
(IgG)
50
40
FLAG
2nd IP
ADAM22
Kv1.1
Wt
Tg1
Wt
Tg1
Wt
Tg1
IB:
LGI1
ADAM22
ADAM23
Kv1.1
Na+K+
ATPase

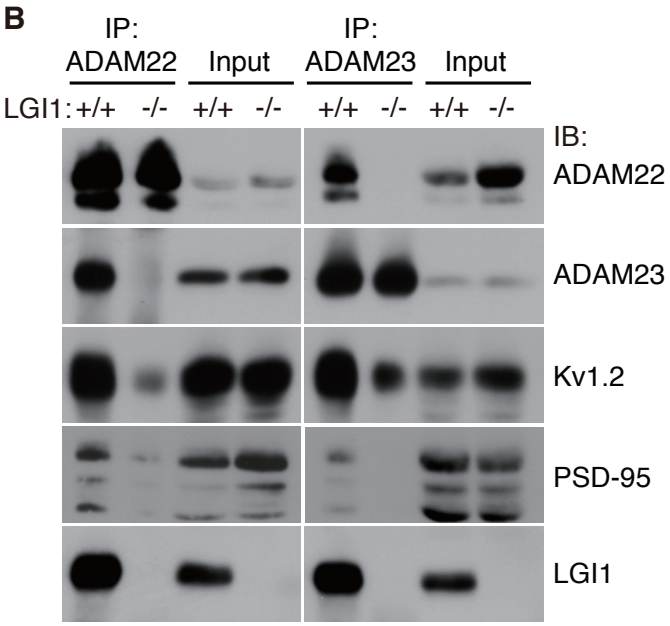
B
IP:
ADAM22
Input
IP:
ADAM23
Input
LGI1:
+/+
-/-
+/+
-/-
+/+
-/-
+/+
-/-
IB:
ADAM22
ADAM23
Kv1.2
PSD-95
LGI1

Figure 8. LGI1, ADAM22 and ADAM23 distribute both pre- and postsynaptically.

(A) LGI1, ADAM22, and ADAM23 displayed similar subcellular distribution. LGI1, ADAM22, and ADAM23 were enriched both in Triton X-100–soluble presynaptic and insoluble PSD fractions. Presynaptic $Kv_{1.1}$ and synaptophysin were enriched in Triton X-100–soluble synaptic fraction, whereas postsynaptic PSD-95 was enriched in PSD fractions. These results suggest that the LGI1/ADAM22/ADAM23 complex is centered between presynapses and postsynapses. H, homogenate; S, supernatant; P, precipitate; Syn, synaptosome; Triton-sol, Triton X-100–soluble presynaptic; PSD, Triton X-100–insoluble postsynaptic density fractions. (B) Expression of LGI1-FH in $LGI1^{-/-}$ mouse restored the interaction between ADAM22 and ADAM23. When ADAM23 was immunoprecipitated from $LGI1^{+/+;+/+}$, $LGI1^{-/-;+/+}$, $LGI1^{-/-;Tg1/+}$ or $LGI1^{-/-;Tg3/+}$ mouse brain extracts, the tripartite complex composed of ADAM22, LGI1(-FH) and ADAM23 was specifically detected in $LGI1^{-/-;Tg1/+}$ mouse expressing LGI1-FH, but not in $LGI1^{-/-;Tg3/+}$ mouse expressing LGI3-FH. Note that LGI3-FH was not co-immunoprecipitated with ADAM23. Closed arrowheads, LGI1-FH; open arrowhead, endogenous LGI1; gray arrowheads, LGI3-FH.

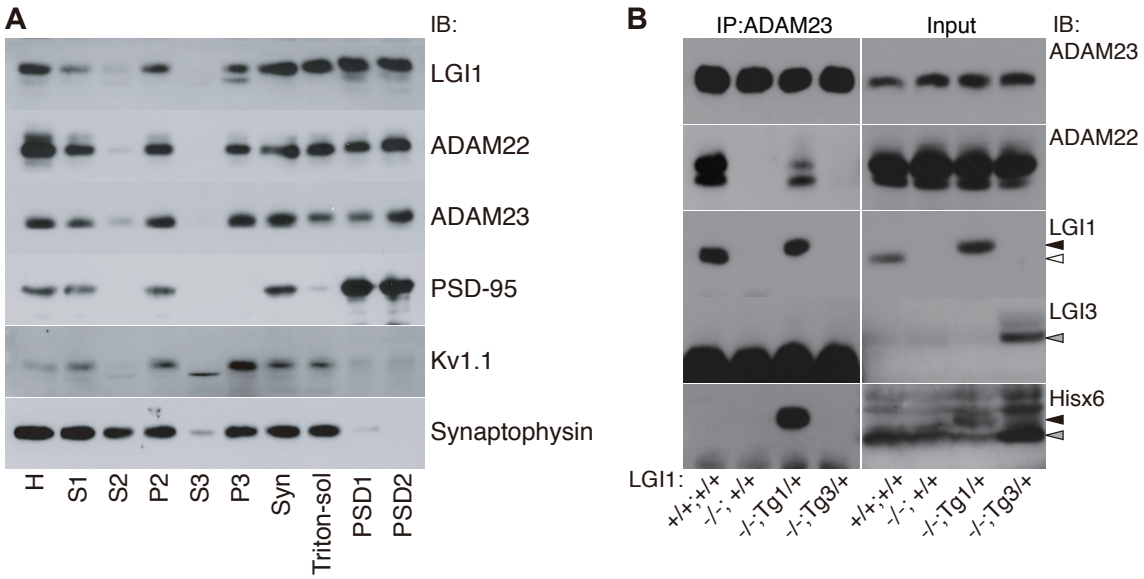
A
IB:
LGI1
ADAM22
ADAM23
PSD-95
Kv1.1
Synaptophysin
H
S1
S2
P2
S3
P3
Syn
Triton-sol
PSD1
PSD2
B
IP:ADAM23
Input
IB:
ADAM23
ADAM22
LGI1
LGI3
Hisx6
LGI1:
+/+;+/+
-/-;+/+
-/-;Tg1/+
-/-;Tg3/+
+/+;+/+
-/-;+/+
-/-;Tg1/+
-/-;Tg3/+

Figure 9. Loss of LGI1/ADAM22/ADAM23 protein complex from the synapse causes epileptic phenotype.

(A) Loss of LGI1 reduces ADAM22, ADAM23, and Kv1 channel in the synaptic fraction (insoluble). Crude synaptic membranes were fractionated by the Triton X-100 solubility, and probed with the indicated antibodies for quantitative Western blotting (Left). Relative band intensities compared with wild-type (+/+) samples are shown in graph. Deep color, $LGI1^{+/-}$; light color, $LGI1^{-/-}$. *$p < 0.05$; **$p < 0.001$. Error bars, ±SD (n = 3). (B) Reduction of synaptic ADAM22 and ADAM23 in $LGI1^{-/-}$ mouse was restored by the addition of an LGI1 transgene allele ($LGI1^{-/-;Tg1/+}$) but not by an LGI3 allele ($LGI1^{-/-;Tg3/+}$). Closed arrowheads, LGI1-FH; open arrowhead, endogenous LGI1. (C) LGI1 protein is highly enriched in the hippocampus and entorhinal cortex (transverse sections at P18). (Scale bar, 1 mm.) (D) Apparent reduction of ADAM22, ADAM23, and Kv1.2, but not Kv4.2, was observed in hippocampus of $LGI1^{-/-}$ mouse. (Scale bar, 0.2 mm.) (E) Immunofluorescence labeling of LGI1. LGI1 was often apposed to or colocalized with postsynaptic PSD-95 (arrowheads) at the molecular layer of the hippocampal regions. (Scale bar, 1 μm.) (F) Electronmicrography of hippocampal dentate gyrus shows that LGI1 localizes at the synaptic site (arrowheads). (Scale bar, 100 nm.)

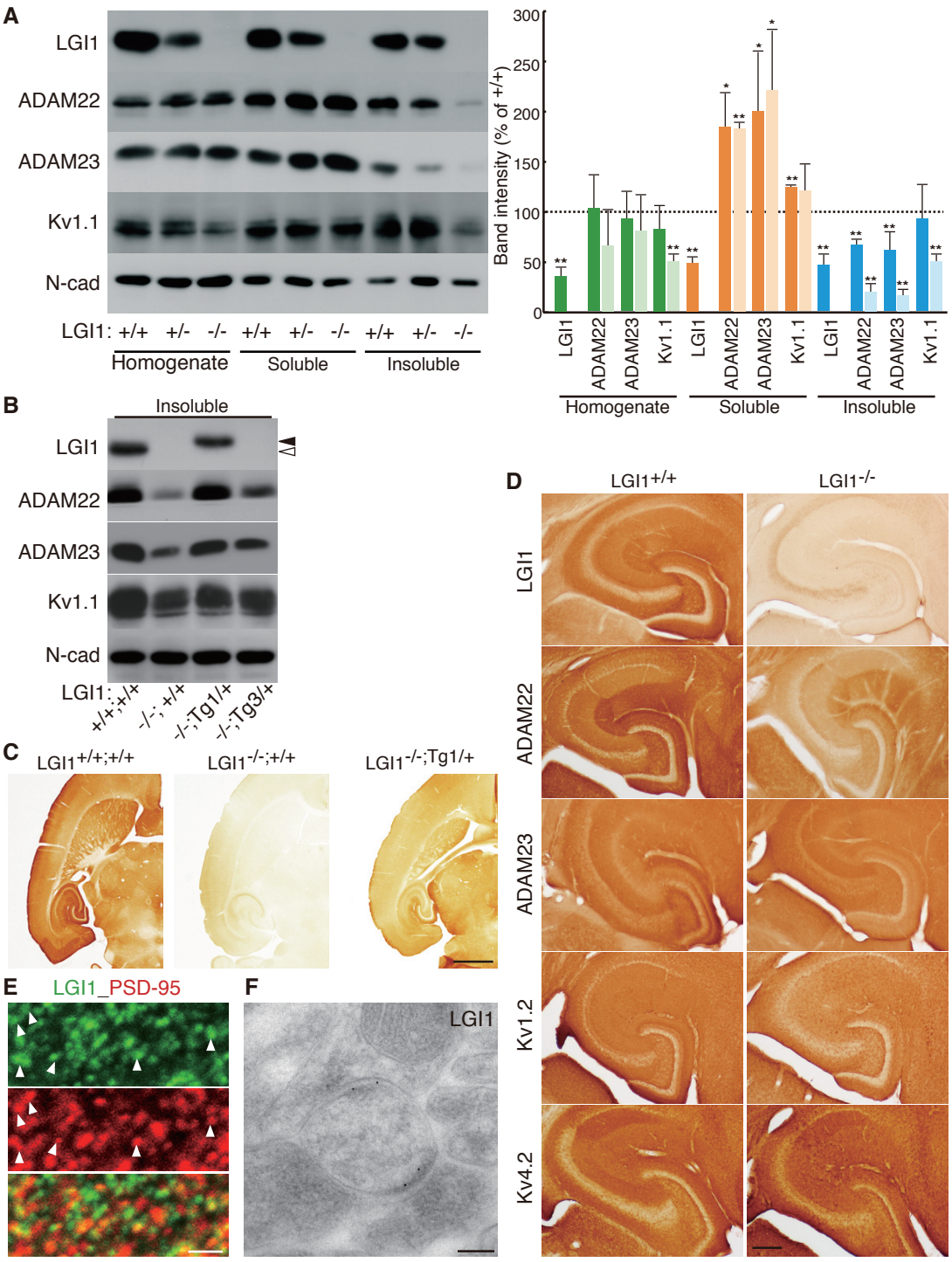
A
LGI1
ADAM22
ADAM23
Kv1.1
N-cad
LGI1: +/+ +/- -/- +/+ +/- -/- +/+ +/- -/-
Homogenate
Soluble
Insoluble
Band intensity (% of +/+)
300
250
200
150
100
50
0
LGI1
ADAM22
ADAM23
Kv1.1
Homogenate
Soluble
Insoluble
B
Insoluble
LGI1
ADAM22
ADAM23
Kv1.1
N-cad
LGI1: +/+;+/+ -/-; +/+ -/-;Tg1/+ -/-;Tg3/+
C
LGI1+/+;+/+
LGI1-/-;+/+
LGI1-/-;Tg1/+
D
LGI1+/+
LGI1-/-
LGI1
ADAM22
ADAM23
Kv1.2
Kv4.2
E
LGI1_PSD-95
F
LGI1

Figure 10. LGI1 is essential for AMPAR-mediated synaptic currents.

(A) Loss of LGI1 results in a significantly reduced (*$p < 0.01$) AMPA/NMDA ratio. (B) No difference in paired-pulse ratio is observed between wild-type ($LGI1^{+/+}$) and $LGI1^{-/-}$ mice ($p = 0.46$). (C) Cumulative distribution plot and average amplitude, inset, showing a significant decrease (*$p < 0.05$) in mEPSC amplitude in $LGI1^{-/-}$ mice. (D) No change in frequency of mEPSCs was observed ($p = 0.80$).

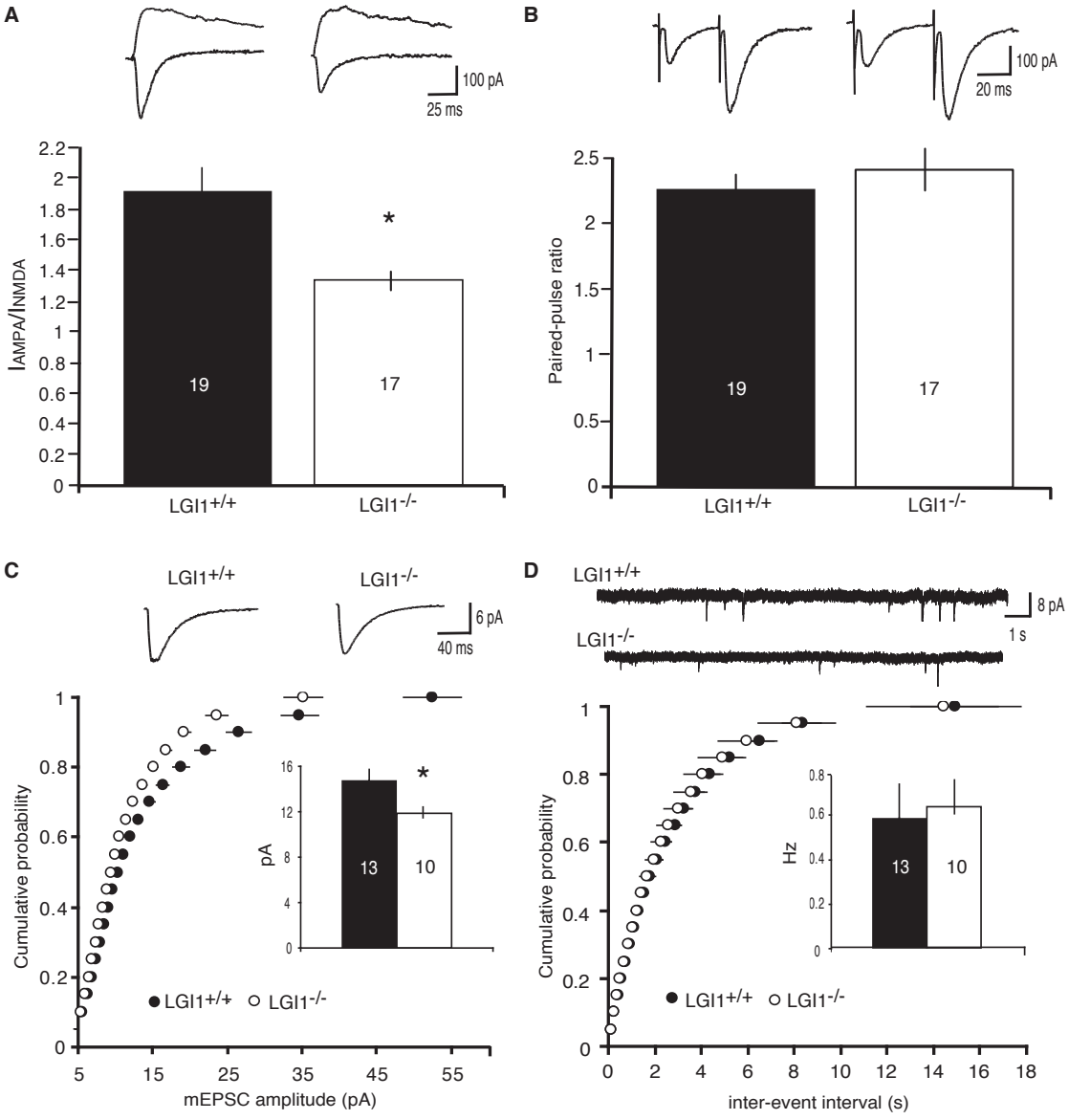
A
100 pA
25 ms
I_{AMPA}/I_{NMDA}
2.2
2
1.8
1.6
1.4
1.2
1
0.8
0.6
0.4
0.2
0
*
19
17
LGI1+/+
LGI1-/-
B
100 pA
20 ms
Paired-pulse ratio
2.5
2
1.5
1
0.5
0
19
17
LGI1+/+
LGI1-/-
C
LGI1+/+
LGI1-/-
6 pA
40 ms
Cumulative probability
1
0.8
0.6
0.4
0.2
0
5
15
25
35
45
55
mEPSC amplitude (pA)
LGI1+/+
LGI1-/-
pA
16
12
8
4
0
*
13
10
D
LGI1+/+
8 pA
LGI1-/-
1 s
Cumulative probability
1
0.8
0.6
0.4
0.2
0
0
2
4
6
8
10
12
14
16
18
inter-event interval (s)
LGI1+/+
LGI1-/-
Hz
0.8
0.6
0.4
0.2
0
13
10

Table 1. Results of mass spectrometry (gel-based) analysis.

Isolated protein*	Protein†	Probability‡ (protein)	Score§	Hits‖
P100	ADAM22	1.82E-08	50.21	6
	PSD-95	2.62E-05	20.19	2
P90	ADAM22	2.10E-12	110.25	13
P80	ADAM22	1.50E-06	78.20	8
	ADAM23	8.11E-08	50.20	5
P65	LGI1	3.56E-09	144.23	23
P55	Tubulin β2	6.78E-06	44.16	5
	Tubulin β6	4.68E-05	48.21	6
	Tubulin α1	1.85E-04	20.15	2
P30	14-3-3zeta	4.45E-07	20.13	2

*p100, p90, p80, p65 p55, and p30 were major bands copurified during the TAP (FLAG-His purification). p100 is a reproducible smear band just above p90. They were found in both FLAG and His eluates.
†Proteins with probability value (<1.0E-04) and score (>20) are listed.
‡Probability (protein) of finding a match as good as or better than the observed match by chance.
§SEQUEST scores.
‖Number of unique parent peptides found.

CHAPTER 4:

ADAM22 and ADAM23 are essential synaptic organizing proteins that mediate paracrine signaling by LGI1

Introduction

Chemical synapses form the anatomical connections and mediate functional transmission between neurons. The development of synapses involves recruitment of proteins that establish presynaptic release sites and postsynaptic densities, and, later, coordinate maturation, maintenance, and plasticity of the synapse. In the last decade, a number of transmembrane synaptic adhesion proteins and secreted proteins that initiate and modulate excitatory synapses—termed synaptic organizing proteins—have been identified. Most recent research has focused on the proteins involved in the first steps of synaptogenesis—such as neuroligins, neurexins, and LRRTMs (de Wit et al., 2009; Graf et al., 2004; Ko et al., 2009; Linhoff et al., 2009; Nam and Chen, 2005; Scheiffele et al., 2000; Siddiqui and Craig, 2011). However, much less is known about the synaptic organizing proteins involved in synapse maintenance and maturation (McMahon and Diaz, 2011).

We recently identified leucine-rich, glioma-inactivated protein 1 (LGI1) as a novel, secreted synaptic organizing protein (Fukata et al., 2006; Fukata et al., 2010). Functionally, we have found that LGI1 regulates synaptic AMPAR content, though the mechanism of action remains unclear. Secreted LGI1 is localized to synapses, where it is poised to mediate multiple protein interactions (Fukata et al., 2010; Leonardi et al., 2011). Specifically, LGI1 has been found to organize a transsynaptic protein complex, binding to the extracellular domain of a disintegrin and metalloprotease proteins 22 and 23 (ADAM22 and ADAM23)—transmembrane proteins located pre- and postsynaptically—which interact with the MAGUK family of scaffolding proteins intracellularly. Genetic deletion of either LGI1, ADAM22, or ADAM23 in mice results in a similar lethal epilepsy phenotype, with seizure onset in the second week of life

resulting in 100% fatality by postnatal week three (Chabrol et al., 2010; Fukata et al., 2010; Mitchell et al., 2001; Owuor et al., 2009; Sagane et al., 2005; Yu et al., 2010), indicating that this transsynaptic structure is critical to maintaining normal synaptic function.

Here, we sought to determine how the LGI1-ADAM complex regulates synaptic transmission. Biochemical data indicate that LGI1 is acting through ADAM transmembrane proteins, though the function of ADAM22 and ADAM23 in synaptic transmission has yet to be explored. Moreover, the source and destination of secreted LGI1 remains unknown. We find that reduction in ADAM22 and ADAM23 expression results in an almost complete loss of excitatory synaptic transmission. We also confirm that the members of this complex are specifically required for localization of receptors to the synapse, and not for expression on the cell surface. Further, we show that LGI1 originates from axons and dendrites, and acts in a paracrine fashion to regulate synaptic transmission. Finally, we provide evidence that the expression of LGI1 regulates synaptic MAGUK function. Given these findings, we conclude that the LGI1-ADAM synaptic organizing complex is a critical regulator of excitatory synapse maintenance and strength.

Results

Loss of ADAM22 results in a decreased number of functional excitatory synapses

LGI1 does not bind AMPARs directly (Fukata et al., 2010), so it must work through a network of interactions to regulate synaptic strength. Based on biochemical data (Fukata et al., 2006; Fukata et al., 2010), we hypothesized that LGI1 regulation of

synaptic transmission is mediated by the transmembrane proteins ADAM22 and ADAM23. Thus, we sought first to explore the role of ADAMs at excitatory synapses.

We began by examining the consequence of ADAM22 deletion on synaptic activity. Using biolistic transfection of Cre into slice cultures prepared from mice with the gene encoding ADAM22 flanked by loxP homologous recombination sites ($ADAM22^{fl/fl}$), we were able to directly compare AMPAR and NMDAR-mediated transmission in the presence and absence of ADAM22. Paired recordings from untransfected, wildtype cells and Cre-transfected, ADAM22-lacking (herein referred to as $ADAM22^{fl/fl}$) neurons showed that loss of ADAM22 results in a significant decrease in both AMPAR and NMDAR-mediated EPSCs (Figure 1A).

The reduction in both AMPAR and NMDAR-mediated currents after loss of ADAM22 could represent a decrease in the number of functional synapses, the probability of vesicle release at a single synapse, the receptor content at each synapse, or a combination of these changes. To distinguish amongst these possibilities, we carried out a coefficient of variation analysis in wildtype and $ADAM22^{fl/fl}$ neurons, which allows for determination of changes in quantal size and quantal content. Changes in quantal size result in changes in variance relative to the change in mean EPSC amplitude, such that the normalized ratio of $mean^2/variance$ (CV^{-2}) is unaffected and data points on a graph showing the relationship of mean versus CV^{-2} lie along the y=1 line. Conversely, changes in quantal content result in correlated changes in CV^{-2}, such that data points on a graph showing the relationship of mean versus CV^{-2} lie along the y=x line (Bekkers and Stevens, 1990; Del Castillo and Katz, 1954; Malinow and Tsien, 1990). Analysis of evoked AMPAR-mediated EPSCs from wildtype versus $ADAM22^{fl/fl}$

cells show correlated changes in mean amplitude and variance, indicative of a change in quantal content after loss of ADAM22 (Figure 1B).

Changes in quantal content can reflect a difference in the number of functional synapses or release probability at individual synapses. To test for presynaptic effects, we analyzed paired-pulse ratios from wildtype and ADAM22$^{fl/fl}$ cells. No difference in PPR was observed, indicating that ADAM22 does not regulate probability of release (Figure 1C). Thus, the change in quantal content observed after the loss of ADAM22 is due to a decreased number of functional synapses.

The LGI1-mediated protein complex contains both pre and postsynaptic proteins (Fukata et al., 2010) and thus may act as a transsynaptic scaffold at excitatory synapses. It is possible that the decreased number of functional synapses observed after loss of ADAM22 is the result of a structural defect decreasing the number of dendritic spines, the site of excitatory synapses. To determine if ADAM22 plays a structural role at excitatory synapses, we quantified the spine density in apical dendrites of ADAM22$^{fl/fl}$ slice cultures biolistically transfected with GFP or GFP and Cre-mCherry (Figure 2A). No significant difference was found in the spine density between wildtype and ADAM22$^{fl/fl}$ neurons (Figure 2B), indicating that the decrease in excitatory synapses observed after loss of ADAM22 is not a result of a structural deficit but rather a reduction in functional excitatory synapses.

ADAM22, though clustered at synapses, is also spread diffusely along the surface of the neuron (Fukata et al., 2006). Thus, it is possible that ADAM22 is required for the delivery or stabilization of AMPARs at the surface. However, glutamate-evoked currents recorded in outside-out patches from wildtype and ADAM22$^{fl/fl}$ cells are not

different, demonstrating that ADAM22 is not required for proper surface localization of AMPARs (Figure 1D).

ADAM22 function is dependent upon PDZ interactions

We next turned to a molecular replacement strategy to dissect the mechanism by which ADAM22 regulates excitatory synapse number. First, we tested whether expression of ADAM22 in ADAM22$^{fl/fl}$ neurons was sufficient to restore transmission. Paired recordings were carried out in untransfected, wildtype cells and cells expressing both Cre and ADAM22 in ADAM22$^{fl/fl}$ slice cultures. Co-expression of ADAM22 resulted in normal levels of AMPAR and NMDAR-mediated transmission (Figure 3A), indicating that ADAM22 expression is sufficient to rescue transmission but not to induce new synapse formation.

ADAM22 contains a PDZ binding motif (Fukata et al., 2006), a unique feature among the ADAM family proteins that bind LGI1. To assess whether ADAM22 function depends on PDZ domain interactions, we tried rescuing with an ADAM22 mutant lacking the PDZ binding motif, ADAM22dC4. Both AMPAR and NMDAR-mediated EPSCs were significantly reduced in cells expressing ADAM22dC4 (Figure 3B), similar to ADAM22$^{fl/fl}$ neurons expressing Cre alone (Figure 3C). We considered that the c-terminal truncation of ADAM22 might result in improper processing of the ADAM22dC4 mutant, impacting surface localization and subsequent LGI1 binding to ADAM22dC4. However, immunostaining of ADAM22dC4 revealed that it has normal surface localization and binds extracellular LGI1 (Figure 4). Thus, PDZ interactions are specifically required for proper ADAM22 function at the synapse.

ADAM22 and ADAM23 are required for excitatory synaptic transmission

LGI1 also interacts with ADAM23 at the synapse (Fukata et al., 2010), thus we were interested in investigating the role of ADAM23 in synaptic transmission. For this, we biolistically transfected a previously verified ADAM23 shRNA (Sun et al., 2007) into wildtype slice cultures. shRNA-mediated knockdown of ADAM23 results in a significant decrease in AMPAR and NMDAR-mediated EPSCs (Figure 5A), while having no effect on paired-pulse ratio (Figure 5B). This reduction in synaptic transmission is similar in magnitude to that of ADAM22 deletion. It is possible that ADAM22 and ADAM23 act in concert, so that deletion of either is enough to eliminate the function of both, and other synaptic organizing protein(s) mediates the remaining 50% of synaptic transmission. Alternatively, ADAM22 and ADAM23 may have complementary roles in synaptic transmission, so that loss of both would have an additive effect. To test this, we biolistically transfected ADAM23 shRNA into slice cultures prepared from ADAM22 germline-knockout mice, and recorded AMPAR and NMDAR-mediated EPSCs. Loss of both ADAM22 and ADAM23 resulted in a dramatic reduction in transmission, with remaining EPSCs barely distinguishable from noise (Figure 5C). This effect was specific to synaptic content, as paired-pulse ratio was not significantly different in cells lacking ADAM22 and ADAM23 (Figure 5D).

LGI1 expression specifically regulates excitatory synaptic strength

Having established that ADAM22 and ADAM23 are critical for maintaining excitatory synapses, we sought next to further explore our previous finding that loss of LGI1 results specifically in a decrease in synaptic AMPAR content (Fukata et al., 2010). It was

recently shown that overexpression of an epilepsy-associated mutant LGI1 (mLGI1) results in increased EPSC amplitude and miniature EPSC (mEPSC) frequency in dentate gyrus granule cells (Zhou et al., 2009). Moreover, a different germline knockout mouse also exhibited an increase in mEPSC frequency, but not amplitude, in CA1 neurons (Yu et al., 2010). We considered that because LGI1$^{-/-}$ mice suffer chronic seizures— shown to inflict significant damage to the hippocampus by P14 in LGI1$^{-/-}$ mice (Chabrol et al., 2010) and known to impact excitatory transmission (Lynch et al., 1996)—the variability in results might reflect the effects of epilepsy, and not the function of LGI1.

Thus, we turned to hippocampal slice culture, a system in which we are able to study the effects of LGI1 expression without the confounding effects of repeated seizures *in vivo*, to verify our results in acute slice. Slice cultures were prepared from P6-P8 animals, before any LGI1$^{-/-}$ mice have developed an epileptic phenotype, and recordings made at DIV8 (Figure 6A), a time at which LGI1 and other major synaptic proteins are robustly expressed (Fukata et al., 2006; Fukata et al., 2010; Thomas et al., 2010). Recordings of AMPA/NMDA ratios made from CA1 neurons in LGI1$^{-/-}$ cultures versus wildtype littermate cultures were significantly decreased (Figure 6B), confirming that the previously observed decrease in AMPA/NMDA ratio in acute slice is due to loss of LGI1 and not an effect of chronic seizures *in vivo*. Moreover, no difference was found in the paired-pulse ratio between wildtype and LGI1$^{-/-}$, akin to our previous findings in acute slice (Figure 6C).

We wanted next to define the nature of the change in AMPA/NMDA ratios observed after loss of LGI1. It is possible that the decrease in transmission observed in the LGI1$^{-/-}$ is due to the changing strength of individual synapses, or to a decrease in the total number of AMPAR-containing synapses. Recording miniature EPSCs (mEPSCs) in

wildtype versus LGI1$^{-/-}$ cells, we found a significant reduction in amplitude but not frequency (Figure 6D), consistent with a deficit in synapse strength, not number. This was specifically due to decreased synaptic localization of AMPARs and not overall expression level, as no difference was observed in glutamate-evoked currents recorded from LGI1$^{-/-}$ and wildtype neurons (Figure 6E), indicating that surface expression is normal in the absence of LGI1.

Because our recordings were made in CA1, and the mLGI1 recordings in the dentate gyrus, we were interested in determining if LGI1 plays distinct roles in different regions of the hippocampus. Recording EPSCs in granule cells of LGI1$^{-/-}$ and wildtype littermates, we observed a decrease in AMPA/NMDA ratio similar in magnitude to our findings in CA1 (Figure 7A). Zhou *et al.* (2009) found that mLGI1 expression slowed NMDAR kinetics (Zhou et al., 2009), which in our preparation might artificially produce a decrease in the AMPA/NMDA ratio; we calculate the NMDAR EPSC amplitude 100 ms after stimulus delivery in order to avoid contamination by the AMPAR EPSC, but this makes our measurement sensitive to changes in receptor kinetics. To avoid this confound, we recorded isolated NMDAR EPSCs in the presence of AMPAR antagonist NBQX, and observed no difference in receptor kinetics between wildtype and LGI1$^{-/-}$ neurons (Figure 7B). Also similar to our findings in CA1, we did not see any change in paired-pulse ratio after loss of LGI1 (Figure 7C). Thus, loss of LGI1 is functionally distinct from mutant LGI1 expression.

LGI1 is a paracrine signal derived from the pre- and postsynaptic cell

How does LGI1 control the strength of excitatory synapses? We looked to molecular replacement strategies to dissect the mechanism of LGI1 effects at the synapse, beginning with a rescue of wildtype LGI1. LGI1$^{-/-}$ hippocampal slice cultures were biolistically transfected with LG1, and simultaneous recordings were made from neighboring CA1 pyramidal cells in response to stimulation of stratum radiatum. Curiously, we observed no difference in AMPAR or NMDAR-mediated EPSCs in the LGI1 expressing cell relative to the LGI1$^{-/-}$ control (Figure 8A).

In our paired-recording set-up, it is possible that secreted LGI1 from the transfected cell acts in a paracrine fashion, increasing receptor content in the neighboring LGI1$^{-/-}$ control cells and masking a change in EPSCs induced by LGI1 expression. To test if secreted LGI1 alters nearby cells, we compared the AMPA/NMDA ratios of untransfected LGI1$^{-/-}$ cells near LGI1-transfected cells to LGI1$^{-/-}$ cells from untransfected LGI1$^{-/-}$ slices (Figure 8B). Consistent with LGI1 having paracrine activity, the AMPA/NMDA ratio of LGI1$^{-/-}$ cells near to transfected cells were rescued to wildtype levels, and significantly increased relative to cells from the untransfected LGI1$^{-/-}$ slices (Figure 8C).

A recently identified missense mutation of *LGI1* implicated in human autosomal dominant temporal lobe epilepsy (ADTLE), LG1S473L, is secretion-competent but has reduced binding to ADAM22 and cannot maintain normal levels of ADAM22 and ADAM23 at the synapse (Yokoi et al., 2014). Using the paracrine signal assay above, we tested whether the LGI1-ADAM interaction is necessary for LGI1 function. Comparing AMPA/NMDA ratios of LGI1$^{-/-}$ cells near to LGI1S473L transfected cells and LGI1$^{-/-}$ cells from untransfected slices, we found that LGI1S473L is unable to rescue AMPA/NMDA ratios as wildtype LGI1 did (Figure 8C). This result is not specific to the

paracrine signaling function of LGI1, as the cells transfected with LGI1S473L also did not have increased AMPAR or NMDAR-meditated EPSCs relative to LGI1$^{-/-}$ cells (Figure 9).

LGI1 mediates a complex with pre- and postsynaptic components (Fukata et al., 2010), though the source of the secreted protein remains unknown. Our previous experiment showed the expression of LGI1 in the postsynaptic cell is sufficient to rescue AMPA/NMDA ratios. To test if presynaptic expression of LGI1 is sufficient to alter transmission, we used lentiviral injections in slice culture to specifically express LGI1 in CA3 neurons and recorded AMPA/NMDA ratios in CA1 pyramidal cells (Figure 8D). These experiments revealed that expression of LGI1 in CA3 rescues AMPA/NMDA ratios of CA1 neurons (Figure 8E) to wildtype levels.

This finding might indicate that LGI1 is promiscuous in its ability to modulate synaptic transmission. It may be that LGI1 is secreted from axons, dendrites, and cell bodies, or diffuses great distances from the site of secretion and impact far away synapses. To test for this, we again used viral rescue of LGI1 in LGI1$^{-/-}$ slices, though this time in the dentate gyrus instead of CA3 (Figure 8D). In slice culture, the somas of dentate gyrus granule cells and CA3 pyramidal neurons are roughly equidistant from CA1 neurons, however their axons and dendrites never come in close contact. Recordings of AMPA/NMDA ratios in CA1 cells of slices with LGI1 expressed in the dentate gyrus were not significantly different from naïve LGI1$^{-/-}$ slices (Figure 8E). This suggests that LGI1 is secreted from axons and dendrites, and only impacts synapses near to the site of secretion.

Supporting this, LGI1 expression is localized to the axons and dendrites, and does not travel far from the cells that secrete it. In transgenic mice expressing LGI1 exclusively in dentate gyrus granule cells (LGI1$^{-/-}$; Prox1-LGI1), immunohistochemical analysis shows LGI1 labeling specifically in the molecular layer and along the mossy fiber axon tract (Figure 10). Moreover, LGI1 does not have a graded effect on synapses, which might be expected of a somatically secreted protein. Stimulation in stratum radiatum (SR) or stratum lacunosum moleculare (SLM)—the site of proximal and distal synapses, respectively—reveals an equal decrease in AMPA/NMDA ratio after loss of LGI1 (Figure 11A). Similarly, the decrease in AMPAR and NMDAR-mediated EPSCs is the same in SR and SLM after deletion of ADAM22 (Figure 11B).

MAGUK function is dependent on LGI1 expression

Extracellular LGI1 directly regulates AMPAR-content at the synapse (Fukata et al., 2006; Fukata et al., 2010). We have shown here that LGI1 must bind ADAM22 to regulate transmission, and that the function of ADAM22 requires PDZ interactions. Like LGI1, expression of PSD-95, a critical PDZ-containing scaffolding protein that binds ADAM22, modulates synaptic AMPAR localization (Elias et al., 2006). Therefore, we wondered if LGI1 expression regulates MAGUK function at the synapse.

Using paired-recordings, we compared the effect of changing PSD-95 expression levels in the wildtype and LGI1$^{-/-}$ slice cultures. As expected, overexpression of the MAGUK family member PSD-95 greatly increases AMPAR but not NDMAR-mediated EPSCs in neurons (Figure 12A). If the LGI1-ADAM22 complex is required for MAGUK function, increased MAGUKs at the synapse should not increase transmission, as is the

case in wildtype neurons. Paired-recordings of LGI1$^{-/-}$ cells and LGI1$^{-/-}$ cells expressing PSD-95 showed that loss of LGI1 significantly decreases PSD-95 induced increases in synaptic transmission (Figure 12B). Thus, LGI1 is a crucial synaptic organizing protein, playing a necessary role in mediating effects of the critical postsynaptic scaffolding protein PSD-95.

Discussion

Here, we identify a novel and essential role for ADAM22 and ADAM23 in maintaining excitatory synaptic transmission. Moreover, we show that LGI1, which binds to ADAMs and regulates their synaptic localization (Fukata et al., 2006; Fukata et al., 2010; Sagane et al., 2008; Thomas et al., 2010; Yokoi et al., 2014), acts as a paracrine signal and controls synaptic AMPAR content through postsynaptic MAGUKs.

Previous analysis of LGI-interacting proteins revealed three candidate transmembrane proteins to mediate the LGI1 functional effect – ADAM11, ADAM22, and ADAM23 (Fukata et al., 2010). However, mice lacking ADAM11 do not have the lethal epileptic phenotype (Takahashi et al., 2006) shared by LGI1, ADAM22, and ADAM23 mice (Fukata et al., 2010; Mitchell et al., 2001; Sagane et al., 2005). Consistent with this phenotypic difference, LGI1 also has a much weaker affinity for ADAM11 than ADAM22 and ADAM23 (Sagane et al., 2008), suggesting that this interaction is not the primary intermediary of LGI1 synaptic effects. Thus, we focused on the role of ADAM22 and ADAM23 at the synapse, and found a previously undescribed and complete requirement for these proteins in excitatory synaptic function.

Though we identified the necessity for PDZ-binding in ADAM22 function, it is unclear how ADAM23 maintains excitatory synaptic function. In addition to binding LGI1, the extracellular domain of ADAM23 has been shown to interact with integrins in heterologous systems (Cal et al., 2000; D'Abaco et al., 2006), though the specific integrins to which it can bind do not appear to be expressed in the brain (Lein et al., 2007). The very short, intracellular c-terminus of ADAM23 has no known interactions or protein homology domains. Further research on the functional interactions of ADAM23 will indeed prove useful in determining its mechanism of action at the synapse.

We also verified our previous results in an *in vitro* model, demonstrating that the loss of LGI1—not repeated seizures—reduces AMPAR-mediated transmission, and extended this finding to show that LGI1 specifically regulates synaptic content and not receptor surface expression. This role for LGI1 is comparable in different regions of the hippocampus, and is distinct from what has been observed in the mLGI1 transgenic mouse (Zhou et al., 2009). Because ADTLE is found in humans that are heterozygous for an LGI1 mutation, it is conceivable that the physiology in the mLGI1 is more representative of the human state than our knockout mouse. However, these mice do not have spontaneous seizures, so it is unclear how well they reflect the pathology in ADTLE patients. Regardless, we believe that our knockout mouse and molecular replacement techniques provide a valuable model for studying the endogenous function of LGI1 in synaptic transmission.

Secreted factors can originate from the presynaptic neuron, neighboring neurons, or nearby astrocytes (Siddiqui and Craig, 2011). LGI1 was initially identified as a potential tumor suppressor, due in part to its low level of expression in malignant gliomas (Chernova et al., 1998). However, in situ and immunohistochemical data

indicate sparse labeling of LGI1 expressing glia (Fukata et al., 2006; Fukata et al., 2010; Morante-Redolat et al., 2002; Piepoli et al., 2006; Senechal et al., 2005), implying that LGI1 may not have robust expression in healthy glia either. Our results show that presynaptic and neighboring neurons both serve as sufficient sources of LGI1.

We have previously demonstrated that exogenous application of LGI1 increases AMPAR-mediated transmission above wildtype levels (Fukata et al., 2006), though here we find that single cell expression of the protein rescues synaptic transmission to that of control cells. This implies that secretion of LGI1 may be regulated, such that the amount of extracellular LGI1 is tightly controlled to support healthy levels of transmission. An interesting subject of future research will be the mechanisms that controls LGI1 secretion and, in turn, normal synaptic transmission.

We have also shown here that in the absence of LGI1, PSD-95 function is greatly diminished—overexpression of PSD-95 in LGI1$^{-/-}$ neurons fails to enhance AMPAR-mediated transmission as it does it wildtype cells. LGI1 binds and regulates ADAM22 and ADAM23 synaptic localization (Yokoi et al., 2014). Moreover, LGI1 can oligomerize—forming homodimers, -trimers, and –tetramers (Fukata et al., 2010; Yokoi et al., 2014) giving it the ability to stabilize increasing numbers of ADAMs at the synapse (Leonardi et al., 2011). We propose a model in which increased extracellular LGI1 binds ADAMs, and acts through MAGUKs to strengthen excitatory synapses (Figure 13). This is supported by work showing that in juxtaparanodal regions ADAM22 is required for proper MAGUK localization (Ogawa et al., 2010).

Because ADAM23 lacks a PDZ binding domain, we believe that LGI1 preferentially acts through ADAM22, such that the effects of LGI1 expression are

mediated by ADAM22-PDZ domain interactions. This fits with our data showing that LGI1S473L, which cannot bind ADAM22 but still interacts with ADAM23 (Yokoi et al., 2014), is unable to rescue deficits in AMPAR-mediated transmission. Moreover, LGI1 preferentially binds ADAM22 *in vitro* (Yokoi et al., 2014), and is found bound to ADAM22 most often *in vivo* (Fukata et al., 2010). Thus, while ADAM22 and ADAM23 are important for the maintenance of synapses, it is likely the LGI1 acts through ADAM22 to regulate AMPAR-content.

What might account for the remaining synaptic ADAMs in the absence of LGI1? Previous work has shown that LGI2, implicated in canine epilepsy (Seppala et al., 2011), and LGI4, found to regulate myelination in the PNS (Ozkaynak et al., 2010) bind ADAM22 and ADAM23 (Nishino et al., 2010; Ozkaynak et al., 2010; Sagane et al., 2008; Seppala et al., 2011). Both family members are also found in CA1, though are expressed at much lower overall levels than LGI1 (Herranz-Perez et al., 2010), and appear to be localized to a specific subset of neurons (Lein et al., 2007). However, these proteins lack a unique insertion in the c-terminal epitempin (EPTP) domains that is thought to contribute to the ability of LGI1 to oligomerize (Leonardi et al., 2011). It is possible, then, that in the absence of LGI1, LGI2 and LGI4 act to stabilize ADAMs at the synapse, though lack the ability to oligomerize and recruit more AMPARs, rendering the remaining synapses weaker.

Over the last decade, the importance of synaptic organizing complexes in proper development and maturation of excitatory synapses has begun to be appreciated. This work uncovers two novel synaptic organizing proteins, ADAM22 and ADAM23, which are essential for excitatory transmission. Together with LGI1, these proteins form an epilepsy-associated transsynaptic organizing complex. A deeper understanding of this

critical complex is certain to contribute not only to our knowledge of the basic mechanisms of synaptic transmission, but also to the dysfunctions that produce these devastating neurological disorders.

Figure 1. Loss of ADAM22 results in a decreased number of functional excitatory synapses.

(A) Paired EPSC recordings made in ADAM22$^{fl/fl}$ slice culture show a significant reduction in AMPAR- (left, $p = 0.002$) and NMDAR-mediated (right, $p = 0.003$) EPSCs after Cre-mediated deletion of ADAM22. Scatter plots show individual paired recordings (open circles) and mean ± SEM (filled circle). Insets are representative traces from a paired recording of a wildtype (black) and ADAM22$^{fl/fl}$ cell (green). Scale bars represent 50 ms and 50 pA. Bar graphs show EPSC amplitude normalized to control (mean ± SEM). (B) Coefficient of variation analysis of AMPAR-mediated EPSCs in wildtype and ADAM22$^{fl/fl}$ cells reveals a change in quantal content after loss of ADAM22. Scatter plots show individual paired recordings (open circles), mean (filled circle), y=x line, and 95% confidence interval (dotted lines). (C) No difference in paired-pulse ratio was observed after Cre-mediated deletion of ADAM22 ($p = 0.27$, $n = 14$). Scale bar is 40 ms. Bar graphs show mean ratio ± SEM. (D) Loss of ADAM22 does not alter surface currents in CA1 pyramidal cells. Above, representative traces of glutamate-evoked currents in outside-out patches pulled from wildtype and ADAM22$^{fl/fl}$ neurons. Scale bars represent 2 s and 100 pA. Bar graphs show mean amplitude ± SEM.

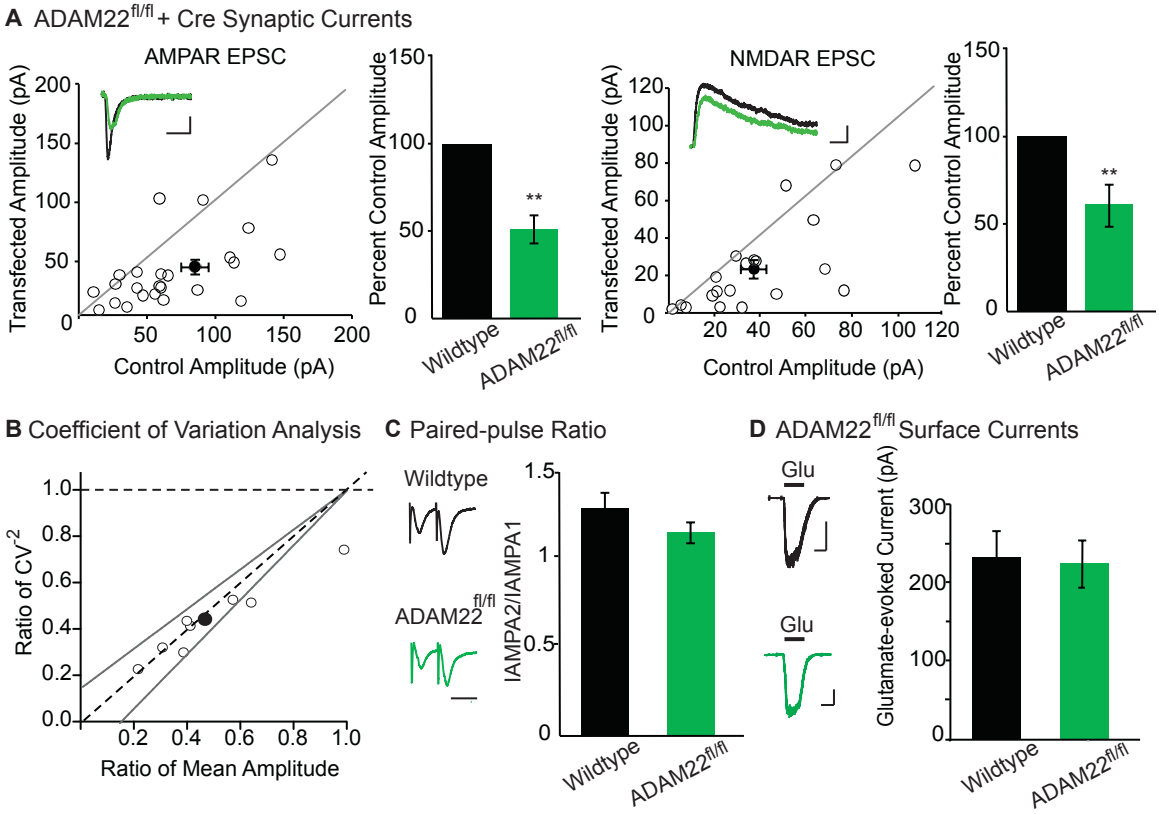
A ADAM22fl/fl + Cre Synaptic Currents
AMPAR EPSC
Transfected Amplitude (pA)
Control Amplitude (pA)
Percent Control Amplitude
Wildtype
ADAM22fl/fl
NMDAR EPSC
B Coefficient of Variation Analysis
Ratio of CV-2
Ratio of Mean Amplitude
C Paired-pulse Ratio
IAMPA2/IAMPA1
D ADAM22fl/fl Surface Currents
Glu
Glutamate-evoked Current (pA)

Figure 2. Loss of ADAM22 does not alter dendritic spine density.

(A) Diagram showing region of apical dendrite where spine density was quantified, and representative images of dendritic spines acquired from GFP or Cre expressing ADAM22$^{fl/fl}$ neurons. Scale bar represents 5 μm. (B) No significant difference in spine density was found in the presence or absence of ADAM22 ($p = 0.77$, $n = 9$). Bar graphs show mean density, error bars represent SEM.

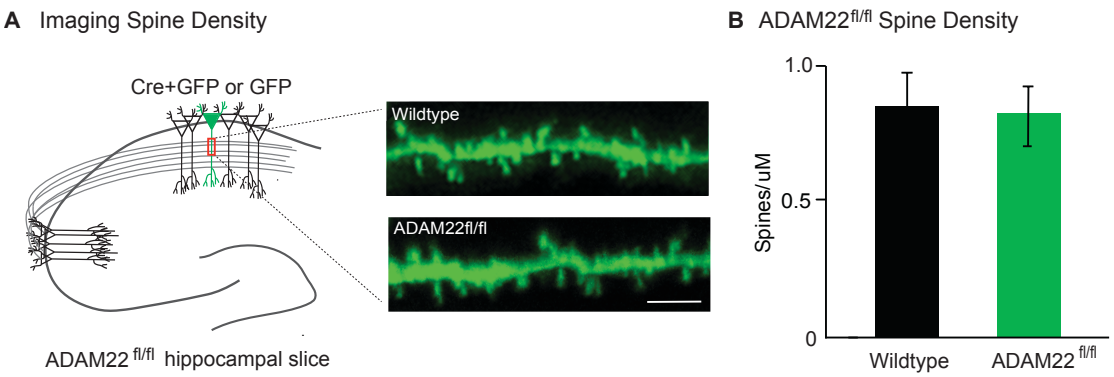
A Imaging Spine Density
Cre+GFP or GFP
Wildtype
ADAM22fl/fl
ADAM22 fl/fl hippocampal slice
B ADAM22fl/fl Spine Density
1.0
0.5
0
Spines/uM
Wildtype
ADAM22 fl/fl

Figure 3. ADAM22 function is dependent upon PDZ interactions.

(A) ADAM22 expression fully rescues the decrease in AMPAR and NMDAR-mediated transmission observed in ADAM22$^{fl/fl}$ cells. Left, diagram of protein domains in wildtype ADAM22. Scatter plots show individual paired recordings (open circles) and mean ± SEM (filled circle). Insets are representative traces from a paired recording of a wildtype (black) and ADAM22$^{fl/fl}$ cell (green). Scale bars represent 50 ms and 50 pA. (B) Expression of ADAM22 lacking the c-terminal PDZ binding domain (ADAM22dC4, left) is unable to rescue the AMPAR or NMDAR EPSC deficit in ADAM22$^{fl/fl}$ cells. (C) Summary bar graphs showing normalized mean ± SEM AMPAR and NMDAR EPSCs in wildtype, Cre, Cre +ADAM22 and Cre + ADAM22dC4 expressing cells. While wildtype ADAM22 is able to rescue both AMPAR and NDMAR-mediated EPSCs to wildtype levels ($p = 0.16$ and $p = 0.47$, respectively), expression of ADAM22dC4 fails to rescue AMPAR and NMDAR-mediated transmission ($p = 0.01$ and $p = 0.02$, respectively).

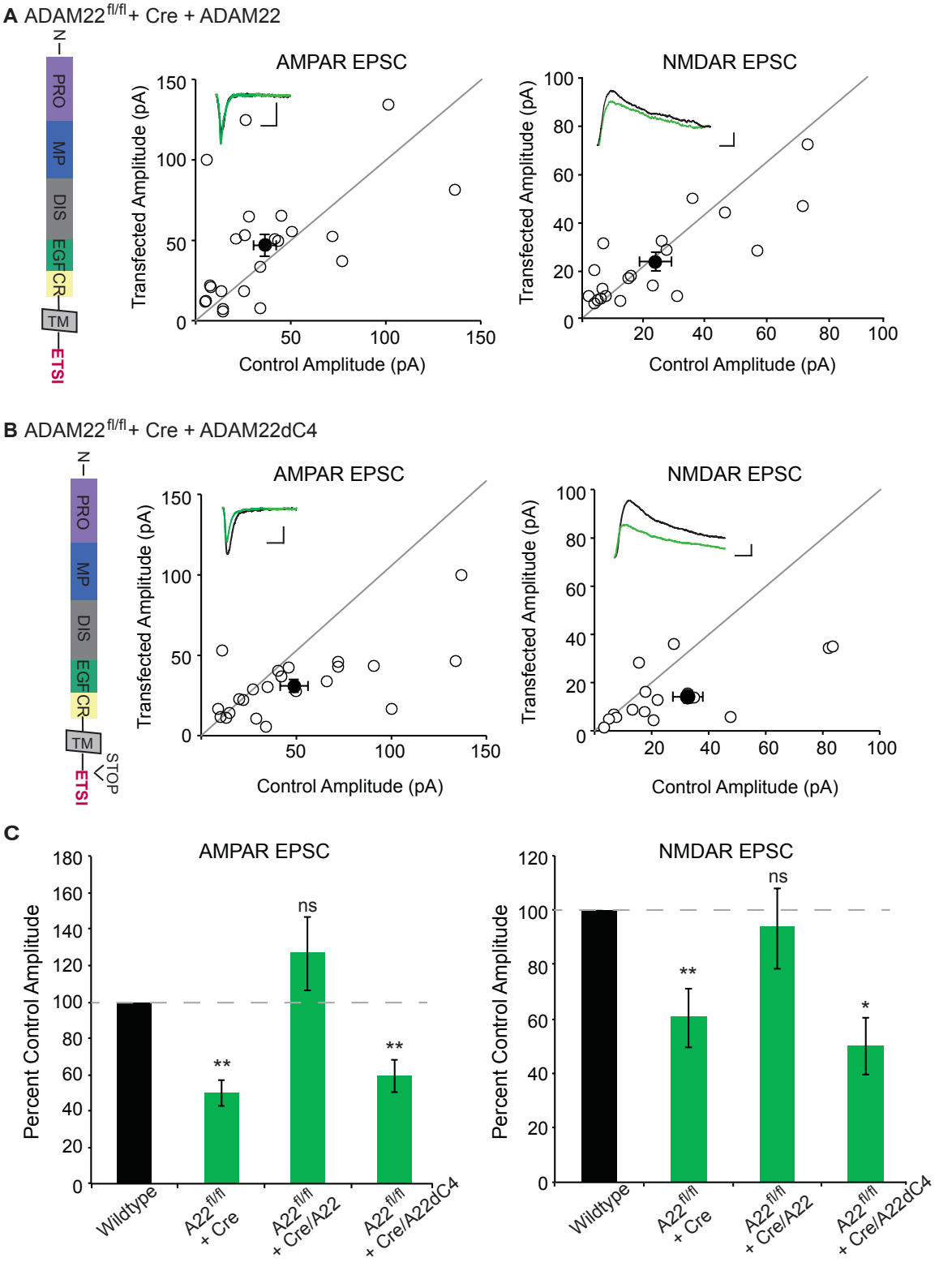
A ADAM22fl/fl + Cre + ADAM22
N
PRO
MIP
DIS
EGF
CR
TM
ETSI
AMPAR EPSC
Transfected Amplitude (pA)
Control Amplitude (pA)
NMDAR EPSC
Transfected Amplitude (pA)
Control Amplitude (pA)
B ADAM22fl/fl + Cre + ADAM22dC4
N
PRO
MIP
DIS
EGF
CR
TM
ETSI
STOP
AMPAR EPSC
Transfected Amplitude (pA)
Control Amplitude (pA)
NMDAR EPSC
Transfected Amplitude (pA)
Control Amplitude (pA)
C
AMPAR EPSC
Percent Control Amplitude
ns
**
**
Wildtype
A22fl/fl + Cre
A22fl/fl + Cre/A22
A22fl/fl + Cre/A22dC4
NMDAR EPSC
Percent Control Amplitude
ns
**
*
Wildtype
A22fl/fl + Cre
A22fl/fl + Cre/A22
A22fl/fl + Cre/A22dC4

Figure 4. Surface localization and LGI1 binding of ADAM22dC4 mutant.

(A) FAH-tagged ADAM22 was expressed in dissociated neurons. (B) Surface bound LGI1 (red), surface ADAM22 (green), and total ADAM22 (blue) were labeled. Wildtype ADAM22 is surface localized and binds extracellular LGI1. ADAM22 lacking the PDZ binding motif (ADAM22dC4) is also surface localized and able to bind extracellular LGI1. Scale bar represents 10 μm.

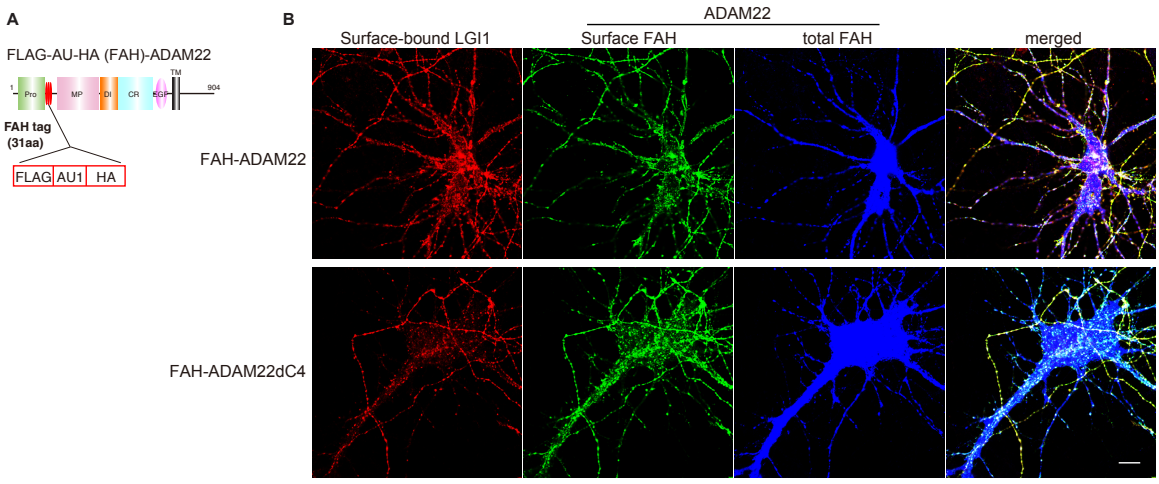
A
FLAG-AU-HA (FAH)-ADAM22
1
Pro
MP
DI
CR
EGF
TM
904
FAH tag
(31aa)
FLAG
AU1
HA
B
ADAM22
Surface-bound LGI1
Surface FAH
total FAH
merged
FAH-ADAM22
FAH-ADAM22dC4

Figure 5. ADAM22 and ADAM23 are essential for excitatory synaptic transmission.

(A) Knockdown of ADAM23 in wildtype neurons results in reduced AMPAR ($p < 0.001$) and NMDAR-mediated ($p < 0.01$) currents. Scatter plots show individual paired recordings (open circles) and mean ± SEM (filled circle). Scale bars represent 50 ms and 50 pA. Bar graphs show normalized mean ± SEM. (B) Reduced ADAM23 expression has no effect on paired-pulse ratio ($p = 0.96$, $n = 9$). Bar graphs shows mean ratio ± SEM. (C) Knockdown of ADAM23 in ADAM22$^{-/-}$ neurons leads to an almost complete abolishment of synaptic transmission. Both AMPAR and NMDAR-mediated EPSCs are reduced by 90%. (D) Loss of ADAM23 in ADAM22KO does not significantly affect paired-pulse ratio ($p = 0.19$, $n = 5$). Bar graphs shows mean ratio ± SEM.

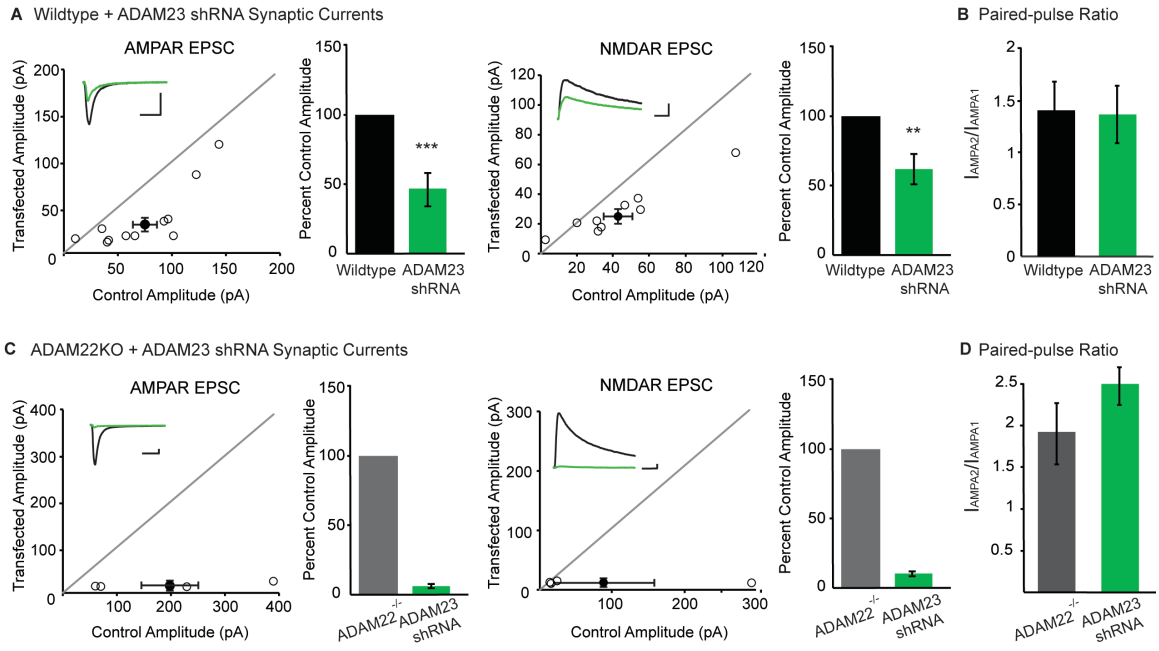
A Wildtype + ADAM23 shRNA Synaptic Currents
AMPAR EPSC
Transfected Amplitude (pA)
Control Amplitude (pA)
Percent Control Amplitude
***
Wildtype
ADAM23 shRNA
NMDAR EPSC
Transfected Amplitude (pA)
Control Amplitude (pA)
Percent Control Amplitude
**
Wildtype
ADAM23 shRNA
B Paired-pulse Ratio
I_{AMPA2}/I_{AMPA1}
Wildtype
ADAM23 shRNA
C ADAM22KO + ADAM23 shRNA Synaptic Currents
AMPAR EPSC
Transfected Amplitude (pA)
Control Amplitude (pA)
Percent Control Amplitude
ADAM22 -/-
ADAM23 shRNA
NMDAR EPSC
Transfected Amplitude (pA)
Control Amplitude (pA)
Percent Control Amplitude
ADAM22 -/-
ADAM23 shRNA
D Paired-pulse Ratio
I_{AMPA2}/I_{AMPA1}
ADAM22 -/-
ADAM23 shRNA

Figure 6. Loss of LGI1 selectively alters postsynaptic strength.

(A) Timeline of experimental preparation for hippocampal slice cultures and recordings as compared to the LGI1$^{-/-}$ phenotype. (B) AMPA/NMDA ratios recorded in slice cultures made from LGI1$^{-/-}$ mice are significantly reduced ($p = 0.03$, $n = 15$) compared to wildtype. Left, sample traces of wildtype (black) and LGI1$^{-/-}$ (gray) recorded at -70 mV and +40 mV. Scale bar represents 50 ms and 50 pA. Right, bar graphs showing average AMPA/NMDA ratios ± SEM in wildtype and LGI1$^{-/-}$. (C) Paired-pulse stimulation reveals no significant difference ($p = 0.46$, $n = 16$) in presynaptic release probability in LGI1$^{-/-}$ relative to wildtype. Left, sample traces. Scale bar represents 40 ms. Right, average ratio ± SEM. (D) Miniature EPSC recordings in wildtype and LGI1$^{-/-}$. Loss of LGI1 results in a significant decrease in amplitude ($p = 0.05$, $n = 15$), but not frequency ($p = 0.21$, $n = 16$), of mEPSCs. Bar graphs of average amplitude and frequency of mEPSCs ± SEM, with example traces for each condition shown above. Scale bars represent 25 ms and 10 pA (amplitude traces), and 100 ms and 10 pA (frequency traces). (E) Outside-out patch recordings in wildtype and LGI1$^{-/-}$ cells have similar glutamate-evoked currents ($p = 0.84$, $n = 13$). Top, sample traces of wildtype and LGI1$^{-/-}$ surface currents. Scale bars represent 2s and 100 pA. Bottom, average glutamate-evoked currents ± SEM.

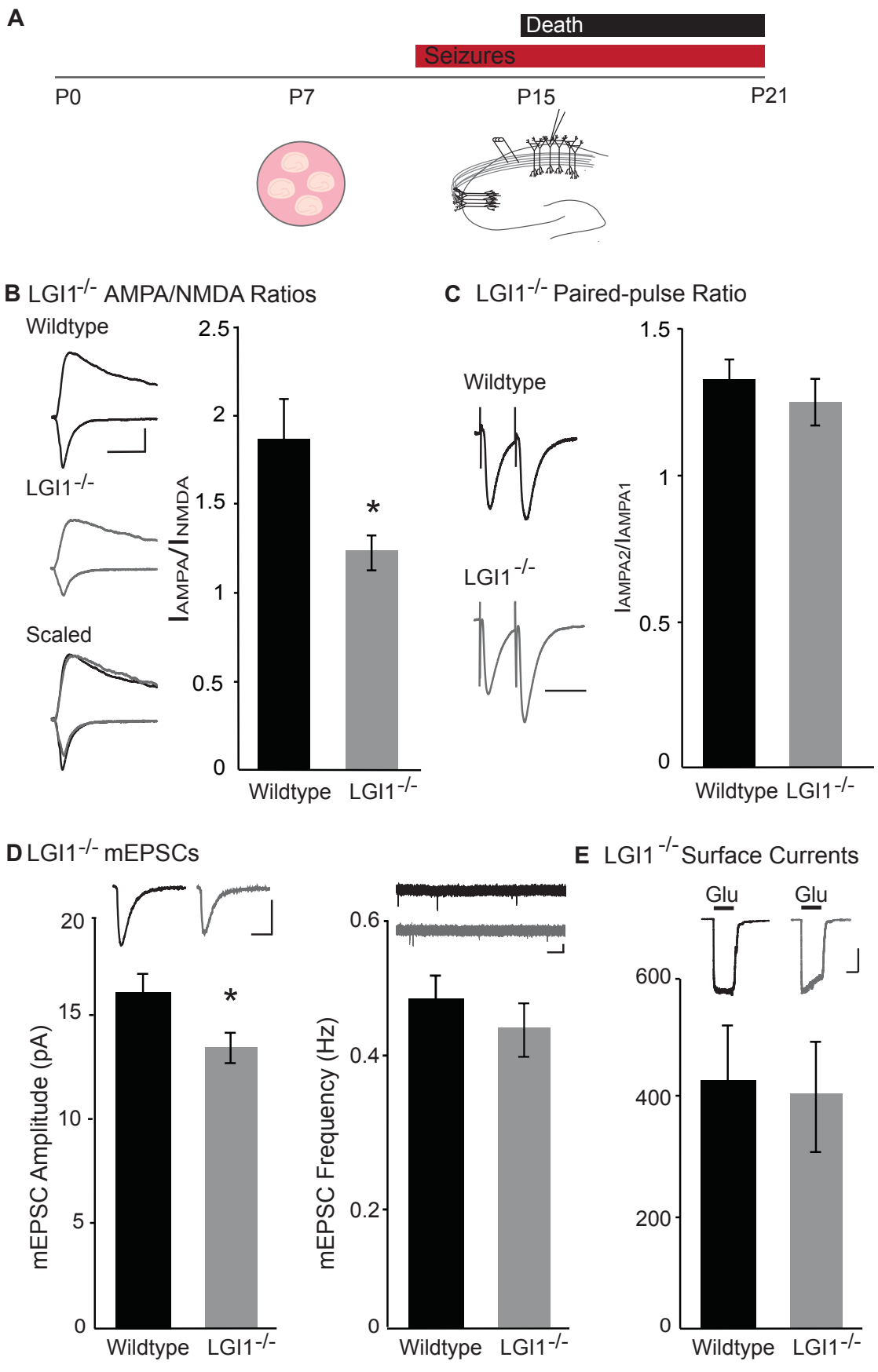
A
Death
Seizures
P0
P7
P15
P21
B LGI1-/- AMPA/NMDA Ratios
Wildtype
LGI1-/-
Scaled
IAMPA/INMDA
2.5
2
1.5
1
0.5
0
*
Wildtype
LGI1-/-
C LGI1-/- Paired-pulse Ratio
Wildtype
LGI1-/-
IAMPA2/IAMPA1
1.5
1
0.5
0
Wildtype
LGI1-/-
D LGI1-/- mEPSCs
mEPSC Amplitude (pA)
20
15
10
5
0
*
Wildtype
LGI1-/-
mEPSC Frequency (Hz)
0.6
0.4
0.2
0
Wildtype
LGI1-/-
E LGI1-/- Surface Currents
Glu
Glu
600
400
200
0
Wildtype
LGI1-/-

Figure 7. The LGI1$^{-/-}$ mouse phenotype is distinct from the LGI1 835delC transgenic.

(A) Loss of LGI1 leads to a significant decrease in AMPA/NMDA ratio in dentate gyrus granule cells ($p = 0.03$, $n = 8$). Bar graphs show average ratio ± SEM. (B) The decay rates of NMDAR-mediated currents recorded in the presence of NBQX were the same between wildtype and LGI1$^{-/-}$ ($p = 0.65$, $n = 15$). Bar graphs show mean decay rate ± SEM. (C) LGI1 expression has no impact on paired-pulse ratio recorded in the dentate gyrus ($p = 0.96$, $n = 8$). Bar graphs show average PPR ± SEM.

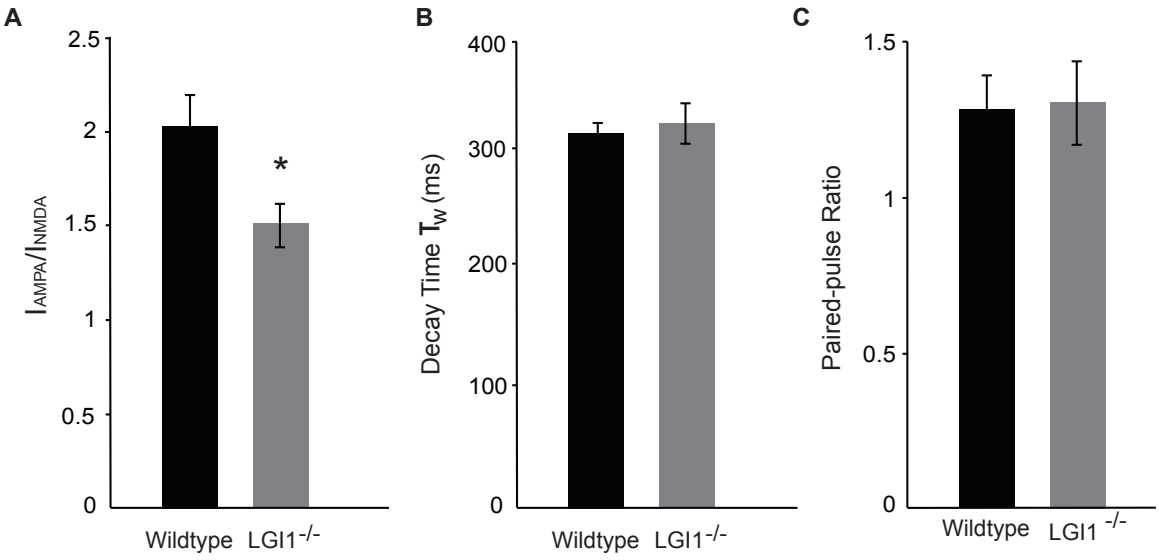
A
2.5
2
1.5
1
0.5
0
I_{AMPA}/I_{NMDA}
*
Wildtype
LGI1-/-
B
400
300
200
100
0
Decay Time T_W (ms)
Wildtype
LGI1-/-
C
1.5
1
0.5
0
Paired-pulse Ratio
Wildtype
LGI1 -/-

Figure 8. LGI1 is a paracrine signal derived from the pre and postsynaptic cell.

(A) The size of AMPAR- and NMDAR-mediated EPSCs in LGI1$^{-/-}$ cells expressing LGI1 are the same as nearby untransfected LGI1$^{-/-}$ cells ($p = 0.09$, $p = 0.49$, $n = 17$). Scatter plots show individual paired recordings (open circles) and mean ± SEM (filled circle). Example traces of LGI1$^{-/-}$ (black) and LGI1$^{-/-}$ + LGI1 (gray), inset. Scale bars represent 50 ms and 50 pA. (B) Recording set up of naïve control cell in LGI1$^{-/-}$ slice and control cell nearby LGI1 overexpressing cell in LGI1$^{-/-}$ slice. (C) The AMPA/NMDA ratio of untransfected, nearby control cells in the LGI1$^{-/-}$ biolistically transfected slices is significantly higher than cells from naïve LGI1$^{-/-}$ slices ($p = 0.03$, $n = 15$). Unlike wildtype LGI1, LGI1S473L does not alter the AMPA/NMDA ratio of nearby cells ($p = 0.71$, $n = 13$). Bar graphs show average ratio ± SEM. (D) Viral injections of LGI1 in CA3 and dentate gyrus neurons were carried out to test the source of active LGI1. Injection sites in CA3 (presynaptic) and DG (nonsynaptic) of LGI1 lentivirus are shown in green. Recordings were made in CA1 pyramidal cells for both experiments. (E) Following LGI1 expression in CA3, neurons of CA1 have an AMPA/NMDA ratio similar to that of wildtype CA1 cells ($p = 0.55$, $n = 20$). However, AMPA/NMDA ratios remain similar to LGI1$^{-/-}$ levels when LGI1 is expressed in the dentate gyrus ($n = 20$, $p = 0.81$). Bar graphs show mean AMPA/NMDA ratio in wildtype, LGI1$^{-/-}$, LGI1$^{-/-}$ with CA3 expression, and LGI1$^{-/-}$ with dentate gyrus expression.

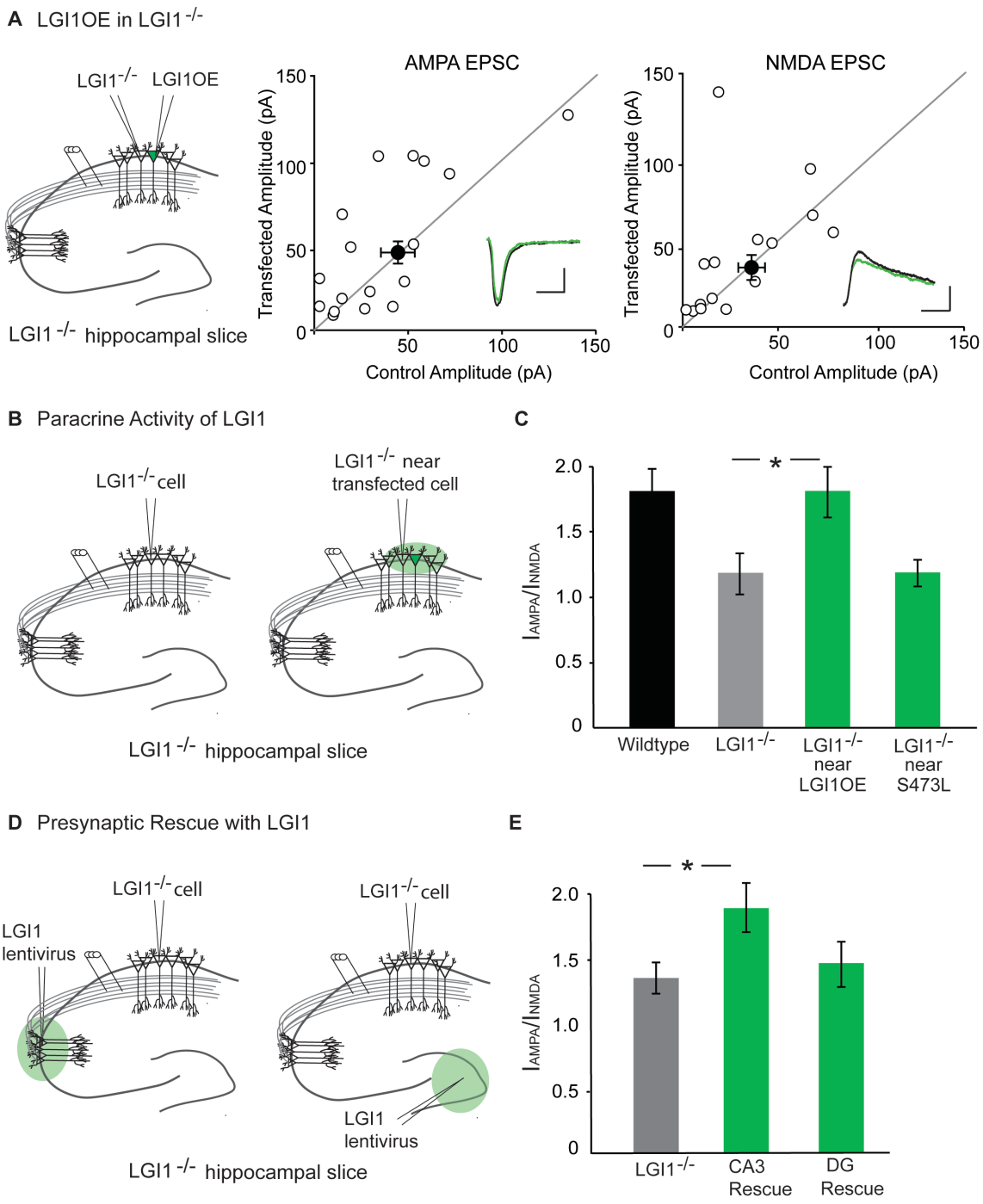
A LGI1OE in LGI1 -/-
LGI1 -/-
LGI1OE
LGI1 -/- hippocampal slice
AMPA EPSC
NMDA EPSC
Transfected Amplitude (pA)
Control Amplitude (pA)
150
100
50
0
50
100
150
B Paracrine Activity of LGI1
LGI1 -/- cell
LGI1 -/- near transfected cell
LGI1 -/- hippocampal slice
C
*
IAMPA/INMDA
2.0
1.5
1.0
0.5
0
Wildtype
LGI1 -/-
LGI1 -/- near LGI1OE
LGI1 -/- near S473L
D Presynaptic Rescue with LGI1
LGI1 -/- cell
LGI1 lentivirus
LGI1 -/- hippocampal slice
E
LGI1 -/-
CA3 Rescue
DG Rescue

Figure 9. LGI1S473L has no effect on AMPAR or NMDAR EPSCs.

(A) Paired recordings were carried out in control, LGI1$^{-/-}$ and neighboring, biolistically transfected LGI1S473L-expressing cells in LGI1$^{-/-}$ slices. (B) Expression of LGI1S473L does not alter AMPAR-mediated EPSCs ($p = 0.67$). Scatter plots show individual paired recordings (open circles) and mean ± SEM (filled circle). Scale bars represent 25 ms and 25 pA. (C) NMDAR-mediated EPSCs are also unchanged relative to LGI1$^{-/-}$ cells ($p = 0.60$, $n = 8$). Scale bars represent 50 ms and 50 pA.

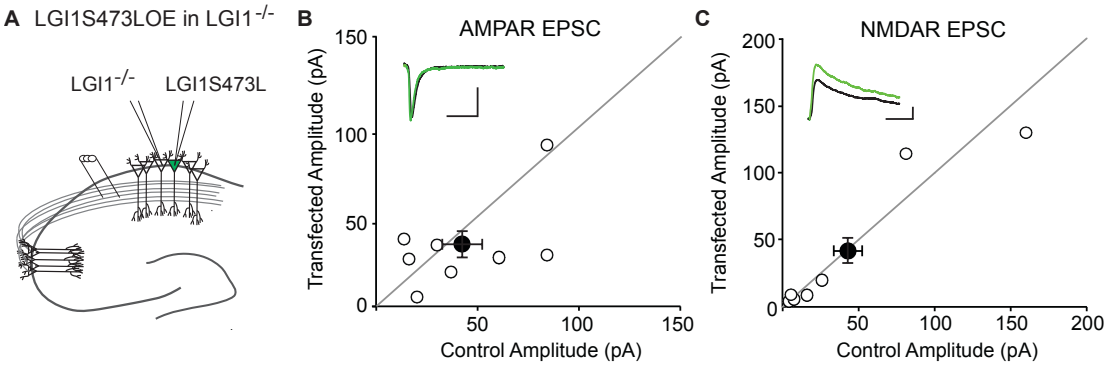
A LGI1S473LOE in LGI1 -/-
LGI1 -/-
LGI1S473L
B
AMPAR EPSC
Transfected Amplitude (pA)
Control Amplitude (pA)
0
50
100
150
C
NMDAR EPSC
Transfected Amplitude (pA)
Control Amplitude (pA)
0
50
100
150
200

Figure 10. LGI1 is localized to the axons and dendrites of a neuron.

(A) Diagram of insertion site of LGI1 after Prox1 promoter. (B) Labeling of LGI1 in wildtype and LGI1$^{-/-}$; Prox1-LGI1 slices. While LGI1 expression is uniform across the hippocampus in the wildtype slice, it is specifically localized to the molecular layer (site of granule cell dendrites) and mossy fiber axon tract.

A Generation of Prox1-LGI1 mouse

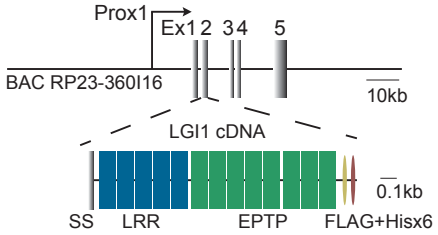

B Hippocampal Slice LGI1 Immunoreactivity

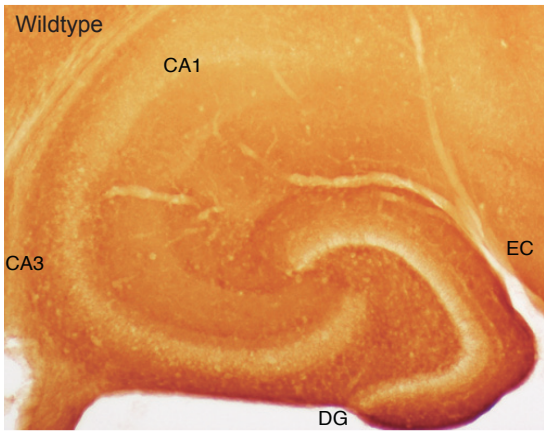

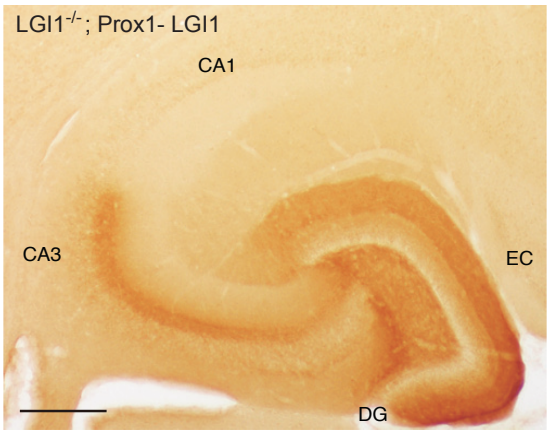

Figure 11. LGI1 and ADAM22 have a similar role in proximal, SR and distal, SLM synapses.

(A) Recordings of AMPA/NMDA ratios in wildtype and LGI1$^{-/-}$ acute slices show that loss of LGI1 results in a similar decrease in synaptic transmission in SR (n = 6, p = 0.05) and SLM (n = 5, p = 0.10). Bar graphs show mean ± SEM. (B) Acute slices were made from Cre-electroporated ADAM22$^{fl/fl}$ mice and paired-recordings collected from wildtype and ADAM22$^{fl/fl}$ cells. Effects on AMPAR and NMDAR-mediated transmission are similar in SR (p = 0.004 and p = 0.01, respectively) and SLM (p = 0.05 and p = 0.01, respectively) of ADAM22$^{fl/fl}$. Scatter plots show individual paired recordings (open circles) and mean ± SEM (filled circle). Black points are pairs recorded after stimulation in SR, gray points are recordings from the same cell after the stimulation electrode was moved to SLM. Bar graphs show mean ± SEM.

A LGI1$^{-/-}$ AMPA/NMDA Ratios

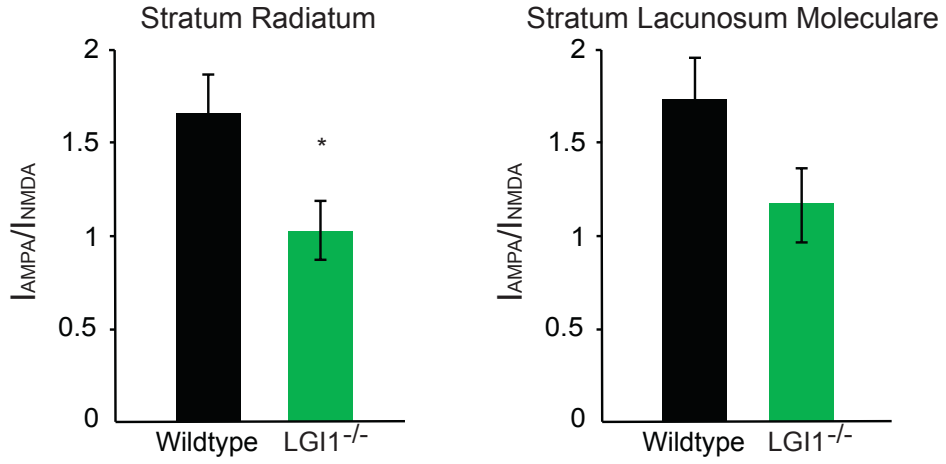

B ADAM22$^{fl/fl}$ Synaptic Currents

AMPAR EPSC

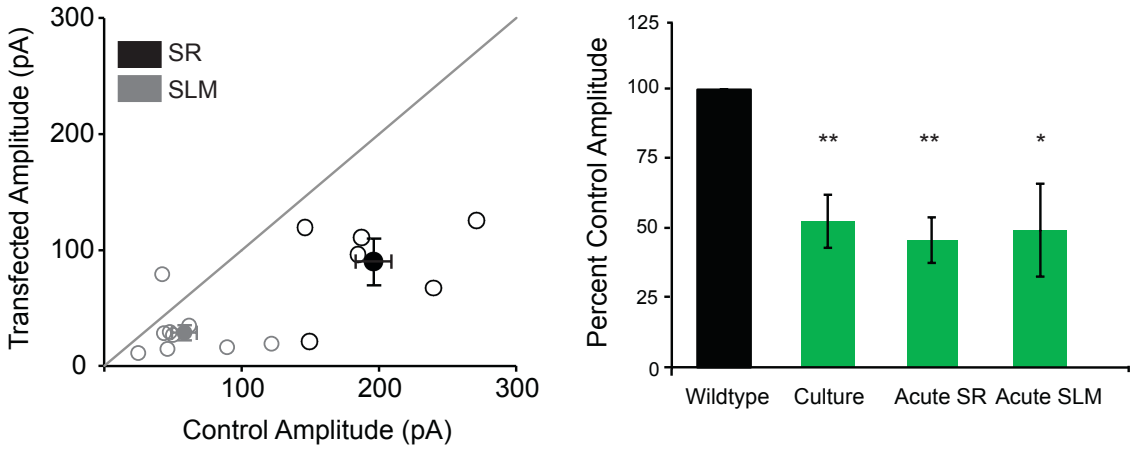

NMDAR EPSC

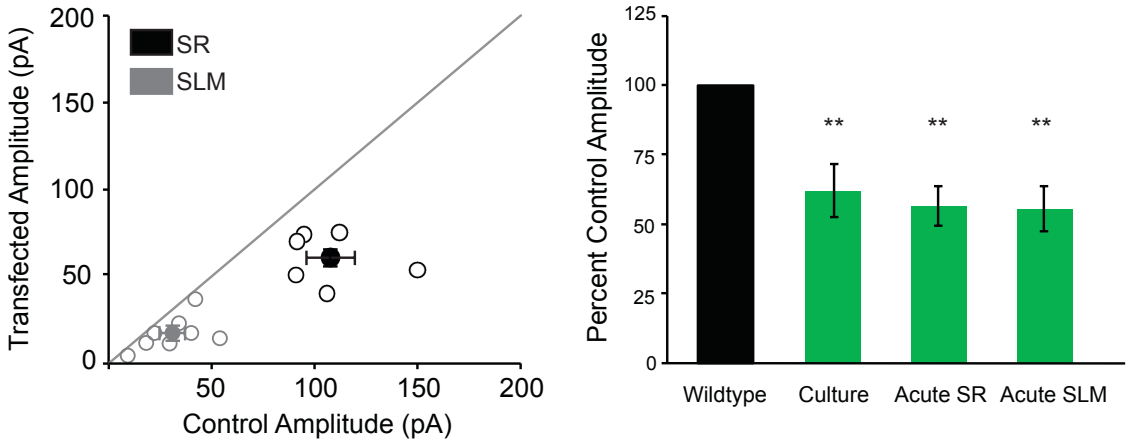

Figure 12. LGI1 is required for MAGUK function at excitatory synapses.

(A) Scatter plot of AMPAR, left, and NMDAR, right, EPSC amplitudes recorded from wildtype and PSD-95 overexpressing cells. Representative traces of paired recordings are shown as insets. Scale bars represent 50 ms and 50 pA. (B) Scatter plot of AMPAR, left, and NMDAR, right, EPSC amplitudes recorded from LGI1$^{-/-}$ control and LGI1$^{-/-}$ cells overexpressing PSD-95. Scale bars represent 50 ms and 25 pA. (C) Summary bar graphs showing the mean ± SEM AMPAR EPSC and NMDAR EPSC of experiments in A and B. Overexpression of PSD-95 in wildtype slice culture results in a 3 fold increase in AMPAR-mediated transmission ($p = 0.0001$) and no change in NMDAR EPSCs ($p = 0.69$). Overexpression of PSD-95 in LGI1$^{-/-}$ slices has a slight, but significant effect on AMPAR EPSCs ($p = 0.05$), without altering NMDAR EPSCs ($p = 0.88$).

A PSD-95 Overexpression in Wildtype

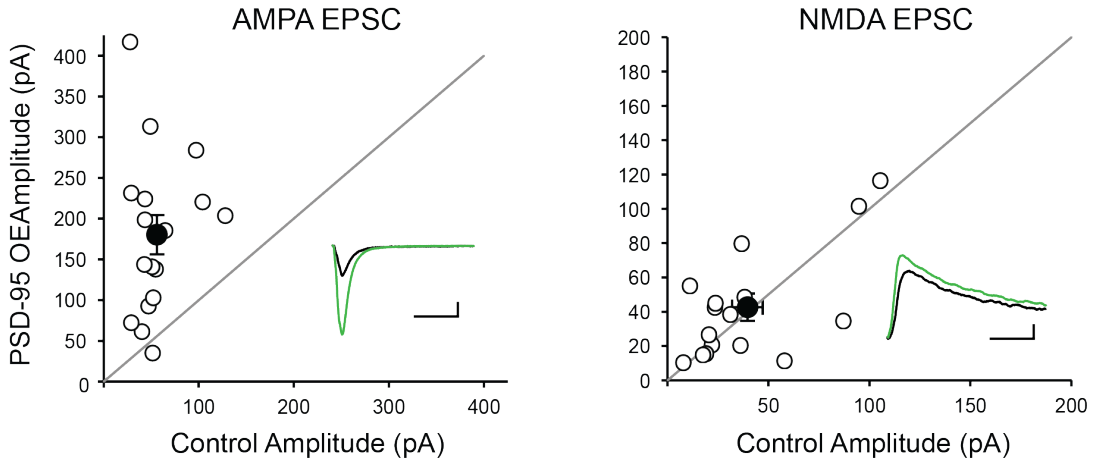

B PSD-95 Overexpression in LGI1$^{-/-}$

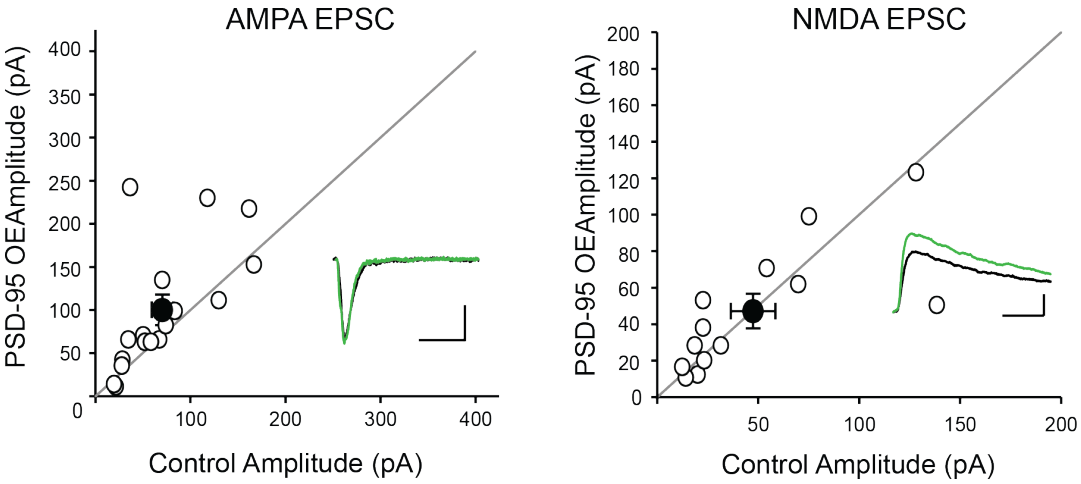

C Summary graph of PSD-95 Overexpression

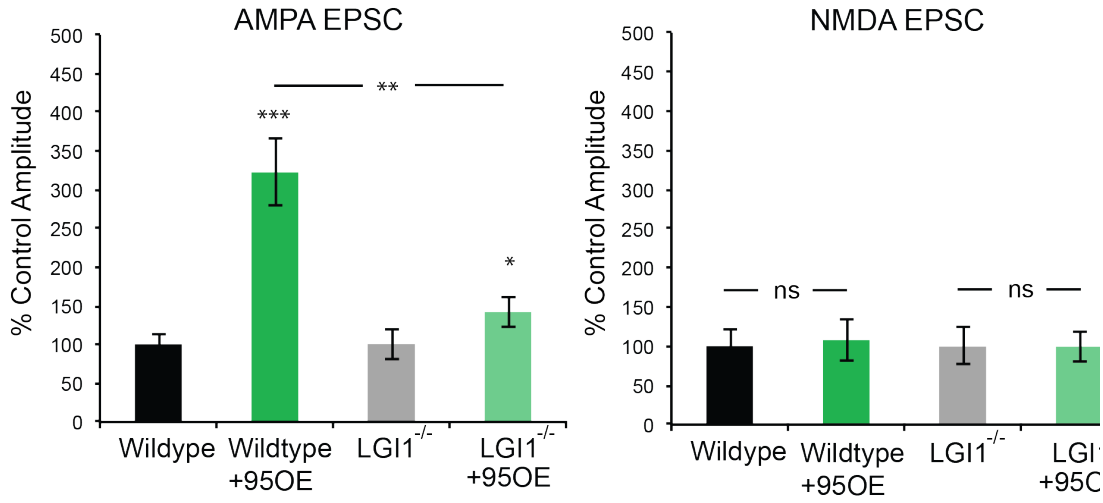

Figure 13. Proposed model of the LGI1-ADAM organizing complex

Left, ADAM22 and ADAM23 act to maintain excitatory synapses. Right, LGI1 secreted from pre and postsynaptic neurons increases the synaptically localized ADAMs and, in turn, functional MAGUK interactions, resulting in increased AMPAR-content at the synapse.

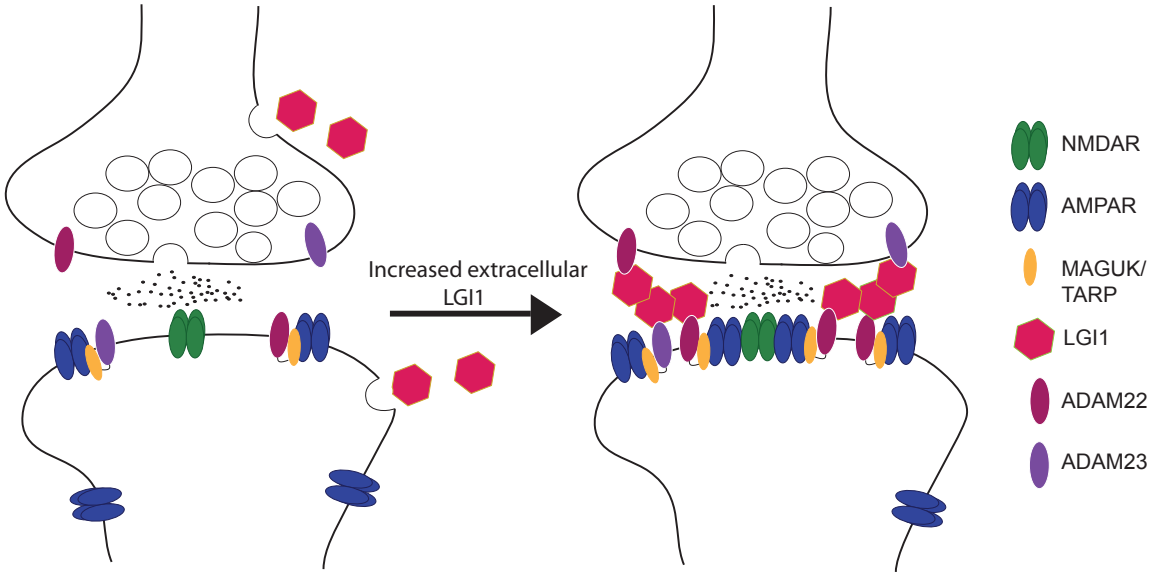
Increased extracellular
LGI1
NMDAR
AMPAR
MAGUK/
TARP
LGI1
ADAM22
ADAM23

CHAPTER 5:

SynDIG1 promotes excitatory synaptogenesis independent of AMPA receptor trafficking and biophysical regulation

Introduction

The AMPA-type ionotropic glutamate receptors (AMPARs) underlie fast, excitatory synaptic transmission and plasticity in the brain (Jonas, 2000) (Malinow and Malenka, 2002). For years, the functional diversity of these tetrameric receptors was thought to originate solely from their subunit composition, which confer different biophysical properties and roles in synaptic transmission (Traynelis et al., 2010) (Mayer, 2005). Over the last decade, however, it has become clear that AMPAR function is also dependent on a multitude of interacting proteins, termed auxiliary subunits. AMPAR auxiliary subunits are typically defined as transmembrane proteins that bind directly to AMPARs, and, similar to other ion channel auxiliary subunits, alter ER trafficking, surface localization, subcellular targeting, and modulation of receptor biophysical properties (Arikkath and Campbell, 2003) (Vacher et al., 2008) (Pongs and Schwarz, 2010) (Jackson and Nicoll, 2011). Studies of the different known AMPAR auxiliary subunits—including TARPs, CNIHs, CKAMP44, and GSG1L—have begun to elucidate the varying impact each has on AMPAR function and localization (Schwenk et al., 2009) (von Engelhardt et al., 2010) (Shi et al., 2010) (Jackson et al., 2011) (Shanks et al., 2012), contributing greatly to our understanding of the diverse functional roles of AMPARs in the brain.

Recently, Synapse Differentiation Induced Gene 1 (SynDIG1) was identified as an AMPAR-interacting protein that regulates synaptic AMPAR content (Kalashnikova et al., 2010). A type II transmembrane protein, its extracellular c-terminus was shown to bind directly to the AMPAR subunit GluA2 in COS-7 cells. Overexpression of SynDIG1 in dissociated hippocampal neurons led to a dramatic increase in miniature excitatory postsynaptic current (mEPSC) amplitude and frequency, along with increases in the

density and size of AMPAR-containing synaptic puncta. shRNA-mediated knockdown of SynDIG1 had the opposite effect, greatly reducing mEPSC frequency and amplitude, while also decreasing the density and size of AMPAR-containing synaptic puncta. Yet, the mechanism by which changing SynDIG1 levels altered synaptic AMPAR-mediated transmission remains unstudied. Imaging of dissociated neurons showed a larger percentage of SynDIG1 colocalized with AMPARs at extrasynaptic than synaptic sites, and SynDIG1 expression levels positively correlated with surface AMPAR labeling (Kalashnikova et al., 2010), implying that SynDIG1 may regulate the surface trafficking of AMPARs. Additionally, owing to its binding to AMPARs, it is also possible that SynDIG1 alters AMPAR-mediated synaptic transmission by direct modification of channel gating properties.

In this study, we set out to further characterize the effect of SynDIG1 on excitatory transmission and determine if SynDIG1 acts as an auxiliary subunit of AMPARs. Through a battery of electrophysiological measurements, we show that SynDIG1 has no direct effect on AMPAR gating properties modulated by known auxiliary subunit interaction—including ligand binding affinity, deactivation, desensitization, and rectification—nor does SynDIG1 alter the surface trafficking of AMPARs. Instead, using hippocampal slice cultures, we make the surprising finding that in addition to regulating synaptic AMPARs, SynDIG1 also regulates NMDA receptor (NMDAR)-mediated transmission. We go on to show that SynDIG1 expression levels control the number of functional excitatory synapses in the hippocampus. Thus, we conclude that SynDIG1 does not act as a typical auxiliary subunit of AMPARs, but rather is a regulatory protein for excitatory synaptogenesis.

Results

SynDIG1 does not influence channel gating or surface trafficking

Because SynDIG1 can bind directly to GluA2 (Kalashnikova et al., 2010), we questioned if SynDIG1 acts as an auxiliary subunit and alters AMPAR-mediated transmission by directly regulating biophysical properties and surface expression of AMPARs. We first examined the effect SynDIG1 expression has on AMPAR biophysical properties. Coexpression of the AMPAR auxiliary subunit TARP γ-2 with GluA2(Q)—the unedited form of the receptor that generates much larger currents—in HEK cells results in a highly significant increase in the response to kainate versus glutamate application, in agreement with previous findings that TARP association greatly increases kainate sensitivity of AMPARs (Jackson and Nicoll, 2011). In contrast, whole cell current responses to either glutamate or kainate application recorded from HEK cells expressing both GluA2 and SynDIG1 were indistinguishable from the responses of HEK cells expressing GluA2 alone (Figure 1A and B).

A signature of the TARP and CNIH auxiliary subunit interaction with AMPA receptors is a decrease in the block by intracellular polyamines at positive membrane potentials, detectable in the current-voltage relationship as reduced inward rectification (Soto et al., 2007) (Shi et al., 2010). We recorded current-voltage relationships from outside-out patches obtained from HEK cells expressing GluA1 and GluA2 alone or in combination with SynDIG1 and found that SynDIG1 expression did not result in a change in AMPAR rectification, indicating that SynDIG1 expression does not affect intracellular polyamine affinity (Figure 1C).

Additionally, AMPAR-interacting proteins, such as TARPs and CKAMP44, have been shown to slow the deactivation time constant of AMPAR-mediated currents (Tomita et al., 2005) (Schwenk et al., 2009) (von Engelhardt et al., 2010). Yet, when we compared the deactivation rates after co-expression of SynDIG1 with GluA2, we observed no significant change in the deactivation time constant as compared to cells expressing GluA2 alone (Figure 1D). Similarly, when we measured AMPAR desensitization, another biophysical property altered by auxiliary subunit binding (von Engelhardt et al., 2010) (Shi et al., 2010) (Shanks et al., 2012) (Tomita et al., 2005), no difference was observed in cells expressing GluA2 alone or coexpressing GluA2 and SynDIG1 (Figure 1E).

Finally, it has been shown that CNIH, TARP, CKAMP44, GSGL1 auxiliary subunits alter the surface expression of AMPARs (Herring et al., 2013) (Shi et al., 2010) (Chen et al., 2000) (von Engelhardt et al., 2010) (Shanks et al., 2012). To test if SynDIG1 regulates surface trafficking of AMPARs, S-AMPA was applied locally to the cell bodies of simultaneously recorded neighboring control and SynDIG1 shRNA expressing neurons in biolistically transfected slice cultures. The amplitude of the current in response to S-AMPA was indistinguishable in wildtype and transfected neurons, indicating that surface expression of AMPARs remains unchanged after loss of SynDIG1 (Figure 1F). As a positive control, we repeated this experiment with shRNA against the known AMPAR auxiliary subunit CNIH2 instead of SynDIG1. Conditional knockout of CNIH2 has been shown to reduce the current response to fast application of glutamate by 50%, as measured through outside-out patch recordings (Herring et al., 2013). Using our local application method, we find a similar reduction in surface AMPARs, with CNIH2 shRNA expressing neurons having an average current response that is 60%

smaller than wildtype (Figure 1F). Taken together, the gating, pharmacological, and surface expression data indicates that SynDIG1 does not act as a typical AMPAR auxiliary subunit by modulating biophysical properties or trafficking of AMPARs.

Overexpression of SynDIG1 increases excitatory synaptic transmission

Having found that SynDIG1 does not act as an auxiliary subunit to AMPARs, we sought to better understand the effects of SynDIG1 on excitatory transmission by further characterizing the changes in synaptic transmission that occur in response to varying SynDIG1 levels. Previous research on SynDIG1's role in synaptic transmission was carried out in dissociated hippocampal culture and only examined mEPSCs. We chose to more closely examine the effect of varying SynDIG1 levels using hippocampal slice cultures—a system that largely maintains the complex architecture of hippocampus, allowing for measurements of evoked transmission and the study of multiple features of synaptic transmission. Using biolistic transfection of hippocampal slice culture, we first overexpressed SynDIG1 in single hippocampal CA1 neurons and simultaneously recorded synaptic activity from transfected and neighboring control neurons in response to stimulation of Schaffer collaterals. We found that overexpression of SynDIG1 caused a doubling in AMPAR EPSCs compared to untransfected control neurons (Figure 2A). Surprisingly, in addition to the effect on AMPAR EPSCs, we also observed a significant increase in NMDAR-mediated EPSCs (Figure 2B).

Knockdown of SynDIG1 decreases excitatory synaptic transmission

If the increase in baseline synaptic transmission upon SynDIG1 overexpression reflects the endogenous role of the protein, reducing SynDIG1 expression should result in the opposite effect. To test this, we knocked down SynDIG1 using biolistic transfection of an shRNA that reduces SynDIG1 protein levels by 75% (Kalashnikova et al., 2010). Simultaneous recordings of shRNA-expressing neurons and neighboring control neurons revealed a 40% decrease in both AMPAR-mediated (Figure 3A) and NMDAR-mediated EPSCs (Figure 3B), consistent with the conclusion that SynDIG1 expression levels regulate both AMPAR- and NMDAR-mediated transmission.

SynDIG1 expression does not alter presynaptic release probability

A simultaneous change in both AMPAR- and NMDAR-mediated EPSCs can reflect a change in presynaptic transmitter release. To determine if the effect of SynDIG expression on excitatory transmission was driven by a change in presynaptic release probability, we compared the paired-pulse ratio of control neurons and neurons transfected with SynDIG1 or SynDIG1 shRNA. We did not detect a significant difference in the paired-pulse ratio between control and SynDIG1-overexpressing neurons (Figure 4A), nor did we observe a change in paired-pulse ratio after knockdown of SynDIG1 (Figure 4B), indicating that the change in EPSCs after manipulation of SynDIG1 expression reflects an change in total synapse number or postsynaptic strength, not a difference in presynaptic release properties.

SynDIG1 supports excitatory synaptogenesis

Because SynDIG1 does not regulate presynaptic probability of release (Figure 4), the observed influence of SynDIG1 on synaptic transmission can either be due to a change in the number of synapses or the strength of existing synapses. To determine which of these two possibilities underlies the effects of SynDIG1 on EPSCs, we performed a coefficient of variation analysis of paired AMPAR EPSCs recorded from control cells and cells expressing SynDIG1 shRNA. In this analysis, a positive correlation between the ratio of transfected versus control coefficient of variation and the ratio of mean EPSC size indicates that fewer synapses are activated during smaller EPSCs, whereas no correlation indicates that fewer receptors per synapse are activated during smaller EPSCs (Bekkers and Stevens, 1990; Del Castillo and Katz, 1954; Manabe et al., 1993). We found that the shRNA-induced reduction in mean EPSC amplitude is correlated with a reduction in the ratio of the coefficient of variation (Figure 5A), suggesting that loss of SynDIG1 leads to a loss of excitatory synapses. To more directly quantify these changes, we also recorded mEPSCs after expression of SynDIG1 shRNA in hippocampal slice culture. Consistent with the coefficient of variation analysis, we observed a 40% decrease in the frequency of mEPSCs and no change in amplitude, supporting the conclusion that SynDIG1 regulates the number of excitatory synapses (Figure 5B).

Discussion

All previously characterized AMPAR auxiliary subunits have been shown to regulate the biophysical properties of AMPARs (Jackson and Nicoll, 2011) (Tomita et al., 2005) (von Engelhardt et al., 2010) (Schwenk et al., 2009) (Shanks et al., 2012). Measuring kainate sensitivity, inward rectification, desensitization and deactivation rates, we found

that SynDIG1 does not behave like known AMPAR auxiliary subunits by regulating receptor gating or pharmacology. Additionally, knockdown of SynDIG1 has no effect on whole-cell AMPAR currents, indicating that SynDIG1 does not play a role in surface trafficking of these receptors. Thus, it seems that despite its ability to bind directly to GluA2 in heterologous cells, SynDIG1 does not share the characteristics of a typical auxiliary subunit in hippocampal neurons.

To further investigate how SynDIG1 expression impacted excitatory synaptic transmission, we studied the effect of varying SynDIG levels in organotypic slice cultures. We found that SynDIG1 positively regulates both evoked AMPAR- and NMDAR-mediated currents; overexpression of SynDIG1 in neurons resulted in an increase in both AMPA and NMDA EPSCs, and knockdown of SynDIG1 decreased AMPA and NMDA EPSCs. While our AMPAR data is very much in agreement with the data published by Kalashnikova et al. (Kalashnikova et al., 2010), they did not observe a change in NMDA mEPSCs following overexpression or knockdown of SynDIG1 in dissociated culture, which contrasts with our results on evoked NMDA EPSCs. This difference could well be due to a difference in the sensitivity of the methodology; mEPSC recordings require a threshold for detection, which is made difficult with the slow NMDA currents. Kalashnikova et al. (Kalashnikova et al., 2010) did observe an increase in NR1 puncta in response to SynDIG1 overexpression, indicating that SynDIG1 does alter NMDAR levels in dissociated neurons as well, though perhaps not to an extent that can be discerned in NMDA mEPSC recordings from dissociated culture.

Because we found no difference in paired-pulse ratio, the observed change in synaptic AMPAR and NMDAR EPSCs can be attributed to a change in the number or strength of synapses. To determine whether SynDIG1 was necessary for synaptogenesis

or synaptic strengthening, we performed a coefficient of variation analysis and mEPSC recordings in neurons expressing SynDIG1 shRNA. In agreement with previous findings (Kalashnikova et al., 2010), these experiments revealed a change in frequency of synaptic responses, consistent with a change in the number of synapses. However, Kalashnikova et al. also observed a significant decrease in mEPSC amplitude, though to a smaller extent than the change in frequency (50% decrease in amplitude versus 70% decrease in frequency) (Kalashnikova et al., 2010). Again, this may be a result of the difference in our preparations, as dissociated cultures have larger mEPSC amplitudes on average, and the small decrease in amplitude we observed after SynDIG1 knockdown may have been larger and more pronounced in their system. Our coefficient of variation analysis, however, argues against this amplitude change contributing to the change seen with the evoked EPSC. Moreover, even in dissociated neurons, Kalashnikova et al. found a reduction in VGLUT1 puncta density after knockdown of SynDIG1, supporting our conclusion that loss of SynDIG1 leads to a loss of synapse number.

Recently, a number of groups have taken large-scale proteomics approaches to identifying AMPAR-interacting proteins(von Engelhardt et al., 2010) (Schwenk et al., 2012) (Shanks et al., 2012). In each of these, SynDIG1 was not identified as a primary binding partner of AMPARs. Along with our data ruling out SynDIG1's function as a traditional subunit, it is likely then that, despite its ability to bind AMPARs directly in a heterologous system, SynDIG1 may not interact with AMPARs directly in neurons, but instead acts as part of a larger postsynaptic complex that controls excitatory synapse formation. SynDIG1 has no known sequence homology with other postsynaptic proteins (Kalashnikova et al., 2010) (Jackson and Nicoll, 2011), so we are not able to predict what type of protein-protein interactions SynDIG1 may form to regulate synaptogenesis.

Interestingly, SynDIG4 (PRRT1) is thought to bind AMPARs directly *in vivo* (von Engelhardt et al., 2010) (Schwenk et al., 2012) (Shanks et al., 2012) and SynDIG1 was found to be capable of homodimerization (Kalashnikova et al., 2010), so it may be that SynDIG1 forms heterodimers with other SynDIG family members to exert its effects. Further research on binding partners of SynDIG1 will certainly prove useful in determining the specific mechanism by which SynDIG1 regulates excitatory synapse number.

Figure 1. SynDIG1 does not alter biophysical properties or surface expression of AMPARs.

(A) Representative whole cell currents recorded in response to application of 1mM kainate (red) or 1mM glutamate (blue) in HEK293T cells expressing GluA2(Q), GluA2(Q) and SynDIG1, or GluA2(Q) and TARP γ-2. Scale bar represents 10 s and 1000 pA. (B) Quantification of conditions shown in A showing the average current responses (left) and kainate to glutamate ratio (right) ± SEM. Note that while co-expression of the TARP γ-2 significantly increases kainate-induced current responses (n = 8, p = 0.0004), co-expression of SynDIG1 does not (n = 8, p = 0.91). (C) Normalized average current-voltage relationships for GluA1(Q)flip (n = 2), GluA1(Q)flip + SynDIG1 (n = 5), GluA2(Q)flip (n = 3), and GluA2(Q)flip + SynDIG1 (n = 3). The addition of SynDIG1 does not alter the current-voltage relationship in GluA1 (p = 0.94) or GluA2 (p = 0.83). (D) Sample traces and average time course of deactivation recorded from HEK293T cells expressing GluA2(Q) (black, n = 10) or GluA2(Q) + SynDIG1 (gray, n = 6). Error bars represent SEM. No significant difference is found in the tau of deactivation after addition of SynDIG1 (p = 0.80). (E) Sample traces and average time course ± SEM of desensitization recorded from HEK293T cells expressing GluA2(Q) (black, n = 9) or GluA2(Q) + SynDIG1 (gray, n = 7). No significant difference is found in the tau of desensitization after addition of SynDIG1 (p = 0.38). Scale bar represents 10 ms. (F) Whole cell currents of wildtype, SynDIG1 shRNA, and CNIH2 shRNA expressing neurons recorded in response to application of 500 nM S-AMPA. Knockdown of the AMPAR auxiliary subunit CNIH2 leads to a dramatic decrease in surface responses (n = 6, p = 0.003), while no change in surface AMPARs is observed after knockdown of SynDIG1 (n = 7, p = 0.93). Bar graphs show mean response amplitude ± SEM.

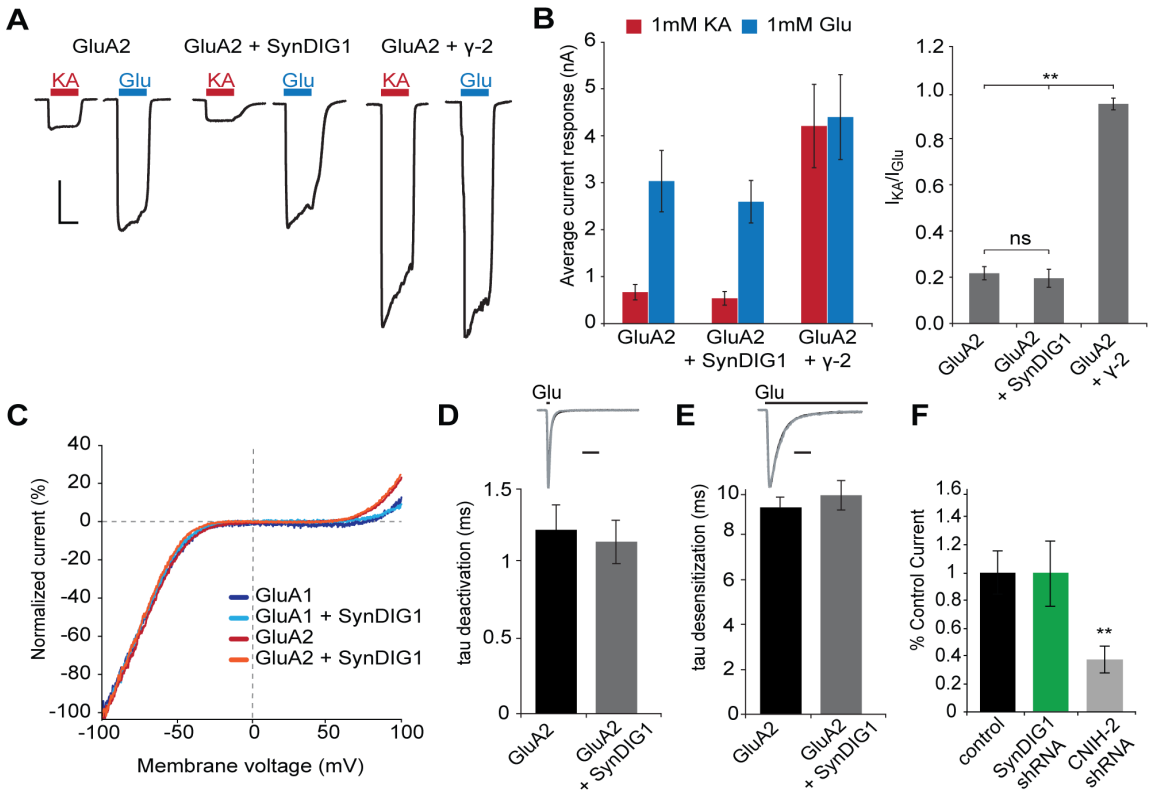
A
GluA2
GluA2 + SynDIG1
GluA2 + γ-2
KA
Glu
B
1mM KA
1mM Glu
Average current response (nA)
GluA2
GluA2 + SynDIG1
GluA2 + γ-2
I_{KA}/I_{Glu}
**
ns
C
Normalized current (%)
Membrane voltage (mV)
GluA1
GluA1 + SynDIG1
GluA2
GluA2 + SynDIG1
D
tau deactivation (ms)
E
tau desensitization (ms)
F
% Control Current
control
SynDIG1 shRNA
CNIH-2 shRNA

Figure 2. SynDIG1 overexpression increases both AMPAR and NMDAR EPSCs.

(A + B) AMPAR- and NMDAR-mediated EPSCs recorded simultaneously from a neuron overexpressing SynDIG1 and a neighboring control neuron. Scatter plots show amplitudes of EPSCs for single pairs (open circles) and means ± SEM (filled circles). Insets are example traces for wildtype (black) and transfected (green) neurons. Scale bars represent 20 ms and 20 pA. Bar graphs (right) show average AMPAR and NMDAR EPSCs normalized to control (AMPA n = 33, $p < 0.0001$; NMDA n = 25, $p = 0.0009$). Error bars denote SEM.

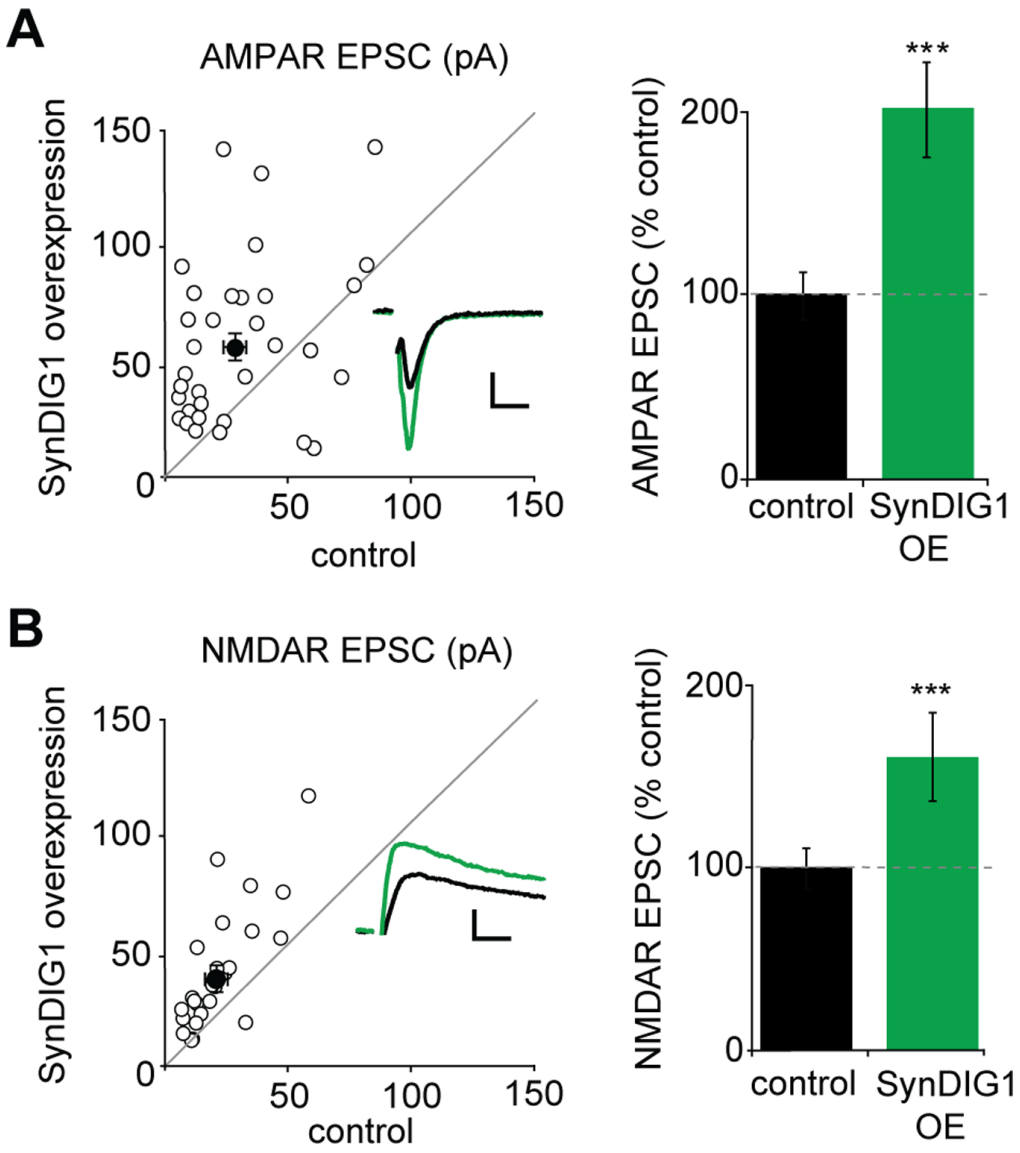
A
AMPAR EPSC (pA)
SynDIG1 overexpression
150
100
50
0
50
100
150
control
***
AMPAR EPSC (% control)
200
100
0
control
SynDIG1 OE
B
NMDAR EPSC (pA)
SynDIG1 overexpression
150
100
50
0
50
100
150
control
***
NMDAR EPSC (% control)
200
100
0
control
SynDIG1 OE

Figure 3. Knockdown of SynDIG1 results in a reduction in both AMPA and NMDA EPSCs.

(A + B) AMPAR- and NMDAR-mediated EPSCs recorded simultaneously from a neuron expressing shRNA to knockdown SynDIG1 and a neighboring control neuron. Scatter plots show amplitudes of EPSCs for single pairs (open circles) and mean ± SEM (filled circles). Scale bars represent 20 ms and 10 pA. Bar graphs plotting average AMPAR and NMDAR EPSCs reveal a 40% decrease in transmission after knockdown (AMPA n = 25, $p = 0.01$; NMDA n = 20, $p = 0.01$). Error bars denote SEM.

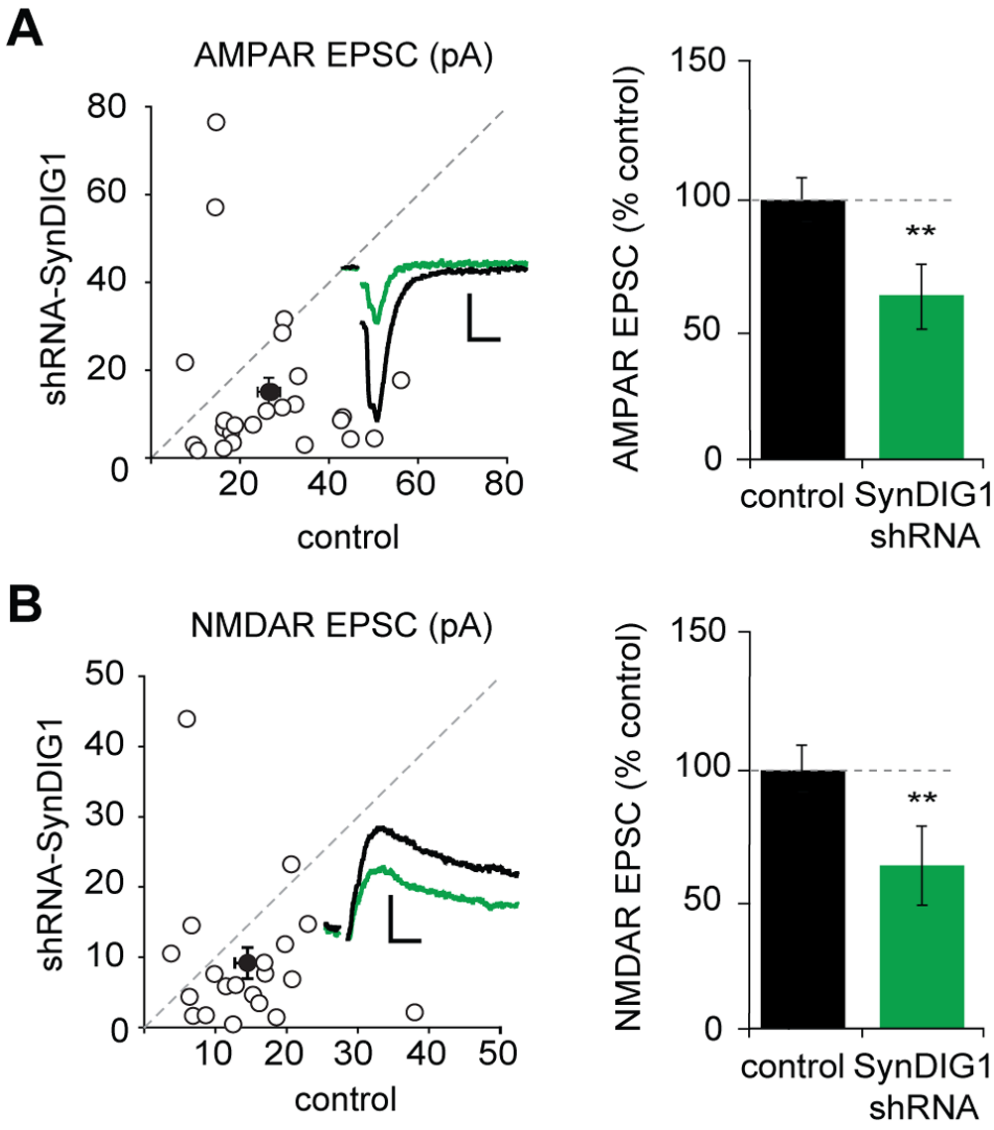
A
AMPAR EPSC (pA)
shRNA-SynDIG1
control
0
20
40
60
80
AMPAR EPSC (% control)
150
100
50
0
**
control
SynDIG1 shRNA
B
NMDAR EPSC (pA)
shRNA-SynDIG1
control
0
10
20
30
40
50
NMDAR EPSC (% control)
150
100
50
0
**
control
SynDIG1 shRNA

Figure 4. SynDIG1 expression does not alter probability of release.

(A) Sample traces (above) and bar graph showing paired-pulse ratio mean ± SEM of control and SynDIG overexpressing cells. No change in paired pulse ratio was detected (n = 11, p = 0.47).

(B) Sample traces (above) and bar graph showing paired-pulse ratio mean ± SEM of control and SynDIG shRNA-transfected cells. No change in paired pulse ratio was detected (n = 10, p = 0.90). Scale bars represent 15 ms and 10 pA.

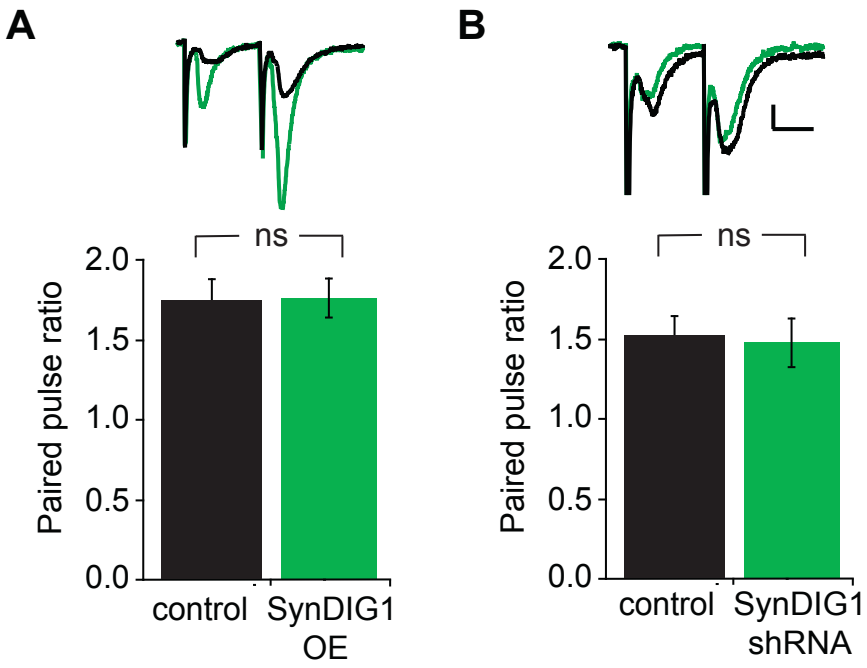
A
ns
2.0
1.5
1.0
0.5
0.0
Paired pulse ratio
control
SynDIG1
OE
B
ns
2.0
1.5
1.0
0.5
0.0
Paired pulse ratio
control
SynDIG1
shRNA

Figure 5. SynDIG1 regulates the number of functional excitatory synapses.

(A) Coefficient of variation analysis for paired recordings of control and SynDIG1 shRNA expressing cells. Open circles represent pairs of neurons, filled circle represents mean ± SEM. Values on the y=x line indicate a change in the number of functional synapses, whereas values along the y=1 line represent changes in synaptic strength of functional synapses.

(B) Bar graphs depicting average mEPSC amplitude and frequency for control and SynDIG1 shRNA-expressing neurons. Reduction in SynDIG1 expression significantly reduces mEPSC frequency (n = 15, p = 0.02), but not amplitude (n = 15, p = 0.31). Error bars represent SEM.

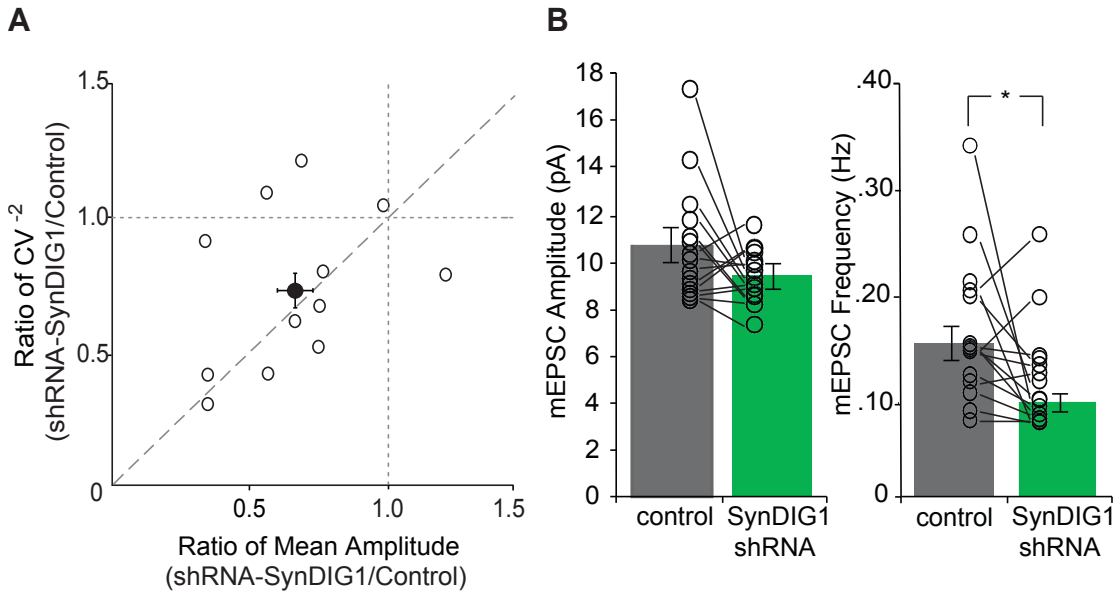
A
B
Ratio of CV -2 (shRNA-SynDIG1/Control)
Ratio of Mean Amplitude (shRNA-SynDIG1/Control)
mEPSC Amplitude (pA)
mEPSC Frequency (Hz)
control
SynDIG1 shRNA
control
SynDIG1 shRNA
*

CHAPTER 6:

General Conclusions

The development and maintenance of excitatory synapses is critical to proper neurological function. Here we have characterized four novel synaptic organizing proteins—LGI1, ADAM22, ADAM23, and SynDIG1—and describe the unique impacts they have on excitatory transmission.

LGI1 supports a transsynaptic complex and regulates excitatory synaptic content

Building off previous evidence that application of LGI1 increases AMPAR-mediated transmission, we sought to determine the mechanism by which LGI1 controls synaptic function. Through the generation of an LGI1 knockout mouse, we provide evidence that LGI is required for strengthening excitatory synapses, in addition to its previously established sufficiency. Further, using mass spectrometry, we were able to identify the proteins that interact with LGI1, including transmembrane ADAM proteins and members of the MAGUK family of cytoplasmic presynaptic and postsynaptic scaffolding proteins. Biochemical analysis of this complex in the LGI1$^{-/-}$ mouse indicated that the presence of LGI1 is critical to the proper synaptic localization and interaction of this protein complex.

We also provide the first direct evidence showing a causal relationship between loss of LGI1 function and epilepsy. Though mutations in *LGI1* have been implicated in autosomal dominant temporal lobe epilepsy (ADTLE) in humans, this data is based only on genetic correlations. Notably, though mice lacking ADAM22 or ADAM23 also suffer from a similar form of lethal epilepsy as LGI1, one study has shown that families with ADTLE lack mutations in ADAM22 (Chabrol et al., 2007). It is unclear if the 18 families included in this research are representative of all families with ADTLE. However, it is

possible that the redundancy of ADAM22 and ADAM23 is such that loss of a single functional ADAM22 or ADAM23 allele is not sufficient to produce epilepsy. Still, research including a larger sample size and also looking for mutations in ADAM23 should prove useful in identifying if this critical synaptic complex underlies human ADTLE.

Paracrine signaling by LGI1 originates from axons and dendrites

Though LGI1 mediates a transsynaptic complex, we only identified a role for LGI1 in postsynaptic composition. Immunohistological analysis showed that LGI1 is expressed in axons and dendrites, but it was unknown if LGI1 is actively secreted from these processes or diffuses great distances after being released from one compartment. Using biolistic and viral introduction of LGI1, we showed that LGI1 secreted from axons or dendrites is able to functionally rescue transmission.

Exogenous application of LGI1, however, has been shown to increase transmission beyond baseline (Fukata et al., 2006). How is it that our single-cell manipulations rescue to baseline whereas addition of LGI1 to the media potentiates synapses? It is possible that the amount of LGI1 protein made in the biolistic and viral rescues is such that the amount of extracellular LGI1 is exactly as it would be in a wildtype brain. Yet, when we look at single-cell overexpression we still find that LGI1 does not increase AMPAR-mediated transmission, NMDAR-mediated transmission, or the AMPA/NMDA ratio (Figure 1). Together, this data suggests an active mechanism for regulating extracellular LGI1, and, in turn, normal levels of synaptic transmission. As manipulations of activity in neuronal culture have significant homeostatic effects on

synaptic content (Turrigiano and Nelson, 2004), it will be difficult to parse out effects of LGI1 loss versus synaptic scaling using electrophysiology. However, innovations in imaging techniques, such as total internal reflection fluorescence (TIRF), allow for visualization of single secretion events. In the future, it will be interesting to use this technique to directly observe the effects of changing levels in activity on LGI1 secretion in real time.

ADAM22 and ADAM23 maintain functional excitatory synapses

In addition to characterizing the role of LGI1 in synaptic maturation, we also identified two novel synaptic organizing proteins, ADAM22 and ADAM23. These proteins are unique members of the ADAM family transmembrane proteins in that they are both catalytically inactive and their expression is restricted to the nervous system (Novak, 2004; Sagane et al., 1999). Despite this, their role in synaptic transmission had never been studied. Here, we demonstrate that ADAM22 and ADAM23 are absolutely essential for excitatory synapse maintenance. While we were able to identify a requirement for PDZ-binding in ADAM22 regulation of synaptic transmission, we were not able to determine the mechanism by which ADAM23 maintains excitatory synapses.

Unlike ADAM22, ADAM23 does not have an intracellular PDZ-binding domain, thus it is unlikely to interact with postsynaptic MAGUKs. There are no other known protein domains in the ADAM23 intracellular c-terminal tail, though there are a number of potentially interesting protein interactions suggested by the domain structure in the extracellular region of ADAM23. The cysteine-rich region of ADAM12 can interact with syndecans (Iba et al., 2000), which have been shown to regulate the maturation of

dendritic spines (Ethell et al., 2001; Ethell and Yamaguchi, 1999). The EGF-like domain of ADAM23 may interact with the EGF-like growth factor receptor ErbB4, a modulator of excitatory synapse structural and functional maturation (Li et al., 2007). ADAM23 has also been shown to bind various members of the integrin family, which have been implicated in synapse maturation (Chavis and Westbrook, 2001). Future studies will be needed to determine if any of these potential interactions of ADAM23 occur in the brain, and the relationship between these interactions and LGI1 binding.

It is also still unclear if LGI1 interaction is important for ADAM baseline synaptic localization and function. Loss of LGI1 does lead to decreased ADAM22 and ADAM23 at the synapse (Yokoi et al., 2014), though some protein remains and no change in synapses number is observed in these mice. Our results indicate that LGI1 is not necessary for ADAM22 and ADAM23 to maintain synapses, but is required for more ADAMs, and, in turn, AMPARs, to be stabilized during synaptic maturation. An interesting question is if any interaction is required for ADAMs to maintain synapses, and, more specifically, if LGI2 and LGI4 are sufficient. Both of these family members can bind ADAM22 and ADAM23 (Kegel et al., 2013), and are expressed in the hippocampus (Herranz-Perez et al., 2010). Though neither appears to be in pyramidal cells, they may act as paracrine signals originating in nearby interneurons, or are produced at undetectably low, but sufficient levels in pyramidal cells.

The LGI1-ADAM complex is required for synaptic MAGUK function

We also present data here indicating that LGI1 is required for MAGUK function at the synapse. Preliminary data indicates that expression of LGI1, however, is not required

for MAGUK localization to dendritic spines (personal correspondence Y. Fukata and M. Fukata). How might LGI1 regulate MAGUK function, while not impacting its synaptic localization?

Quantitative analysis of postsynaptic proteins indicates the MAGUK family proteins far outnumber NMDARs and AMPARs in the postsynaptic density (Sheng and Hoogenraad, 2007). Thus, there must be other factors that control the function of MAGUKs once they have reached the synapse. Our data indicates that LGI is required for MAGUKs to increase synaptic transmission. It is possible that LGI1 localizes MAGUKs into a functional microdomain within the synapse; it may be that the transsynaptic structure that LGI1 creates is able to guide MAGUKs into the functional synaptic space in line with the presynaptic active zone. It also may be that LGI1-ADAM22 interactions with MAGUKs compete with a different MAGUK interaction that negatively regulates their synaptic function.

Another interesting aspect of the LGI1-MAGUK interaction is that SAP-102, a member of the MAGUK family that is functional during early development but is replaced by PSD-93 and PSD-95 (Elias et al., 2006), has not been found to be part of the LGI1-mediated transsynaptic complex (Fukata et al., 2010). The timeline of LGI1 and PSD-95/PSD-93 expression at the synapse is similar (Fukata et al., 2006; Sans et al., 2000). Moreover, loss of PSD-95 and PSD-93 leads to a reduction in AMPA/NMDA ratio, similar to loss of LGI1 – though mEPSC data indicates an underlying change in frequency in the former and change in amplitude in the latter (Elias et al., 2006; Fukata et al., 2010). It is a tempting proposition that LGI1 guides synaptic development by stabilizing the replacement of SAP-102 with the mature MAGUKs, PSD-95 and PSD-93.

Future experiments examining the impact of changing SAP-102 expression in the absence of LGI1 should shed light on this question.

Presynaptic effects of the LGI1-ADAM complex

The shaker-related potassium channels (Kv1s) are a part of the transsynaptic complex LGI1 mediates, and LGI1 has previously been shown to modulate the function of Kv1 (Schulte et al., 2006), yet we saw no effect on presynaptic release properties in any of our experiments. The LGI1-Kv interaction is likely mediated by ADAM22, as LGI1 does not directly interact with the extracellular domain of potassium channels (Fukata et al., 2010), and ADAM22 was identified through proteomic analysis of Kv1 interacting proteins (Schulte et al., 2006). Though significantly reduced, the ADAM22 and Kv1.2 interaction is still somewhat preserved in the LGI1$^{-/-}$ mouse brain (Fukata et al., 2010), and may be sufficient to properly modulate potassium channel conductance in the absence of LGI1.

The majority of our ADAM22 and ADAM23 manipulations were exclusively postsynaptic, and did not alter the presynaptic probability of release. However, it should be noted that in the germline ADAM22$^{-/-}$ recordings, where ADAM22 is absent from both the pre- and postsynaptic cell, we saw a slightly higher paired-pulse ratio than observed in our other experiments, indicative of decreased probability of release, and an even larger effect was observed in ADAM22$^{-/-}$ cells expressing ADAM23 shRNA. This difference was not significant, and requires a larger n and more controlled studies to make conclusions from, but presents an interesting lead in the question of presynaptic function of the LGI1-ADAM complex.

LGI1 and ADAMs in neuronal development versus synaptic maturation

Previous research has demonstrated that LGI1 can act as an antagonist for myelin-based growth cone inhibition (Thomas et al., 2010), and application of LGI1 to dissociated hippocampal neurons increases neurite outgrowth (Owuor et al., 2009). This increase is dependent upon interaction with ADAM23, and ADAM23-lacking neurons exhibit reduced dendritic arborization *in vivo* (Owuor et al., 2009). However, decreases in neurite outgrowth would not explain the specific change in synaptic AMPAR-content in LGI1$^{-/-}$ mice we observe, and our postnatal knockdown of ADAM23 should not alter dendritic arborization. This suggests that LGI1 and ADAMs may have independent roles in neurite development and synaptic maturation.

Recently, LGI1 has been identified as the target of antibodies made in the autoimmune disorder limbic encephalitis. Patients with limbic encephalitis develop adult-onset epilepsy and neuropsychiatric symptoms, such as memory deficits and psychosis (Lai et al., 2010). So, while it may be argued that the epilepsy phenotype related to mutations in *LGI1* is a result of improper neurite development, it is certain that disruption of the LGI1-ADAM complex in the mature adult brain can also produce disease, indicating a critical function for this complex in synaptic maintenance as well as development.

SynDIG1 is a synaptic organizing protein, not an auxiliary subunit

In addition to identifying the role of the LGI1-ADAM complex in synaptic transmission, we also characterized the recently discovered synaptic organizing protein, SynDIG1. Found in a screen for developmentally regulated proteins, SynDIG1 was later shown to

directly interact with AMPARs and contribute to synapse maturation (Diaz et al., 2002; Kalashnikova et al., 2010). All other transmembrane proteins that bind AMPARs, termed auxiliary subunits, have been shown to regulate both receptor trafficking and biophysical properties (Jackson and Nicoll, 2011).

We sought to examine if SynDIG1 acts as a traditional auxiliary subunit, and determine whether the previously identified role in synapse maturation was a result of its effect on receptor trafficking. Our data indicates that SynDIG1 does not act as an auxiliary subunit, having no impact on trafficking or biophysical properties of AMPARs. Instead, we found that SynDIG1 is a synaptogenic protein, modulating both AMPAR and NMDAR mediated EPSCs.

It is unclear how this AMPAR-interacting protein promotes the generation of excitatory synapses. SynDIG1 expression does not alter dendritic spine density (Figure 2), indicating that it does not have structural effects at the synapse. Functionally, SynDIG1 sequence reveals little in the way of protein homology. To begin to understand the mechanism of SynDIG1 action at the synapse, we constructed mutants of SynDIG1 that lacked either the extracellular C-terminus or intracellular N-terminus. We found that both regions of the protein are required for the synaptogenic effects of SynDIG1 (Figure 3), though we are unsure if these proteins are properly processed and if these deficits reflect a specific defect in synaptic activity.

More recently, however, the previously defined direct interaction of SynDIG1 and AMPARs has come into question. Two separate proteomic analyses failed to identify SynDIG1 as a protein that is bound to AMPARs at the synapse, though they did identify SynDIG4 (PRRT2) as an AMPAR interacting protein (Schwenk et al., 2012;

Shanks et al., 2012; von Engelhardt et al., 2010). SynDIG1 was shown to be able to homodimerize, though it's ability to heterodimerize with other SynDIGs is unknown. Future experiments on SynDIG family interactions, and their dependence on the N- and C-termini of SynDIG1 may begin to elucidate the mechanism by which SynDIG1 regulates synaptogenesis.

Concluding Remarks

When considering synaptic organizing proteins, a logical question arises: why are there so many? The answer to this likely lies in two basic features of the brain: proteins need to be specialized enough to support the complexity of information processing, but also must share functional similarity such that loss of one does not lead to failure of the whole system. Specialization in the brain takes the form of synapse location, transmitter identity, and molecular composition. These unique features are driven by the various synaptic organizing proteins that are present at a specific synapse (Siddiqui and Craig, 2011). Here, we add to this body of knowledge and present data on LGI1, a critical regulator of molecular composition at glutamatergic synapses. Redundancy of the system often involves the evolution of a family of proteins that serve similar functions. In our work, we have identified two members of the ADAM family proteins that have parallel roles at the synapse and are absolutely essential to excitatory transmission. We also provide data implicating SynDIG1 in synaptogenesis, though whether it is part of a redundant system or organizes a very specific subset of synapses remains a question ripe for study.

Figure 1. Overexpression of LGI1 does not impact synaptic transmission.

AMPAR-mediated (A) and NMDAR-mediated (B) are both unchanged after expression of LGI1 in wildtype slice culture. Open circles represent pairs of neurons, filled circle represents mean ± SEM. (C) Bar graphs show average AMPAR (left) and NMDAR EPSCs (center) normalized to control, and AMPA/NMDA ratio of wildtype and SynDIG1 overexpressing cells. No significant difference is observed in AMPAR- ($p = 0.44$) or NMDAR-mediated EPSCs ($p = 0.91$), as well as AMPA/NMDA ratio ($p = 0.41$).

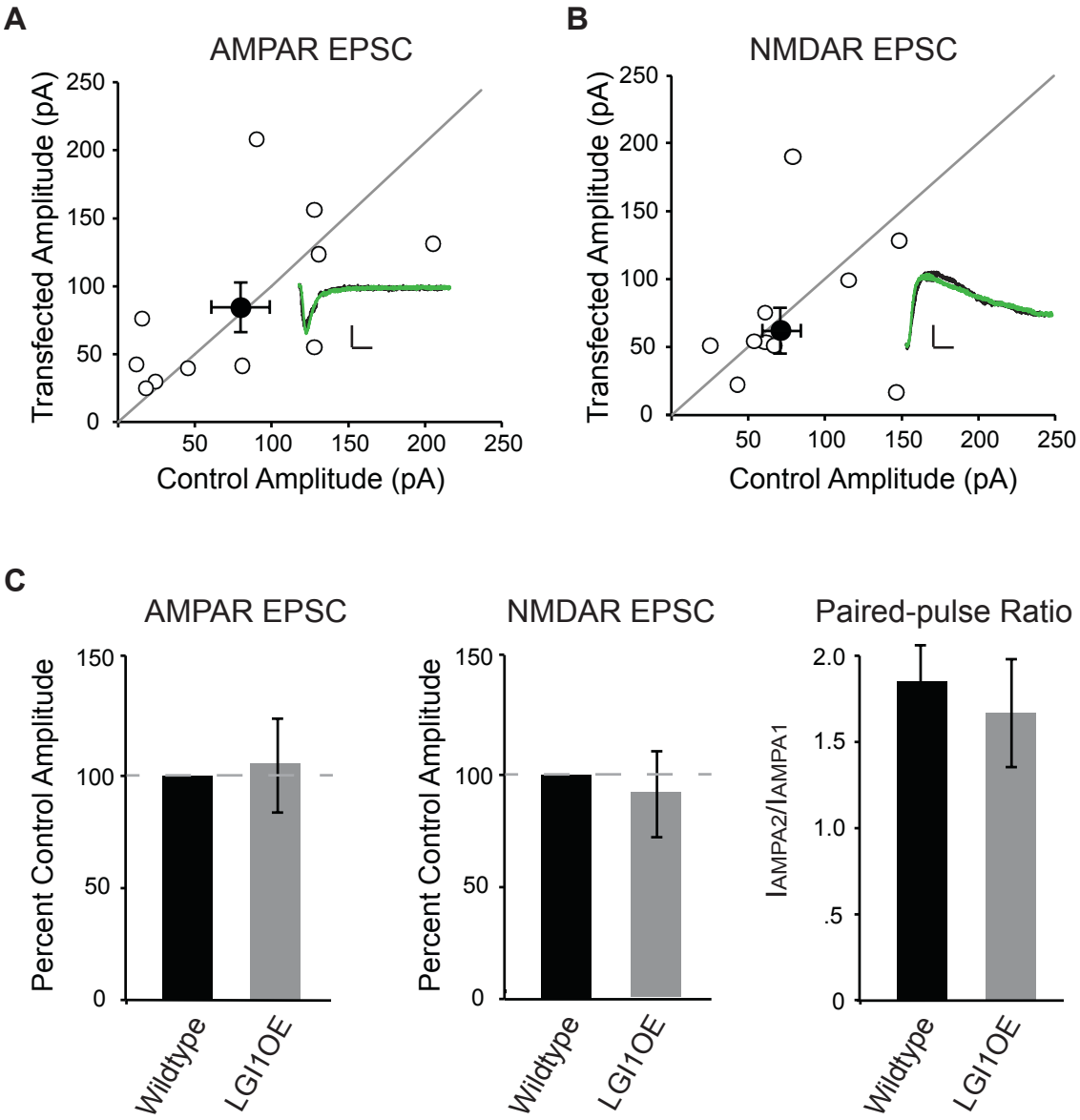
A
AMPAR EPSC
Transfected Amplitude (pA)
Control Amplitude (pA)
0
50
100
150
200
250
B
NMDAR EPSC
Transfected Amplitude (pA)
Control Amplitude (pA)
C
AMPAR EPSC
Percent Control Amplitude
NMDAR EPSC
Percent Control Amplitude
Paired-pulse Ratio
IAMPA2/IAMPA1
0
.5
1.0
1.5
2.0
Wildtype
LGI1OE

Figure 2. SynDIG1 expression does not alter spine density.

(A) Representative images of dendritic spines taken from wildtype (left) and SynDIG1 shRNA-expressing cells (right). (B) Quantification of dendritic spines revealed no difference in density after expression of SynDIG1 shRNA ($n = 7$, $p = 0.84$).

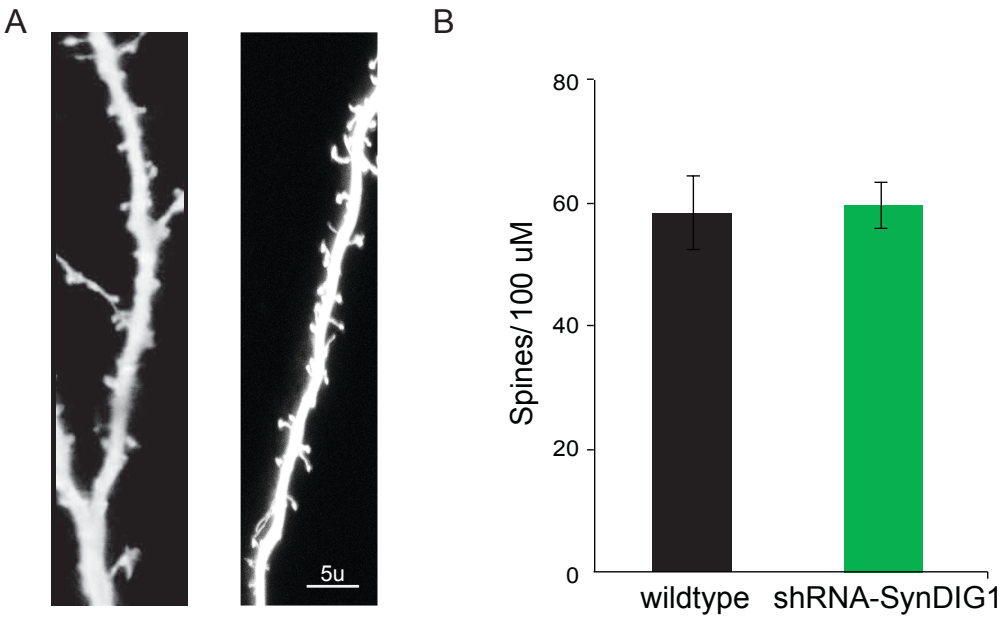
A
5u
B
80
60
40
20
0
Spines/100 uM
wildtype
shRNA-SynDIG1

Figure 3. Both the N- and C-terminal ends of SynDIG1 are required for synaptic function.

(A) Topology of full- length SynDIG1, C-terminally truncated SynDIGd33C, and N-terminally truncated SynDIGd117N. (B) Expression of C- (left) and N- (center) terminally truncated SynDIG has no effect on AMPAR EPSCs ($p = 0.43$ and $p = 0.45$, respectively). (C) Expression of C- (left) and N- (center) terminally truncated SynDIG does not increase NMDAR EPSCs ($p = 0.28$ and $p = 0.70$, respectively), as expression of wildtype SynDIG1 does. Open circles represent pairs of neurons, filled circle represents mean ± SEM. Bar graphs show average AMPAR (left) and NMDAR EPSCs (center) normalized to control, and

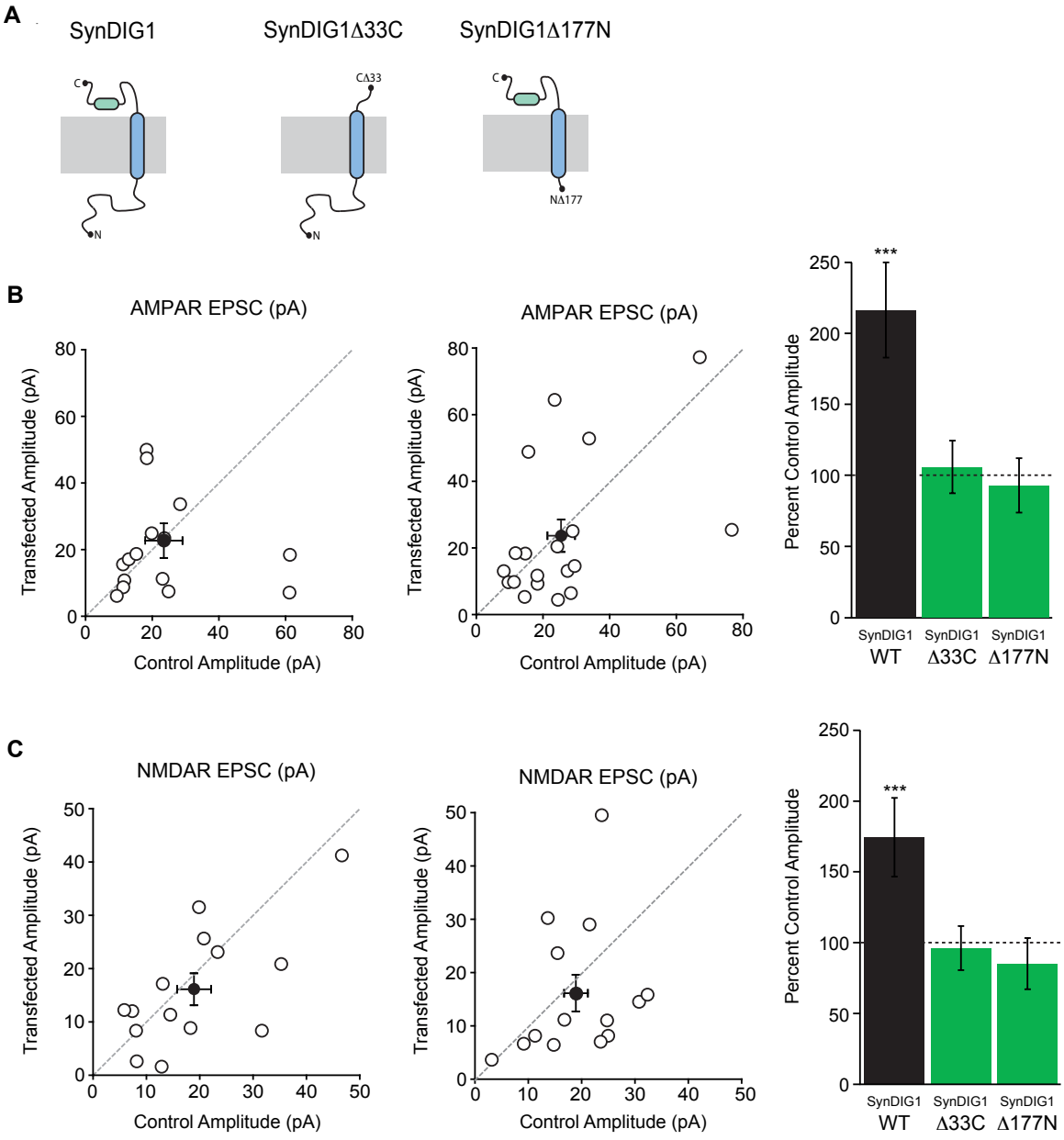
A
SynDIG1
SynDIG1Δ33C
SynDIG1Δ177N
C
CΔ33
NΔ177
N
B
AMPAR EPSC (pA)
Transfected Amplitude (pA)
Control Amplitude (pA)
Percent Control Amplitude
***
SynDIG1 WT
SynDIG1 Δ33C
SynDIG1 Δ177N
C
NMDAR EPSC (pA)

CHAPTER 7:

References

Arikkath, J., and Campbell, K.P. (2003). Auxiliary subunits: essential components of the voltage-gated calcium channel complex. Curr Opin Neurobiol *13*, 298-307.

Bekkers, J.M., and Stevens, C.F. (1990). Presynaptic mechanism for long-term potentiation in the hippocampus. Nature *346*, 724-729.

Berghuis, B., Brilstra, E.H., Lindhout, D., Baulac, S., de Haan, G.J., and van Kempen, M. (2013). Hyperactive behavior in a family with autosomal dominant lateral temporal lobe epilepsy caused by a mutation in the LGI1/epitempin gene. Epilepsy & behavior : E&B *28*, 41-46.

Bredt, D.S., and Nicoll, R.A. (2003). AMPA receptor trafficking at excitatory synapses. Neuron *40*, 361-379.

Brew, H.M., Gittelman, J.X., Silverstein, R.S., Hanks, T.D., Demas, V.P., Robinson, L.C., Robbins, C.A., McKee-Johnson, J., Chiu, S.Y., Messing, A.*, et al.* (2007). Seizures and reduced life span in mice lacking the potassium channel subunit Kv1.2, but hypoexcitability and enlarged Kv1 currents in auditory neurons. J Neurophysiol *98*, 1501-1525.

Cal, S., Freije, J.M., Lopez, J.M., Takada, Y., and Lopez-Otin, C. (2000). ADAM 23/MDC3, a human disintegrin that promotes cell adhesion via interaction with the alphavbeta3 integrin through an RGD-independent mechanism. Molecular biology of the cell *11*, 1457-1469.

Carlin, R.K., Grab, D.J., Cohen, R.S., and Siekevitz, P. (1980). Isolation and characterization of postsynaptic densities from various brain regions: enrichment of different types of postsynaptic densities. J Cell Biol *86*, 831-845.

Chabrol, E., Gourfinkel-An, I., Scheffer, I.E., Picard, F., Couarch, P., Berkovic, S.F., McMahon, J.M., Bajaj, N., Mota-Vieira, L., Mota, R.*, et al.* (2007). Absence of mutations in the LGI1 receptor ADAM22 gene in autosomal dominant lateral temporal epilepsy. Epilepsy research *76*, 41-48.

Chabrol, E., Navarro, V., Provenzano, G., Cohen, I., Dinocourt, C., Rivaud-Pechoux, S., Fricker, D., Baulac, M., Miles, R., Leguern, E.*, et al.* (2010). Electroclinical characterization of epileptic seizures in leucine-rich, glioma-inactivated 1-deficient mice. Brain : a journal of neurology *133*, 2749-2762.

Chavis, P., and Westbrook, G. (2001). Integrins mediate functional pre- and postsynaptic maturation at a hippocampal synapse. Nature *411*, 317-321.

Chen, L., Chetkovich, D.M., Petralia, R.S., Sweeney, N.T., Kawasaki, Y., Wenthold, R.J., Bredt, D.S., and Nicoll, R.A. (2000). Stargazin regulates synaptic targeting of AMPA receptors by two distinct mechanisms. Nature *408*, 936-943.

Chernova, O.B., Somerville, R.P., and Cowell, J.K. (1998). A novel gene, LGI1, from 10q24 is rearranged and downregulated in malignant brain tumors. Oncogene *17*, 2873-2881.

D'Abaco, G.M., Ng, K., Paradiso, L., Godde, N.J., Kaye, A., and Novak, U. (2006). ADAM22, expressed in normal brain but not in high-grade gliomas, inhibits cellular proliferation via the disintegrin domain. Neurosurgery *58*, 179-186; discussion 179-186.

Dalmau, J., Gleichman, A.J., Hughes, E.G., Rossi, J.E., Peng, X., Lai, M., Dessain, S.K., Rosenfeld, M.R., Balice-Gordon, R., and Lynch, D.R. (2008). Anti-NMDA-receptor encephalitis: case series and analysis of the effects of antibodies. The Lancet Neurology *7*, 1091-1098.

de Wit, J., Sylwestrak, E., O'Sullivan, M.L., Otto, S., Tiglio, K., Savas, J.N., Yates, J.R., 3rd, Comoletti, D., Taylor, P., and Ghosh, A. (2009). LRRTM2 interacts with Neurexin1 and regulates excitatory synapse formation. Neuron *64*, 799-806.

Del Castillo, J., and Katz, B. (1954). Quantal components of the end-plate potential. The Journal of physiology *124*, 560-573.

Diaz, E., Ge, Y., Yang, Y.H., Loh, K.C., Serafini, T.A., Okazaki, Y., Hayashizaki, Y., Speed, T.P., Ngai, J., and Scheiffele, P. (2002). Molecular analysis of gene expression in the developing pontocerebellar projection system. Neuron *36*, 417-434.

El-Husseini, A.E., Schnell, E., Chetkovich, D.M., Nicoll, R.A., and Bredt, D.S. (2000). PSD-95 involvement in maturation of excitatory synapses. Science *290*, 1364-1368.

El-Husseini Ael, D., Schnell, E., Dakoji, S., Sweeney, N., Zhou, Q., Prange, O., Gauthier-Campbell, C., Aguilera-Moreno, A., Nicoll, R.A., and Bredt, D.S. (2002). Synaptic strength regulated by palmitate cycling on PSD-95. Cell *108*, 849-863.

Elias, G.M., Funke, L., Stein, V., Grant, S.G., Bredt, D.S., and Nicoll, R.A. (2006). Synapse-specific and developmentally regulated targeting of AMPA receptors by a family of MAGUK scaffolding proteins. Neuron *52*, 307-320.

Ethell, I.M., Irie, F., Kalo, M.S., Couchman, J.R., Pasquale, E.B., and Yamaguchi, Y. (2001). EphB/syndecan-2 signaling in dendritic spine morphogenesis. Neuron *31*, 1001-1013.

Ethell, I.M., and Yamaguchi, Y. (1999). Cell surface heparan sulfate proteoglycan syndecan-2 induces the maturation of dendritic spines in rat hippocampal neurons. J Cell Biol *144*, 575-586.

Fukata, Y., Adesnik, H., Iwanaga, T., Bredt, D.S., Nicoll, R.A., and Fukata, M. (2006). Epilepsy-related ligand/receptor complex LGI1 and ADAM22 regulate synaptic transmission. Science *313*, 1792-1795.

Fukata, Y., Lovero, K.L., Iwanaga, T., Watanabe, A., Yokoi, N., Tabuchi, K., Shigemoto, R., Nicoll, R.A., and Fukata, M. (2010). Disruption of LGI1-linked synaptic complex causes abnormal synaptic transmission and epilepsy. Proc Natl Acad Sci U S A *107*, 3799-3804.

Fukaya, M., and Watanabe, M. (2000). Improved immunohistochemical detection of postsynaptically located PSD-95/SAP90 protein family by protease section pretreatment: a study in the adult mouse brain. J Comp Neurol *426*, 572-586.

Godde, N.J., D'Abaco, G.M., Paradiso, L., and Novak, U. (2006). Efficient ADAM22 surface expression is mediated by phosphorylation-dependent interaction with 14-3-3 protein family members. J Cell Sci *119*, 3296-3305.

Graf, E.R., Zhang, X., Jin, S.X., Linhoff, M.W., and Craig, A.M. (2004). Neurexins induce differentiation of GABA and glutamate postsynaptic specializations via neuroligins. Cell *119*, 1013-1026.

Gu, W., Brodtkorb, E., and Steinlein, O.K. (2002). LGI1 is mutated in familial temporal lobe epilepsy characterized by aphasic seizures. Annals of neurology *52*, 364-367.

Herranz-Perez, V., Olucha-Bordonau, F.E., Morante-Redolat, J.M., and Perez-Tur, J. (2010). Regional distribution of the leucine-rich glioma inactivated (LGI) gene family transcripts in the adult mouse brain. Brain research *1307*, 177-194.

Herring, B.E., Shi, Y., Suh, Y.H., Zheng, C.Y., Blankenship, S.M., Roche, K.W., and Nicoll, R.A. (2013). Cornichon proteins determine the subunit composition of synaptic AMPA receptors. Neuron *77*, 1083-1096.

Iba, K., Albrechtsen, R., Gilpin, B., Frohlich, C., Loechel, F., Zolkiewska, A., Ishiguro, K., Kojima, T., Liu, W., Langford, J.K., *et al.* (2000). The cysteine-rich domain of human

ADAM 12 supports cell adhesion through syndecans and triggers signaling events that lead to beta1 integrin-dependent cell spreading. J Cell Biol *149*, 1143-1156.

Irani, S.R., Alexander, S., Waters, P., Kleopa, K.A., Pettingill, P., Zuliani, L., Peles, E., Buckley, C., Lang, B., and Vincent, A. (2010). Antibodies to Kv1 potassium channel-complex proteins leucine-rich, glioma inactivated 1 protein and contactin-associated protein-2 in limbic encephalitis, Morvan's syndrome and acquired neuromyotonia. Brain : a journal of neurology *133*, 2734-2748.

Jackson, A.C., Milstein, A.D., Soto, D., Farrant, M., Cull-Candy, S.G., and Nicoll, R.A. (2011). Probing TARP modulation of AMPA receptor conductance with polyamine toxins. J Neurosci *31*, 7511-7520.

Jackson, A.C., and Nicoll, R.A. (2011). The expanding social network of ionotropic glutamate receptors: TARPs and other transmembrane auxiliary subunits. Neuron *70*, 178-199.

Jonas, P. (2000). The Time Course of Signaling at Central Glutamatergic Synapses. News Physiol Sci *15*, 83-89.

Kalachikov, S., Evgrafov, O., Ross, B., Winawer, M., Barker-Cummings, C., Martinelli Boneschi, F., Choi, C., Morozov, P., Das, K., Teplitskaya, E., *et al.* (2002). Mutations in LGI1 cause autosomal-dominant partial epilepsy with auditory features. Nature genetics *30*, 335-341.

Kalashnikova, E., Lorca, R.A., Kaur, I., Barisone, G.A., Li, B., Ishimaru, T., Trimmer, J.S., Mohapatra, D.P., and Diaz, E. (2010). SynDIG1: an activity-regulated, AMPA- receptor-interacting transmembrane protein that regulates excitatory synapse development. Neuron *65*, 80-93.

Kato, A.S., Zhou, W., Milstein, A.D., Knierman, M.D., Siuda, E.R., Dotzlaf, J.E., Yu, H., Hale, J.E., Nisenbaum, E.S., Nicoll, R.A., *et al.* (2007). New transmembrane AMPA receptor regulatory protein isoform, gamma-7, differentially regulates AMPA receptors. J Neurosci *27*, 4969-4977.

Kawamata, J., Ikeda, A., Fujita, Y., Usui, K., Shimohama, S., and Takahashi, R. (2010). Mutations in LGI1 gene in Japanese families with autosomal dominant lateral temporal lobe epilepsy: the first report from Asian families. Epilepsia *51*, 690-693.

Kegel, L., Aunin, E., Meijer, D., and Bermingham, J.R. (2013). LGI proteins in the nervous system. ASN neuro *5*, 167-181.

Kessels, H.W., and Malinow, R. (2009). Synaptic AMPA receptor plasticity and behavior. Neuron *61*, 340-350.

Kim, E., and Sheng, M. (2004). PDZ domain proteins of synapses. Nature reviews Neuroscience *5*, 771-781.

Ko, J., Fuccillo, M.V., Malenka, R.C., and Sudhof, T.C. (2009). LRRTM2 functions as a neurexin ligand in promoting excitatory synapse formation. Neuron *64*, 791-798.

Koch, S.M., and Ullian, E.M. (2010). Neuronal pentraxins mediate silent synapse conversion in the developing visual system. J Neurosci *30*, 5404-5414.

Lai, M., Hughes, E.G., Peng, X., Zhou, L., Gleichman, A.J., Shu, H., Mata, S., Kremens, D., Vitaliani, R., Geschwind, M.D., *et al.* (2009). AMPA receptor antibodies in limbic encephalitis alter synaptic receptor location. Annals of neurology *65*, 424-434.

Lai, M., Huijbers, M.G., Lancaster, E., Graus, F., Bataller, L., Balice-Gordon, R., Cowell, J.K., and Dalmau, J. (2010). Investigation of LGI1 as the antigen in limbic encephalitis previously attributed to potassium channels: a case series. The Lancet Neurology *9*, 776-785.

Lein, E.S., Hawrylycz, M.J., Ao, N., Ayres, M., Bensinger, A., Bernard, A., Boe, A.F., Boguski, M.S., Brockway, K.S., Byrnes, E.J., *et al.* (2007). Genome-wide atlas of gene expression in the adult mouse brain. Nature *445*, 168-176.

Leonardi, E., Andreazza, S., Vanin, S., Busolin, G., Nobile, C., and Tosatto, S.C. (2011). A computational model of the LGI1 protein suggests a common binding site for ADAM proteins. PloS one *6*, e18142.

Li, B., Woo, R.S., Mei, L., and Malinow, R. (2007). The neuregulin-1 receptor erbB4 controls glutamatergic synapse maturation and plasticity. Neuron *54*, 583-597.

Linhoff, M.W., Lauren, J., Cassidy, R.M., Dobie, F.A., Takahashi, H., Nygaard, H.B., Airaksinen, M.S., Strittmatter, S.M., and Craig, A.M. (2009). An unbiased expression

screen for synaptogenic proteins identifies the LRRTM protein family as synaptic organizers. Neuron *61*, 734-749.

Lynch, M.W., Rutecki, P.A., and Sutula, T.P. (1996). The effects of seizures on the brain. Current opinion in neurology *9*, 97-102.

Malatesta, M., Furlan, S., Mariotti, R., Zancanaro, C., and Nobile, C. (2009). Distribution of the epilepsy-related Lgi1 protein in rat cortical neurons. Histochem Cell Biol *132*, 505-513.

Malinow, R., and Malenka, R.C. (2002). AMPA receptor trafficking and synaptic plasticity. Annu Rev Neurosci *25*, 103-126.

Malinow, R., and Tsien, R.W. (1990). Presynaptic enhancement shown by whole-cell recordings of long-term potentiation in hippocampal slices. Nature *346*, 177-180.

Manabe, T., Wyllie, D.J., Perkel, D.J., and Nicoll, R.A. (1993). Modulation of synaptic transmission and long-term potentiation: effects on paired pulse facilitation and EPSC variance in the CA1 region of the hippocampus. Journal of neurophysiology *70*, 1451-1459.

Matsuda, K., Miura, E., Miyazaki, T., Kakegawa, W., Emi, K., Narumi, S., Fukazawa, Y., Ito-Ishida, A., Kondo, T., Shigemoto, R.*, et al.* (2010). Cbln1 is a ligand for an orphan glutamate receptor delta2, a bidirectional synapse organizer. Science *328*, 363-368.

Mayer, M.L. (2005). Glutamate receptor ion channels. Curr Opin Neurobiol *15*, 282-288.

Menuz, K., and Nicoll, R.A. (2008). Loss of inhibitory neuron AMPA receptors contributes to ataxia and epilepsy in stargazer mice. J Neurosci *28*, 10599-10603.

Migaud, M., Charlesworth, P., Dempster, M., Webster, L.C., Watabe, A.M., Makhinson, M., He, Y., Ramsay, M.F., Morris, R.G., Morrison, J.H., *et al.* (1998). Enhanced long-term potentiation and impaired learning in mice with mutant postsynaptic density-95 protein. Nature *396*, 433-439.

Mitchell, K.J., Pinson, K.I., Kelly, O.G., Brennan, J., Zupicich, J., Scherz, P., Leighton, P.A., Goodrich, L.V., Lu, X., Avery, B.J., *et al.* (2001). Functional analysis of secreted and transmembrane proteins critical to mouse development. Nature genetics *28*, 241-249.

Morante-Redolat, J.M., Gorostidi-Pagola, A., Piquer-Sirerol, S., Saenz, A., Poza, J.J., Galan, J., Gesk, S., Sarafidou, T., Mautner, V.F., Binelli, S., *et al.* (2002). Mutations in the LGI1/Epitempin gene on 10q24 cause autosomal dominant lateral temporal epilepsy. Human molecular genetics *11*, 1119-1128.

Nam, C.I., and Chen, L. (2005). Postsynaptic assembly induced by neurexin-neuroligin interaction and neurotransmitter. Proc Natl Acad Sci U S A *102*, 6137-6142.

Nishino, J., Saunders, T.L., Sagane, K., and Morrison, S.J. (2010). Lgi4 promotes the proliferation and differentiation of glial lineage cells throughout the developing peripheral nervous system. J Neurosci *30*, 15228-15240.

Nobile, C., Michelucci, R., Andreazza, S., Pasini, E., Tosatto, S.C., and Striano, P. (2009). LGI1 mutations in autosomal dominant and sporadic lateral temporal epilepsy. Hum Mutat *30*, 530-536.

Noebels, J.L. (2003). The biology of epilepsy genes. Annual review of neuroscience *26*, 599-625.

Novak, U. (2004). ADAM proteins in the brain. Journal of clinical neuroscience : official journal of the Neurosurgical Society of Australasia *11*, 227-235.

Ogawa, Y., Oses-Prieto, J., Kim, M.Y., Horresh, I., Peles, E., Burlingame, A.L., Trimmer, J.S., Meijer, D., and Rasband, M.N. (2010). ADAM22, a Kv1 channel-interacting protein, recruits membrane-associated guanylate kinases to juxtaparanodes of myelinated axons. J Neurosci *30*, 1038-1048.

Ottman, R., Risch, N., Hauser, W.A., Pedley, T.A., Lee, J.H., Barker-Cummings, C., Lustenberger, A., Nagle, K.J., Lee, K.S., Scheuer, M.L., *et al.* (1995). Localization of a gene for partial epilepsy to chromosome 10q. Nat Genet *10*, 56-60.

Ottman, R., Winawer, M.R., Kalachikov, S., Barker-Cummings, C., Gilliam, T.C., Pedley, T.A., and Hauser, W.A. (2004). LGI1 mutations in autosomal dominant partial epilepsy with auditory features. Neurology *62*, 1120-1126.

Owuor, K., Harel, N.Y., Englot, D.J., Hisama, F., Blumenfeld, H., and Strittmatter, S.M. (2009). LGI1-associated epilepsy through altered ADAM23-dependent neuronal morphology. Molecular and cellular neurosciences *42*, 448-457.

Ozkaynak, E., Abello, G., Jaegle, M., van Berge, L., Hamer, D., Kegel, L., Driegen, S., Sagane, K., Bermingham, J.R., Jr., and Meijer, D. (2010). Adam22 is a major neuronal receptor for Lgi4-mediated Schwann cell signaling. J Neurosci *30*, 3857-3864.

Piepoli, T., Jakupoglu, C., Gu, W., Lualdi, E., Suarez-Merino, B., Poliani, P.L., Cattaneo, M.G., Ortino, B., Goplen, D., Wang, J.*, et al.* (2006). Expression studies in gliomas and glial cells do not support a tumor suppressor role for LGI1. Neuro Oncol *8*, 96-108.

Pongs, O., and Schwarz, J.R. (2010). Ancillary subunits associated with voltage-dependent K+ channels. Physiological reviews *90*, 755-796.

Redies, C., Hertel, N., and Hubner, C.A. (2012). Cadherins and neuropsychiatric disorders. Brain research *1470*, 130-144.

Reid, C.A., Berkovic, S.F., and Petrou, S. (2009). Mechanisms of human inherited epilepsies. Progress in neurobiology *87*, 41-57.

Sagane, K., Hayakawa, K., Kai, J., Hirohashi, T., Takahashi, E., Miyamoto, N., Ino, M., Oki, T., Yamazaki, K., and Nagasu, T. (2005). Ataxia and peripheral nerve hypomyelination in ADAM22-deficient mice. BMC neuroscience *6*, 33.

Sagane, K., Ishihama, Y., and Sugimoto, H. (2008). LGI1 and LGI4 bind to ADAM22, ADAM23 and ADAM11. International journal of biological sciences *4*, 387-396.

Sagane, K., Yamazaki, K., Mizui, Y., and Tanaka, I. (1999). Cloning and chromosomal mapping of mouse ADAM11, ADAM22 and ADAM23. Gene *236*, 79-86.

Sans, N., Petralia, R.S., Wang, Y.X., Blahos, J., 2nd, Hell, J.W., and Wenthold, R.J. (2000). A developmental change in NMDA receptor-associated proteins at hippocampal synapses. J Neurosci *20*, 1260-1271.

Scheiffele, P., Fan, J., Choih, J., Fetter, R., and Serafini, T. (2000). Neuroligin expressed in nonneuronal cells triggers presynaptic development in contacting axons. Cell *101*, 657-669.

Schulte, U., Thumfart, J.O., Klocker, N., Sailer, C.A., Bildl, W., Biniossek, M., Dehn, D., Deller, T., Eble, S., Abbass, K.*, et al.* (2006). The epilepsy-linked Lgi1 protein assembles into presynaptic Kv1 channels and inhibits inactivation by Kvbeta1. Neuron *49*, 697-706.

Schwenk, J., Harmel, N., Brechet, A., Zolles, G., Berkefeld, H., Muller, C.S., Bildl, W., Baehrens, D., Huber, B., Kulik, A.*, et al.* (2012). High-resolution proteomics unravel architecture and molecular diversity of native AMPA receptor complexes. Neuron *74*, 621-633.

Schwenk, J., Harmel, N., Zolles, G., Bildl, W., Kulik, A., Heimrich, B., Chisaka, O., Jonas, P., Schulte, U., Fakler, B., *et al.* (2009). Functional proteomics identify cornichon proteins as auxiliary subunits of AMPA receptors. Science *323*, 1313-1319.

Senechal, K.R., Thaller, C., and Noebels, J.L. (2005). ADPEAF mutations reduce levels of secreted LGI1, a putative tumor suppressor protein linked to epilepsy. Human molecular genetics *14*, 1613-1620.

Seppala, E.H., Jokinen, T.S., Fukata, M., Fukata, Y., Webster, M.T., Karlsson, E.K., Kilpinen, S.K., Steffen, F., Dietschi, E., Leeb, T., *et al.* (2011). LGI2 truncation causes a remitting focal epilepsy in dogs. PLoS genetics *7*, e1002194.

Seppala, E.H., Koskinen, L.L., Gullov, C.H., Jokinen, P., Karlskov-Mortensen, P., Bergamasco, L., Baranowska Korberg, I., Cizinauskas, S., Oberbauer, A.M., Berendt, M., *et al.* (2012). Identification of a novel idiopathic epilepsy locus in Belgian Shepherd dogs. PloS one *7*, e33549.

Shanks, N.F., Savas, J.N., Maruo, T., Cais, O., Hirao, A., Oe, S., Ghosh, A., Noda, Y., Greger, I.H., Yates, J.R., 3rd, *et al.* (2012). Differences in AMPA and kainate receptor interactomes facilitate identification of AMPA receptor auxiliary subunit GSG1L. Cell Rep *1*, 590-598.

Sheng, M., and Hoogenraad, C.C. (2007). The postsynaptic architecture of excitatory synapses: a more quantitative view. Annual review of biochemistry *76*, 823-847.

Shi, Y., Suh, Y.H., Milstein, A.D., Isozaki, K., Schmid, S.M., Roche, K.W., and Nicoll, R.A. (2010). Functional comparison of the effects of TARPs and cornichons on AMPA receptor trafficking and gating. Proc Natl Acad Sci U S A *107*, 16315-16319.

Sia, G.M., Beique, J.C., Rumbaugh, G., Cho, R., Worley, P.F., and Huganir, R.L. (2007). Interaction of the N-terminal domain of the AMPA receptor GluR4 subunit with the neuronal pentraxin NP1 mediates GluR4 synaptic recruitment. Neuron *55*, 87-102.

Siddiqui, T.J., and Craig, A.M. (2011). Synaptic organizing complexes. Curr Opin Neurobiol *21*, 132-143.

Smart, S.L., Lopantsev, V., Zhang, C.L., Robbins, C.A., Wang, H., Chiu, S.Y., Schwartzkroin, P.A., Messing, A., and Tempel, B.L. (1998). Deletion of the K(V)1.1 potassium channel causes epilepsy in mice. Neuron *20*, 809-819.

Soto, D., Coombs, I.D., Kelly, L., Farrant, M., and Cull-Candy, S.G. (2007). Stargazin attenuates intracellular polyamine block of calcium-permeable AMPA receptors. Nat Neurosci *10*, 1260-1267.

Sousa, I., Clark, T.G., Holt, R., Pagnamenta, A.T., Mulder, E.J., Minderaa, R.B., Bailey, A.J., Battaglia, A., Klauck, S.M., Poustka, F., *et al.* (2010). Polymorphisms in leucine-rich repeat genes are associated with autism spectrum disorder susceptibility in populations of European ancestry. Molecular autism *1*, 7.

Steinlein, O.K. (2004). Genetic mechanisms that underlie epilepsy. Nature reviews Neuroscience *5*, 400-408.

Stoppini, L., Buchs, P.A., and Muller, D. (1991). A simple method for organotypic cultures of nervous tissue. J Neurosci Methods *37*, 173-182.

Striano, P., de Falco, A., Diani, E., Bovo, G., Furlan, S., Vitiello, L., Pinardi, F., Striano, S., Michelucci, R., de Falco, F.A., *et al.* (2008). A novel loss-of-function LGI1 mutation linked to autosomal dominant lateral temporal epilepsy. Arch Neurol *65*, 939-942.

Sun, Y., Wang, Y., Zhang, J., Tao, J., Wang, C., Jing, N., Wu, C., Deng, K., and Qiao, S. (2007). ADAM23 plays multiple roles in neuronal differentiation of P19 embryonal carcinoma cells. Neurochemical research *32*, 1217-1223.

Takahashi, E., Sagane, K., Oki, T., Yamazaki, K., Nagasu, T., and Kuromitsu, J. (2006). Deficits in spatial learning and motor coordination in ADAM11-deficient mice. BMC neuroscience *7*, 19.

Thomas, R., Favell, K., Morante-Redolat, J., Pool, M., Kent, C., Wright, M., Daignault, K., Ferraro, G.B., Montcalm, S., Durocher, Y., *et al.* (2010). LGI1 is a Nogo receptor 1 ligand that antagonizes myelin-based growth inhibition. J Neurosci *30*, 6607-6612.

Tomita, S., Adesnik, H., Sekiguchi, M., Zhang, W., Wada, K., Howe, J.R., Nicoll, R.A., and Bredt, D.S. (2005). Stargazin modulates AMPA receptor gating and trafficking by distinct domains. Nature *435*, 1052-1058.

Traynelis, S.F., Wollmuth, L.P., McBain, C.J., Menniti, F.S., Vance, K.M., Ogden, K.K., Hansen, K.B., Yuan, H., Myers, S.J., and Dingledine, R. (2010). Glutamate receptor ion channels: structure, regulation, and function. Pharmacological reviews *62*, 405-496.

Turrigiano, G.G., and Nelson, S.B. (2004). Homeostatic plasticity in the developing nervous system. Nature reviews Neuroscience *5*, 97-107.

Uemura, T., Lee, S.J., Yasumura, M., Takeuchi, T., Yoshida, T., Ra, M., Taguchi, R., Sakimura, K., and Mishina, M. (2010). Trans-synaptic interaction of GluRdelta2 and Neurexin through Cbln1 mediates synapse formation in the cerebellum. Cell *141*, 1068-1079.

Vacher, H., Mohapatra, D.P., and Trimmer, J.S. (2008). Localization and targeting of voltage-dependent ion channels in mammalian central neurons. Physiological reviews *88*, 1407-1447.

von Engelhardt, J., Mack, V., Sprengel, R., Kavenstock, N., Li, K.W., Stern-Bach, Y., Smit, A.B., Seeburg, P.H., and Monyer, H. (2010). CKAMP44: a brain-specific protein attenuating short-term synaptic plasticity in the dentate gyrus. Science *327*, 1518-1522.

Wang, K., Zhang, H., Ma, D., Bucan, M., Glessner, J.T., Abrahams, B.S., Salyakina, D., Imielinski, M., Bradfield, J.P., Sleiman, P.M., *et al.* (2009). Common genetic variants on 5p14.1 associate with autism spectrum disorders. Nature *459*, 528-533.

Winawer, M.R., Ottman, R., Hauser, W.A., and Pedley, T.A. (2000). Autosomal dominant partial epilepsy with auditory features: defining the phenotype. Neurology *54*, 2173-2176.

Yan, J., Oliveira, G., Coutinho, A., Yang, C., Feng, J., Katz, C., Sram, J., Bockholt, A., Jones, I.R., Craddock, N., *et al.* (2005). Analysis of the neuroligin 3 and 4 genes in autism and other neuropsychiatric patients. Molecular psychiatry *10*, 329-332.

Yang, Y., and Calakos, N. (2013). Presynaptic long-term plasticity. Frontiers in synaptic neuroscience *5*, 8.

Yokoi, N., Fukata, Y., Kase, D., Miyazaki, T., Jaegle, M., Ohkawa, T., Takahashi, N., Iwanari, H., Mochizuki, Y., Hamakubo, T., *et al.* (2014). Chemical Correctors Restore LGI1 Functions and Ameliorate Increased Seizure Susceptibility in a Mouse Model of Human Epilepsy.

Yoshimura, Y., Yamauchi, Y., Shinkawa, T., Taoka, M., Donai, H., Takahashi, N., Isobe, T., and Yamauchi, T. (2004). Molecular constituents of the postsynaptic density fraction revealed by proteomic analysis using multidimensional liquid chromatography-tandem mass spectrometry. Journal of neurochemistry *88*, 759-768.

Yu, Y.E., Wen, L., Silva, J., Li, Z., Head, K., Sossey-Alaoui, K., Pao, A., Mei, L., and Cowell, J.K. (2010). Lgi1 null mutant mice exhibit myoclonic seizures and CA1 neuronal hyperexcitability. Human molecular genetics *19*, 1702-1711.

Zhou, Y.D., Lee, S., Jin, Z., Wright, M., Smith, S.E., and Anderson, M.P. (2009). Arrested maturation of excitatory synapses in autosomal dominant lateral temporal lobe epilepsy. Nature medicine *15*, 1208-1214.

Publishing Agreement

It is the policy of the University to encourage the distribution of all theses, dissertations, and manuscripts. Copies of all UCSF theses, dissertations, and manuscripts will be routed to the library via the Graduate Division. The library will make all theses, dissertations, and manuscripts accessible to the public and will preserve these to the best of their abilities, in perpetuity.

Please sign the following statement:

I hereby grant permission to the Graduate Division of the University of California, San Francisco to release copies of my thesis, dissertation, or manuscript to the Campus Library to provide access and preservation, in whole or in part, in perpetuity.

Author Signature

10-27-14

Date